

**WATER USE OF MATURE PECAN ORCHARDS UNDER SEMI-ARID CONDITIONS**

**by**

**WERNER ROSSOUW**

**Submitted in partial fulfillment of the academic requirements of  
M.Sc. (Agric) Horticulture  
in the Department of Plant and Soil Sciences  
University of Pretoria**

**Supervisor: Dr N.J. Taylor**

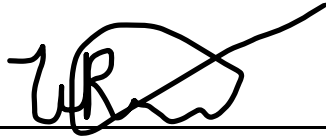
**Co-Supervisor: Prof. J.G. Annandale**

**March 2023**

## Declaration

I, Werner Rossouw, declare that the dissertation, which I hereby submit for the degree M.Sc. (Agric) Horticulture at the University of Pretoria, is my own work and has not previously been submitted by me for a degree at this or any other tertiary institution. I also certify that there was no plagiarism committed in writing this dissertation.

X



---

Werner Rossouw

Date: 25/02/2023

## Abstract

Judicious and sensible water supply is vital for optimal fruit production, and as a result most orchard crops depend on supplemental irrigation, especially in areas in South Africa, where rainfall patterns are unpredictable and sparsely distributed. Through accurate quantification or estimation of crop water use or evapotranspiration (ET), the need for supplemental irrigation can be quantified. In addition, by partitioning ET into its components, a better understanding of the factors that govern water loss from an orchard can be obtained, which is critical for determining where water savings can be made. This study aimed to measure ET and its components (canopy transpiration ( $T_c$ ) and soil evaporation ( $E_s$ )) of a 14-year-old mixed cultivar pecan orchard in the semi-arid Northern Cape Province of South Africa. This is one of the hotter and drier pecan production regions in South Africa and was expected to differ from where most of the pecan water use research was conducted in the United States of America (U.S.A), due mainly to a longer growing season in the Northern Cape. The current data used for water management of pecan orchards are primarily based on research done in other countries or by using an empirical model to estimate water use. As different regions are characterized by its own unique climate and management practices, modeling approaches were developed that adjust pecan crop coefficient curves ( $K_c$ ) to specific climatic conditions and managements practices through weather variables, thermal time, fractional canopy cover and crop height (Allen and Pereira, 2009; Miyamoto, 1983; Samani et al., 2011; Sammis et al., 2004; Taylor et al., 2015). These empirical models may not be applicable to South African growing conditions as they contain artefacts of the regions from where they were developed, potentially leading to inaccurate ET predictions (Ibraimo, 2018). In the study by Ibraimo (2018), it was highlighted that modelling pecan ET according to a four stage  $K_c$  approach (Allen et al., 1998b) yielded accurate results on a seasonal basis, but not at a monthly time step, mainly because pecan exhibit a six stage  $K_c$  curve. A second approach was tested by Ibraimo (2018), whereby a set of reference  $K_c$  were adjusted according for canopy size and growing degree days (GDD) to derive orchard specific  $K_c$  (Samani et al., 2011; Sammis, 2004). The ET estimates correlated well with actual measurements at the study site in Cullinan, South Africa, but it was further hypothesized that the method of adjusting  $K_c$  values for climate would not be transferable to hotter production areas where GDD exceeds 1500. Ibraimo (2018) [proposed that a better method could be to adjust  $K_c$  curve according to observed phenological stages and that the approach would work better in orchards whereby  $E_s$  is a minor component ( $\leq 20\%$ ) of ET. By measuring the two ET components separately it is possible that this approach could be applied to a wider range of orchards, which would allow for improved estimation, as well as the contribution of  $E_s$  towards total ET.

Field trials were conducted over the 2018/2019 production season on a farm in the Vaalharts irrigation scheme to measure  $T_c$  and model  $E_s$  separately, which was then used to obtain seasonal ET values. From the results it was observed that the application of the empirical equation of Sammis et al., (2004) for adjusting  $K_c$  values according to thermal time does not hold true in Vaalharts that has a GDD accumulation exceeding 1500 (1861 for the 2018/19 season) during the growing season. The approach proposed by Ibraimo (2018), whereby the  $K_c$  curve was adjusted according to phenological stages allowed for more accurate estimations of  $K_c$ . The method was shown to successfully estimate monthly ET of mature pecan trees in this study, when the adjusted  $K_{c-ref}$  values were further adjusted for canopy size as described by Samani et al., (2011). There was a slight overestimation by the model between November 2018 and January 2019, ultimately accounting for a 6% overestimation of estimated ET as compared to ET estimated as the sum of  $T_c$  and modelled  $E_s$ . The performance of the model was determined by comparing the accuracy of monthly ET modelling against determined monthly ET. From this comparison the coefficient of determination ( $R^2$ ) value was 0.86, which is considerable to be acceptable. The Willmott index of agreement (D) value was 0.91, root mean square error (RMSE) 23.22, mean absolute error (MAE) of 13.60 and coefficient of residual mass (CRM) of 1.01. The MAE is below the threshold of 20% which indicates that the slight deviation is still within acceptable limits. Based on the positive CRM value the deviation is attributed to an overestimation of the model. This data suggests that by allowing for the adjustment of the  $K_{c-ref}$  curve according to local growing conditions and canopy cover, good estimates of monthly ET can be obtained. Through this method it was possible to determine the main contributing factors that drive water loss, through both  $T_c$  or  $E_s$ , as well as some of the factors driving the water loss.



## TABLE OF CONTENTS

### CHAPTER 1 GENERAL INTRODUCTION 1

1.1.1	Background.....	1
1.1.2	Hypotheses.....	2
1.1.3	Aim of Study .....	3
1.1.4	Objectives.....	3

### CHAPTER 2 LITERATURE REVIEW 4

2.1	Pecan physiology pertaining to water relations	4
2.1.1	Ecophysiology .....	4
2.1.2	The influence of weather variables on transpiration.....	8
2.1.3	Whole-tree hydraulic flow .....	10
2.1.4	Pecan tree response to soil water availability .....	11
2.2	Pecan water use	12
2.2.1	Pecan water use .....	13
2.2.2	Soil evaporation.....	17
2.2.3	Water use efficiency and water use productivity.....	20
2.2.4	Measurement of crop water use.....	23
2.2.5	Modelling pecan water use .....	28

### CHAPTER 3 GENERAL MATERIALS AND METHODS 37

3.1	Site description and experimental layout .....	37
3.2	Weather data.....	38
3.3	Irrigation and water table monitoring.....	39
3.4	Ecophysiological measurements .....	40
3.5	Soil evaporation, drainage patterns and root density .....	40
3.6	Sap flow measurements .....	45
3.7	Evapotranspiration estimates using the Eddy Covariance technique .....	48

3.8	Determination of canopy size .....	49
CHAPTER 4	PECAN EVAPOTRANSPIRATION	51
4.1	Introduction .....	51
4.2	Materials and Methods .....	53
4.3	Results .....	53
4.3.1.	Weather conditions.....	53
4.3.2.	Pecan transpiration and Canopy Development.....	54
4.3.3.	Soil Evaporation .....	57
4.3.4.	Pecan evapotranspiration and partitioning.....	63
4.3.5.	Pecan water use efficiency and productivity .....	65
4.4	Discussion and Conclusion .....	67
CHAPTER 5	KEY FACTORS INFLUENCING PECAN EVAPOTRANSPIRATION	72
5.1.	Introduction.....	72
5.2.	Materials and Methods.....	74
5.3.	Results.....	74
5.3.1.	Factors influencing transpiration .....	74
5.3.2.	Pecan ecophysiology .....	76
5.3.3.	Root distribution and tree water status in relation to soil water content	81
5.4.	Discussion and Conclusion .....	91
CHAPTER 6	MODELLING PECAN EVAPOTRANSPIRATION	94
6.1.	Introduction.....	94
6.2.	Materials and Methods.....	95
6.3.	Results and Discussion.....	99
6.4.	Conclusion.....	103
CHAPTER 7	GENERAL CONCLUSIONS	105
References		110

## **Acknowledgements**

Firstly, would I like to thank Dr. Nicolette Taylor for the opportunity to conduct this M.S.c (Agric) Horticulture degree as well as for all the support and guidance as it proved invaluable to complete this thesis.

I would like to acknowledge the Water Research Commission and SAPPA for providing the necessary funds to pursue this research in pecan water use. Further would I like to thank Marnus Groenewald from Groen Boerdery for being so accommodating with our study site and lending us his trees for the water use studies.

Lastly, my friends, family and wife, Shannon Rossouw, who have been by my side since starting this venture, a big thank you for keeping me motivated when the going got tough. I hope I have made you proud.

## List of Figures

Figure 2.1 Relationship between A) photosynthesis, B) stomatal conductance and C) leaf transpiration and midday stem water potential of trees at two sites just outside Las Cruces, New Mexico. Data was collected during periods when trees were well watered and when they were water stressed during flood irrigation dry down cycles (Othman et al., 2014). .....	6
Figure 2.2 Diurnal variation of stem water potential ( $\Psi_{\text{stem}}$ ) and leaf water potential ( $\Psi_{\text{leaf}}$ ) at tree heights of 2.5 m (lower canopy), 4.6 m (mid canopy) and 7.6 m (upper canopy) and vapor pressure deficit for A) and C) well-watered conditions and B) and D) a dry soil. A) and B) are at site with a sandy loam soil and C) and D) are at a site with silty clay loam soil, both outside Las Cruces in New Mexico (Deb et al., 2012). .....	7
Figure 2.3 Daily pecan transpiration ( $T_c$ ) as influenced by A) wind speed ( $u_2$ ), B) air temperature ( $T_a$ ), C) solar radiation ( $R_s$ ), and D) vapor pressure deficit (VPD). The black circles represents 0.1 of the regression quantiles, the open squares 0.5 and the black triangles 0.9 (Ibraimo, 2018). ..	9
Figure 2.4 Measured ( $\bullet$ ) and calculated ( $\Delta$ ) canopy transpiration and trunk sap flow ( $\circ$ ) from 07hoo until 24hoo (Steinberg et al., 1990). .....	11
Figure 2.5 Relationship between annual pecan ET and fractional cover for 279 orchards in New Mexico's Lower Rio Grande valley. ET was estimated using a regional ET estimation model (Samani et al., 2011). .....	17
Figure 2.6 Relating the amount of energy available for A) the fractions of soil covered by vegetation, wetted and exposed and wetted (fraction of soil covered by vegetation ( $f_c$ ), fraction of soil wetted by rain or irrigation ( $f_w$ ), fraction of soil that is both exposed and wetted ( $f_{ew}$ ), and exposed soil fraction ( $1-f_c$ )) for a partial cover crop when the wetting results from precipitation or B) from irrigation that only wets a fraction of the soil surface (Allen et al., 2005). .....	18
Figure 2.7 Evaporation simulation from a wetted sand column to represent Stage 1 which is governed by capillary flow to the zone of evaporation and Stage 2, which is governed by vapor diffusion (Lehmann et al., 2008). .....	18
Figure 2.8 A) Monthly values of water use efficiency (WUE) of pecan trees (Biomass/ET) and B) the impact of VPD on monthly measured and predicted water use efficiency (WUE) for pecan trees near Las Cruces in New Mexico (Wang et al., 2007a). .....	21
Figure 3.1 A) Orchard layout where the trial is taking place and the position of the two sites where sap flow is measured, B) At site A four trees are measured, Tree 1 and 2 are 'Choctaw' and Tree 3 and 4 are 'Wichita', at site B four trees are measured, Tree 1 and 4 are 'Choctaw' and Tree 2 and 3 are 'Wichita'. .....	37
Figure 3.2 The automatic weather station (AWS) placed within 1 km of the trial site. ....	39

Figure 3.3 Irrigation uniformity test with a series of rain gauges (▲) placed at 1 m intervals within the row from an uncovered macro-sprinkler (○), whilst opposite sprinkler was covered (●). ....	40
Figure 3.4 Initial Micro-lysimeter placement around the tree, ⊗ represents the micro-lysimeters within the row at a 1.25 m spacing. ⊕ Represents the micro-lysimeters perpendicular to the row at a 1.67 m spacing. Micro-lysimeters 1 to 12 represent different wetted and shaded soil surface areas within the ground allocated to the tree. ....	41
Figure 3.5 Final placement of micro-lysimeters around the tree, ⊗ represents the micro-lysimeters across the row at 1.25 m spacing. ⊕ Represents the micro-lysimeters perpendicular and parallel to the row at a 1.67 m spacing. Micro-lysimeters 1 to 24 represent different wetted and shaded soil surface areas within the ground allocated to the tree. ....	42
Figure 3.6 Visual representation of 15 GS-1 Decagon soil water sensor placement at three distances perpendicular to the tree; firstly, within the row at 0 m, secondly at 2.7 m from the tree base and thirdly at 5 m from the tree base at depths of 30 cm, 40 cm, 60 cm, 90 cm and 120 cm at tree 2 site B. ....	43
Figure 3.7 Grid installed in a 1 m x 1 m soil profile pit wall to determine rooting pattern and root distribution. ....	45
Figure 3.8 Schematic representation of the HR method proposed by Burgess et al., (2001), with the heater probe in grey and the thermocouples in blue spaced equally apart (indicated by x). ....	46
Figure 3.9 Core taken from a 'Choctaw' tree indicating bark thickness and presence of heartwood. ....	47
Figure 3.10 Wounding caused as a result of probe insertion into the tree to determine heat pulse velocities and ultimately transpiration. ....	48
Figure 3.11 ■A) Position of the Open Path Eddy Covariance system above the tree canopy. ■ B) Position of the Open Path Eddy Covariance system in relation to the sap flow measurements. ....	49
Figure 3.12 A Hukseflux HFP01 soil heat flux plate in parallel with two TCAV-L soil temperature averaging probes. ....	49
Figure 3.13 Representation of the grid layout for the determination of canopy cover using a Decagon AccuPAR LP-80 ceptometer (Decagon Devices, Pullman, WA, USA). ....	50
Figure 4.1 Weather data from the automatic weather station from 09 September 2018 until 09 September 2019, which included solar radiation ( $\text{MJ m}^{-2} \text{ day}^{-1}$ ), minimum (Temp min) and maximum (Temp max) temperature ( $^{\circ}\text{C}$ ), seasonal rainfall (mm), vapor pressure deficit (VPD) (kPa) and reference evapotranspiration ( $\text{ET}_o$ ) (mm). ....	54

Figure 4.2 Measured daily transpiration rates ( $T_c$ ) of 'Wichita' (Blue line) and 'Choctaw' (Grey line) cultivars and corresponding reference evapotranspiration ( $ET_o$ ) (mm) (Green line) measurements during the 2018-2019 production season. ....55

Figure 4.3 Average leaf area index (LAI) of 'Choctaw' (tree 1 and 2) (Grey line) and 'Wichita' (tree 3 and 4) (Blue line) pecan trees in Vaalharts over the 2018-2019 production season. Error bars indicate the standard error of the two trees. ....56

Figure 4.4 Seasonal transpiration crop coefficient ( $K_t$ ) of 'Wichita' (blue dots) and 'Choctaw' (grey dots) and the daily average of each respective cultivar represented by the black line for 'Wichita' and the orange line for 'Choctaw' through the course of the 2018-2019 production season. ....57

Figure 4.5 Spatial and temporal variation of average daily soil evaporation ( $E_s$ ) (mm day<sup>-1</sup>) from micro-lysimeters throughout the 2018/19 season, Rainfall (mm) and the corresponding  $f_{c\ eff}$  (%) on the secondary y-axis. The first four measurement days represent measurement from the initial micro-lysimeter layout (Figure 3.4), whilst bars with no patterns represent micro-lysimeter measurements from the second layout (Figure 3.5). ....58

Figure 4.6 Photosynthetic active radiation (PAR) ( $\mu\text{mol m}^{-2} \text{s}^{-1}$ ) at the received at the soil surface where the soil-micro-lysimeters were placed on selected days in relation to the leaf area index (LAI) of 'Wichita' tree 4 at Site B (brown line). ....59

Figure 4.7 Irrigation uniformity test ( $L\ h^{-1}$ ) at set 1 m intervals from macro-sprinkler (represented by red triangle) on the second micro-lysimeter layout for reference (numbered 1 to 24).....60

Figure 4.8 A) Estimates of the soil evaporation reduction cycle ( $K_r$ ) and B) soil evaporation ( $E_s$ ) (mm day<sup>-1</sup>), after a respective rainfall (mm day<sup>-1</sup>) and irrigation (mm day<sup>-1</sup>) event, measured on a daily basis during a period when the effective canopy cover ( $f_{c\ eff}$ ) was 75% in Vaalharts. ....61

Figure 4.9 (A) Parameterization (n=8) and (B) validation (n=8) of  $E_s$  estimates using the FAO-56 dual  $K_c$  model for a sandy loam soil in the mature pecan orchard in Vaalharts.....62

Figure 4.10 Seasonal estimated  $E_s$  (mm day<sup>-1</sup>) (grey line) with the varying LAI (m<sup>2</sup> m<sup>-2</sup>) (blue dots) and the accompanying  $ET_o$  (mm day<sup>-1</sup>) (blue line) for the 2018-2019 measurement period. ....63

Figure 4.11 Monthly measured evapotranspiration (ET), ET from Eddy covariance tower and reference evapotranspiration ( $ET_o$ ) with crop coefficients ( $K_c$ ) of a 14-year-old pecan orchard during the 2018/19 production season. ....64

Figure 4.12 Partitioning of pecan evapotranspiration (ET) into total monthly transpiration ( $T_c$ ) and modelled soil evaporation ( $E_s$ ) in the 14-year-old mixed cultivar pecan orchard during the 2018-2019 production season in Vaalharts, South Africa, as well as the percentage contribution of  $T_c$  and  $E_s$  to total ET. ....65

Figure 5.1 The response of hourly transpiration ( $\text{mm h}^{-1}$ ) of ‘Wichita’ (left hand panel) and ‘Choctaw’ (right hand panel) to atmospheric variables, which included (A & B) air temperature ( $^{\circ}\text{C}$ ), (C & D) solar radiation ( $\text{MJ m}^{-2} \text{h}^{-1}$ ), (E & F) vapor pressure deficit (kPa) and (G & H) reference evapotranspiration (mm) for the measurement period of November 2018 until April 2019 and during daylight hours (06:00 to 18:00).....75

Figure 5.2 Average pre-dawn leaf water potential (MPa) measurements of all selected measurement trees for transpiration throughout the season.....76

Figure 5.3 Hourly change in stem water potential ( $\Psi_{\text{Stem}}$ ), sun leaf water potential ( $\Psi_{\text{Sun}}$ ) and shade leaf water potential ( $\Psi_{\text{Shade}}$ ) (MPa) measurements compared to the vapor pressure deficit (VPD, kPa) and transpiration ( $T_c$ ,  $\text{L h}^{-1}$ ) for A) 22/10/2018, B) 04/12/2018 and C) 11/04/2019 with standard error indications. ....78

Figure 5.4 A) The relationship between leaf water potential of A) shaded leaves ( $\Psi_{\text{Shaded}}$  (MPa)), B) sun leaves ( $\Psi_{\text{Sun}}$  (MPa)) and C) stem water potential ( $\Psi_{\text{Stem}}$  (MPa)) against average VPD (KPa) for three selected days (22/10/2018, 04/12/2018 and 11/04/2019).....79

Figure 5.5 Hourly measured canopy transpiration rate ( $\text{L h}^{-1}$ ) throughout the day corresponding to dates of water potential measurements.....80

Figure 5.6 The relationship between  $\Psi_{\text{Sun}}$  (MPa) and canopy transpiration ( $\text{L h}^{-1}$ ) for three measurement days. ....81

Figure 5.7 Matric potential data from Chameleon sensors at A) trial site A at depths of 30, 60 and 90 cm throughout the season and B) trial site B at depths of 30, 60 and 90 cm. C) Average soil temperature ( $^{\circ}\text{C}$ ) of both sites at 30 cm depth for the period of 7 September 2018 until 15 April 2019.....82

Figure 5.8 Accumulative Irrigation and/or Rainfall (mm), Reference Evapotranspiration (mm), Evapotranspiration (mm) and Transpiration (mm) for ‘Choctaw’ and ‘Wichita’ trees during the period of 10 September 2018 until 30 June 2019. ....83

Figure 5.9 The number and diameter of roots found at 1.5 m (n=8093), 2.5 m (n=6967), 3.5 m (n=2915) and 4.5 m (n=1185) from the trunk perpendicular to the tree row.....86

Figure 5.10 Seasonal fluctuating hourly measurements of volumetric water content at various depths and indications of Field Capacity (FC), Plant Available Water (PAW) and Permanent Wilting Point (PWP) at 2.5 m from the tree within the tree row. ....87

Figure 5.11 Seasonal fluctuating hourly measurements of volumetric water content at various depths and indications of Field Capacity (FC), Plant Available Water (PAW) and Permanent Wilting Point (PWP) at 2.5 m from the tree within the working row .....88

Figure 5.12 Seasonal fluctuating hourly measurements of volumetric water content at various depths and indications of Field Capacity (FC), Plant Available Water (PAW) and Permanent Wilting Point (PWP) at 5 m from the tree within the working row. ....89

Figure 5.13 Hourly comparison of various levels of A) volumetric water content in relation to B) canopy transpiration given varying environmental variables such as C) temperature ( $^{\circ}\text{C}$ ), D) solar radiation ( $\text{MJ m}^{-2} \text{h}^{-1}$ ), E) vapor pressure deficit (kPa) and F) reference evapotranspiration ( $\text{mm h}^{-1}$ ) on three selected date which are 24<sup>th</sup> January 2019, 8<sup>th</sup> March 2019 and 4<sup>th</sup> April 2019. ....91

Figure 6.1 Transpiration crop coefficients ( $K_t$ ) for the 2018-2019 production season for ‘Wichita’ (blue dots) and ‘Choctaw’ (grey dots) pecan trees, with the black line representing the average  $K_t$  between the two measured cultivars with red dotted lines indicating on what date changes occurred. ....100

Figure 6.2 The comparison between measured daily growing degree days (GDD) and the derived  $K_c$  values, as described by Sammis et al., (2004) (purple dots), in relation to  $K_t$  values for ‘Choctaw’ (blue dots) and ‘Wichita’ (yellow dots) pecan trees in the Vaalharts region. ....101

Figure 6.3 Six stage reference crop coefficient ( $K_{c-ref}$ ) curve for a mature pecan orchard at Vaalharts for the 2018-2019 production season. ....102

Figure 6.4 Measured (marker) and extrapolated (line) effective fractional interception of photosynthetic active radiation in the Vaalharts pecan orchard for the 2018-2019 season. ....102

Figure 6.5 Comparison between monthly estimated and actual evapotranspiration (ET) as described by Ibraimo (2018) with adjusted  $K_c$  values for a mature pecan orchard in Vaalharts during the 2018-2019 production season, according to phenological stages. ....103



## List of Tables

Table 2.1 Evapotranspiration of pecan orchards reported in literature. $f_c$ is fractional canopy cover, ET is evapotranspiration and T is transpiration.....	14
Table 2.2 Measured monthly pecan reference crop coefficients ( $K_{c-ref}$ ) which has been offset by 6 months to account for southern hemisphere conditions (Samani et al., 2011). .....	30
Table 3.1 Overview of the mixed cultivar orchard at the trial site in Jan Kempdorp, South-Africa. ....	38
Table 4.1 Crop yield, seasonal water use (ET), total income, total water applied, water use efficiency (WUE), water use productivity (WUP), irrigation water use efficiency (IWUE) and transpiration water use efficiency (TWUE) for two pecan cultivars under non-limiting soil water conditions for the 2018/19 production season. ....	67
Table 5.1 Soil sample results of bulk density ( $\text{kg m}^{-3}$ ), clay (%), sand (%), silt (%), permanent wilting point ( $\text{cm}^3$ water $\text{cm}^{-3}$ soil), field capacity ( $\text{cm}^3$ water $\text{cm}^{-3}$ soil) and plant available water ( $\text{cm}^3$ water $\text{cm}^{-3}$ soil) at various depths (cm) down the soil profile with accompanying soil texture classes.....	84
Table 6.1 Monthly pecan reference crop coefficients ( $K_{c-ref}$ ) for New Mexico, which were offset by 6 months to represent southern hemisphere seasons (Ibraimo et al., 2016; Samani et al., 2011). ....	96
Table 6.2 Average monthly pecan reference crop coefficients ( $K_{c-ref}$ ) for the Vaalharts study site during the 2018-2019 production season using the function described by Sammis et al., (2004). ....	96
Table 6.3 Pecan growth stage classification through the course of the season (Herrera, 1990; Wells and Conner, 2007) and corresponding $K_{c-ref}$ values as suggested by Ibraimo et al., (2016) and Samani et al., (2011). ....	97
Table 6.4 Values used to parameterize the FAO-56 dual crop coefficient model in order to estimate soil evaporation coefficient.....	98

## **List of Abbreviations and Symbols**

### Abbreviations

ABA	Abscisic acid
AWS	Automatic weather station
E	East
EBR	Energy balance ratio
GDP	Gross domestic product
HPV	Heat pulse velocity (cm hr <sup>-1</sup> )
HR	Heat ratio
IRGA	Infrared gas analyzer
IWUE	Irrigation water use efficiency (t ha <sup>-1</sup> mm <sup>-1</sup> )
MMs	Method of moments
N	North
OLS	Ordinary least squares
OPEC	Open Path Eddy Covariance
PAR	Photosynthetically active radiation (nm)
RMA	Reduced major axis
S	South
SAPPA	South African Pecan Production Association
SFD	Sap flux density (cm hr <sup>-1</sup> )
TWUE	Transpiration water use efficiency (kg yield/T)
U.S.A	United States of America
W	West
WRC	Water Research Commission

WUE Water use efficiency (kg yield ET<sup>-1</sup>)

WUP Water use productivity (R m<sup>-3</sup>)

### Symbols

A Net CO<sub>2</sub> assimilation for Photosynthesis (μmol m<sup>-2</sup> s<sup>-1</sup>)

c<sub>g</sub> Specific gravity of wood (g cm<sup>-3</sup>)

c<sub>d</sub> Specific heat capacity of dry wood (kJ kg<sup>-1</sup> K<sup>-1</sup>)

c<sub>w</sub> specific heat capacity of water (kJ kg<sup>-1</sup> K<sup>-1</sup>)

c<sub>f</sub> Specific heat capacity of fresh wood (kJ kg<sup>-1</sup> K<sup>-1</sup>)

c<sub>s</sub> Specific heat capacity of sap (kJ kg<sup>-1</sup> K<sup>-1</sup>)

C<sub>a</sub> Ambient CO<sub>2</sub> concentration (ppm)

C<sub>P</sub> Canopy porosity

CR Capillary rise

C<sub>i</sub> Internal CO<sub>2</sub> concentration (ppm)

DP Deep percolation

D<sub>ax</sub> Axial thermal diffusivity of sapwood (W m<sup>-1</sup> K<sup>-1</sup>)

D<sub>e</sub> Cumulative depth of evaporation from the topsoil layer (mm)

e<sub>a</sub> Actual vapor pressure (kPa)

e<sub>s</sub> Saturation vapor pressure (kPa)

ET<sub>o</sub> Reference evapotranspiration (mm day<sup>-1</sup>)

ET Crop evapotranspiration (mm day<sup>-1</sup>)

E<sub>s</sub> Soil evaporation (mm day<sup>-1</sup>)

f<sub>c eff</sub> Effective fractional cover

f<sub>h</sub> Fraction of the orchard floor that is shaded

f<sub>IPAR</sub> Fractional interception of photosynthetically active radiation

$f_d$	Diffuse radiation interception fraction of the orchard floor
$g_a$	Aerodynamic conductance ( $\text{m s}^{-1}$ )
$g_s$	Leaf stomatal conductance ( $\text{mmol m}^{-2} \text{s}^{-1}$ )
$g_c$	Canopy conductance ( $\text{mmol m}^{-2} \text{s}^{-1}$ )
$G$	Soil heat flux ( $\text{MJ m}^{-2} \text{d}^{-1}$ )
GDD	Growing Degree Day
$h$	Mean plant height (m)
$H$	Sensible heat flux density ( $\text{W m}^{-2}$ )
$I$	Irrigation (mm)
$K_{ax}$	Axial thermal heat conductivity ( $\text{W m}^{-1} \text{K}^{-1}$ )
$K_c$	Crop coefficient
$K_{cb}$	Basal crop coefficient
$K_e$	Soil evaporation coefficient
$K_r$	Dimensionless evaporation reduction coefficient
$K_t$	Transpiration crop coefficient
$K_w$	Thermal conductivity of water ( $\text{W m}^{-1} \text{K}^{-1}$ )
LAI	Leaf Area Index
LE	Latent heat flux ( $\text{W m}^{-2}$ )
MC	Water content of the sapwood
$MC_{FSP}$	Water content at fiber saturation point
MPa	Megapascal
$P$	Precipitation (mm)
$P_a$	Atmospheric pressure (kPa)
RH	Relative humidity (%)

RO	Surface runoff (mm)
$R_n$	Net radiation ( $\text{MJ m}^{-2}$ )
$R_s$	Total daily solar radiation ( $\text{MJ m}^{-2}\text{d}^{-1}$ )
$T_c$	Canopy transpiration ( $\text{mm hr}^{-1}$ )
$T_a$	Air temperature ( $^{\circ}\text{C}$ )
t	Time (s or hr)
$T_b$	Base temperature ( $^{\circ}\text{C}$ )
$u_2$	Wind speed ( $\text{m s}^{-1}$ )
$V_c$	Corrected heat pulse velocity ( $\text{cm hr}^{-1}$ )
V	Volume of the wood sample ( $\text{m}^3$ )
VPD	Air vapor pressure deficit (kPa)
$w_f$	Fresh weight of the wood sample (g)
$w_d$	Oven-dried weight of the wood sample (g)
x	Distance (m)
$\Delta$	Slope of the saturation vapor pressure-temperature curve
$\Omega$	Decoupling coefficient
$\beta$	Bowen ratio
$\gamma$	Psychometric constant ( $\text{kPa } ^{\circ}\text{C}^{-1}$ )
$w'$	Vertical wind speed ( $\text{m s}^{-1}$ )
$q'$	Vertical humidity (%)
$\Psi_{\text{leaf}}$	Leaf water potential (mPa)
$\Psi_{\text{shade}}$	Leaf water potential of shaded leaves (mPa)
$\Psi_{\text{sun}}$	Leaf water potential of sun exposed leaves (mPa)
$\Psi_{\text{stem}}$	Stem water potential (mPa)

$\lambda$	Constant of latent heat of vaporization ( $\text{J g}^{-1}$ )
$\rho$	Density of water ( $\text{kg m}^3$ )
$\rho_a$	Air density ( $\text{kg m}^3$ )
$\rho_c$	Volumetric heat capacity ( $\text{J kg}^{-1} \text{ }^\circ\text{C}^{-1}$ )
$\rho_w$	Density of fresh wood ( $\text{kg/m}^3$ )
$\rho_s$	Density of sap ( $\text{kg/m}^3$ )
$\rho_d$	Density of dry wood ( $\text{kg/m}^3$ )
$\Theta$	Volumetric soil water content ( $\text{m}^3 \text{ m}^{-3}$ )

## **DISSERTATION OUTLINE**

This dissertation comprises of six chapters. Chapter 1 provides a general introduction that covers the relevance and importance of the study and how it pertains to the pecan industry. The hypotheses, aims and objectives for the study are also provided in this chapter. Chapter 2 reviews the current literature related to pecan tree phenology and morphology and its relation to consumptive water use. A description of the methods to quantify evapotranspiration and its constituents under various environmental conditions used within this study are described within Chapter 3 along with the site description and modelling approaches. Chapter 4 focusses on the measurement of pecan evapotranspiration, as well as its partitioning into transpiration and evaporation. It further determines the water use efficiency of the pecan orchard in this study. Chapter 5 includes an in-depth analysis of the drivers of pecan water use described in Chapter 4 and some aspects of pecan tree water relations. In Chapter 6 transpiration crop coefficients are adjusted using growing degree days, and limitations to this model are explained. Further to the approach crop coefficients were adjusted according to phenological stages in order to estimate pecan evapotranspiration under various growing conditions. Chapter 7 presents the general conclusions of the study and makes suggestions for future research.

## CHAPTER 1 GENERAL INTRODUCTION

### 1.1.1 Background

The pecan (*Carya illinoensis* (Wangenh.) K. Koch) is a horticultural crop that is indigenous to river bottoms and tributaries in the United States of America (U.S.A) and is regarded as one of the most significant native contributors to the U.S.A agricultural economy (Sande et al., 2009; Wells, 2017; Wood et al., 1994). Perennial pecan trees are highly adaptable to selective pressure caused by diverse climatic conditions, making its widespread cultivation in different countries possible (Sparks, 2005). These adaptive traits can be attributed to the wide range of genetic diversity that exists within the species, where certain populations with genotypes adapted to the specific climatic conditions, will have a competitive advantage over other genotypes adapted for climatic conditions of another region (Sparks, 2005).

The diversity within pecan makes it a popular choice for widespread commercial cultivation and contributes significantly to the South African gross domestic product (GDP), in addition to supplying a wide range of job opportunities. In South Africa the pecan nut industry has been expanding rapidly, as 580 000 trees were planted in 2017 and 2018 compared to only 200 000 in 2010 (SAPPA, 2018). Due to the rapid expansion, it is very difficult to determine the exact area under pecan production. Conservative estimates are between 21 500 and 27 700 ha, with at least 11 000 ha in Vaalharts making it the most important pecan production area in South Africa (A. Coetzee, personal communication, 12 August 2019; SAPPA, 2018). This rapid expansion of the industry places a burden on existing resources, as pecan trees require a large amount of water during the growing season, which is suggested to be more than most row crops (Sparks, 2005). South Africa, and especially Vaalharts, is characterized by semi-arid conditions, with inadequate water supply as a result of erratic rainfall patterns and sparsely distributed water tables, which places increased pressure on limited irrigation water resources. Therefore, accurate estimates of pecan water use are necessary in the Vaalharts region to ensure judicious irrigation practices.

Substantial knowledge of pecan water use, phenology, as well as the accompanying soil and climatic conditions, are required for the efficient management of water resources and maximization of orchard profitability (Ward and Pulido-Velazquez, 2008). The majority of research on pecan water use has been conducted in the U.S.A and there is limited literature available on the water use of pecan trees and orchards in different production areas in South Africa. Local knowledge is critical as different total seasonal water use values are highly likely in different regions, as a result of different climatic conditions and management practices. In addition, as



annual pecan water use measurements are bound by conditions experienced during a specific growing year, is it necessary to model the water use of pecan orchards to ensure that estimates can be made for a vast number of orchards in different regions without having to do measurements. In order to ensure the accuracy of the model for all pecan orchards, it is vital that the model is validated under a range of conditions which impact tree water use.

Once water use of pecan trees has been quantified it is possible to evaluate efficiencies in the system. In this respect water use efficiency (WUE) and water use productivity (WUP) can be determined to assess yield per m<sup>3</sup> of water used by the crop and the Rands earned per m<sup>3</sup> of water used by the crop. The determination of WUE and WUP aids in the benchmarking of growers in terms of how efficiently they are applying irrigation water and making use of rainfall. In addition, by quantifying WUP for a low yielding but high value crop it allows growers to demonstrate the value of the water used by the crop, which could justify the volumes of water used to produce pecans.

#### 1.1.2 Hypotheses

1. Transpiration rates within the same cultivar, as well as between the study cultivars 'Wichita' and 'Choctaw', will differ on a daily basis in accordance with canopy size and prevailing weather conditions, leading to different seasonal crop water use values.
2. When canopy cover is low, soil evaporation will be at its highest and will be the main constituent of evapotranspiration, up until the maximum canopy cover is reached for the season. As canopy cover increases, transpiration will increase, and soil evaporation will decrease due to increased shading of the orchard floor.
3. Pecan water use efficiency (WUE) is comparable to other oil-bearing nut crops but will be lower than other high yielding fruit trees. However, due to the high value of the crop water use productivity will be similar to other fruit tree crops.
4. Through partitioning of evapotranspiration into its constituents, canopy transpiration ( $T_c$ ) and soil evaporation ( $E_s$ ), can a better understanding be obtained of beneficial and non-beneficial consumptive water use which will aid in increasing WUE and in modelling crop water use.
5. Pecans exhibit anisohydric tendencies as minimum diurnal leaf water potentials depend largely on prevailing weather conditions, with leaf water potential falling more on days with high midday vapor pressure deficit than days with a low vapor pressure deficit.
6. The growing degree days (GDD) will exceed 1500 in this growing region leading to inaccurate estimation of reference crop coefficients ( $K_{c-ref}$ ) when using an empirical GDD-

$K_c$  approach, and therefore will have to be adjusted according to observed phenological stages, which will lead to more accurate estimates of ET.

7. Evapotranspiration of irrigated pecan orchards can be more accurately modelled with a dual crop coefficient approach than a single crop coefficient approach.

### 1.1.3 Aim of Study

The aim of this study was to determine pecan water use under semi-arid conditions in South Africa and to gain an understanding of the factors driving water use by evaluating the constituents that make up crop water use. It was further aimed to use this information to evaluate a suitable dual crop coefficient model for the accurate determination of pecan orchard evapotranspiration.

### 1.1.4 Objectives

- 1 Measure the transpiration rates of unstressed 'Choctaw' and 'Wichita' pecan cultivars using the heat ratio method.
- 2 Determine the relationship between transpiration, canopy cover and weather variables in unstressed 'Choctaw' and 'Wichita' pecan trees.
- 3 Estimate soil evaporation of the mature pecan orchard using micro-lysimeters under varying canopy cover conditions.
- 4 Model unstressed pecan evapotranspiration for the Vaalharts region, using methods described by Ibraimo et al., (2016).
- 5 Determine the yield and quality of the nuts in the orchard in which water use was measured to determine water use efficiency and water use productivity.
- 6 Determine leaf and stem water potentials for 'Choctaw' and 'Wichita' pecan cultivars and if a relationship exists with soil water content.
- 7 To estimate evapotranspiration of pecan orchards for targeted window periods using the eddy covariance technique in order to parameterize the dual crop coefficient approach for mature pecan orchards.

## CHAPTER 2 LITERATURE REVIEW

### 2.1 Pecan physiology pertaining to water relations

Pecans are native to the river bottoms and tributaries of the Mississippi River and rivers of central and eastern Texas, and inherently adapted an efficient water transport system to accommodate its high water requirement by means of a large taproot system that serves as a survival adaptation under semi-arid conditions (Andersen and Brodbeck, 1988; Sparks, 2002; Wolstenholme, 1979). Within the pecan species there exists a large genotypic pool that is expressed through numerous cultivars that differ in various aspects of growth and reproductive traits, as well as adaptation to different environmental conditions to ensure survival (Sparks, 2005). From aforementioned traits, a three-way interaction exists between the location, cultivar and year (Wood et al., 1997), that could result in variable results of water use. Using cultivation techniques, such as irrigation, can the survival adaptations that pecans employ become mute, but still play a crucial part in how the plant responds to these practices. Therefore, the physiological responses when subjected to various abiotic conditions outside its native range requires investigation to understand the regulatory mechanism pecans employ to regulate water use.

#### 2.1.1 Ecophysiology

Weather variables are ever changing throughout the course of a day, as well as over a season, and have a pronounced influence on tree water use through the effect on atmospheric evaporative demand. Plants are able to limit water loss if unfavorable conditions arise, mainly through changes in stomatal aperture, which is controlled by both exogenous and endogenous factors (Jones et al., 1985). Exogenous factors include environmental variables such as soil water content, air temperature, humidity, wind speed, solar irradiance and atmospheric CO<sub>2</sub> (Hetherington and Woodward, 2003). Endogenous factors consist of the plant hormone abscisic acid (ABA) and the internal CO<sub>2</sub> concentrations in the stomata (Rico et al., 2013). The role of the stomata is to optimize carbon uptake relative to water loss via transpiration, which is influenced by a number of exogenous factors as mentioned above. Whilst high vapor pressure deficit (VPD), low solar irradiance and water deficits can all cause stomatal closure, conditions such as high solar irradiance, low CO<sub>2</sub> concentrations inside the leaf tissue and its surrounding environment and conditions of low VPD encourage stomatal opening (Rico et al., 2013). Another important consideration is the ability of the xylem to transport water to the leaves to sustain transpiration rates. If water transport to the leaves does not match the rate of water leaving the leaves then the leaf water potential will drop to the point where the gradient between the roots and leaves will be so great that cavitation occurs (Campbell and Turner, 1990; Sperry, 2000; Sperry et al., 2008). It

is therefore important that the plant retains some stomatal control to maintain a more favorable water potential inside its tissues when adverse conditions arise (Jones et al., 1985).

Leaf water potential ( $\Psi_{\text{leaf}}$ ) is highly dependent on whether the leaf is exposed to the sun or shaded throughout the day, with the rate of  $\Psi_{\text{leaf}}$  decline higher for sunlit leaves than for shaded leaves, when compared at the same time of day. It was found in 5 year old pecan trees in Texas that at 14:00 the average  $\Psi_{\text{leaf}}$  of sunlit leaves was -2 MPa, whereas average shaded leaf  $\Psi_{\text{leaf}}$  was -1.3 MPa (Steinberg et al., 1990). These authors concluded that the water transport system in pecans is relatively efficient as  $\Psi_{\text{leaf}}$  of -2 MPa was recorded without a reduction in transpiration, suggesting that pecans may be able to sustain a rate of flow to the leaves that sustains the rate of water loss from the leaf surface under fairly dry conditions. Othman et al., (2014) examined the impact of changes in plant water status on  $A$  and  $g_s$  during a dry down cycle following a flood irrigation event. At midday stem water potential ( $\Psi_{\text{stem}}$ ), defined as the water potential of an enclosed leaf indicative of the whole plant water status, above -0.85 MPa there was no impact on photosynthesis, but as  $\Psi_{\text{stem}}$  dropped below -0.9 MPa the photosynthetic rate ( $A$ ) began to decline (Figure 2.1). Under prolonged periods of water deficits Othman et al., (2014) found that  $A$  was reduced by 50-70%, stomatal conductance ( $g_s$ ), defined as the measure of the degree of stomata opening, by 60-90% and canopy transpiration ( $T_c$ ), defined as the loss of water vapor through the stomata, by 30-70% when subjected to low leaf water potentials of -1.5 to -2 MPa for seven days. As a result of these findings Othman et al., (2014) suggested that in order to prevent any impact of water stress on yield of pecan orchards stem water potential should be maintained above a threshold of -0.9 MPa. This imposed threshold differed from reported values by Wells (2015) whereby water stress in pecan occurred at a lower  $\Psi_{\text{stem}}$  of -0.78 MPa under humid conditions. The difference could be attributed to the prevailing weather conditions influencing  $\Psi_{\text{stem}}$ , where the water potential will have slightly lower thresholds in more arid conditions.

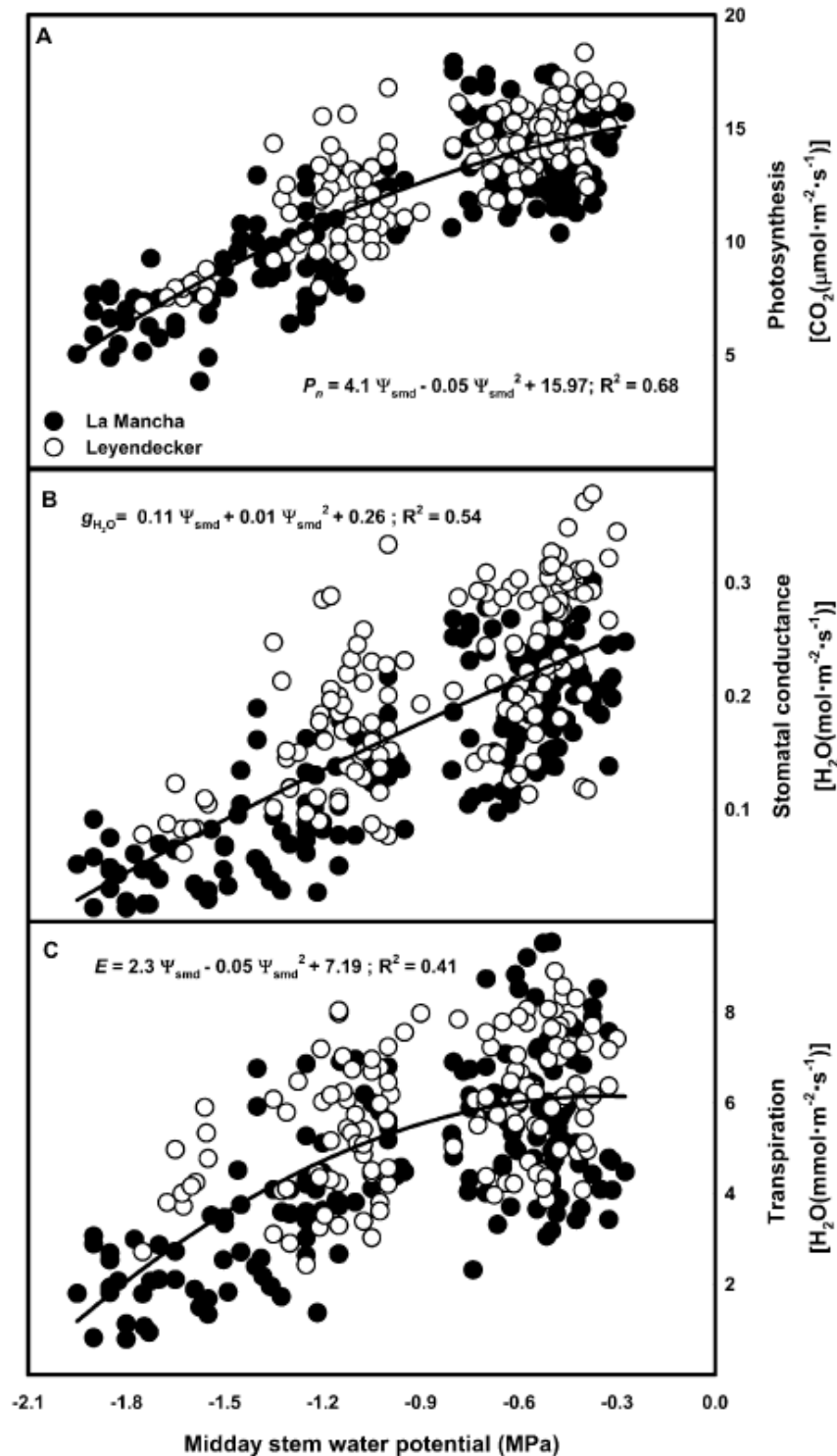
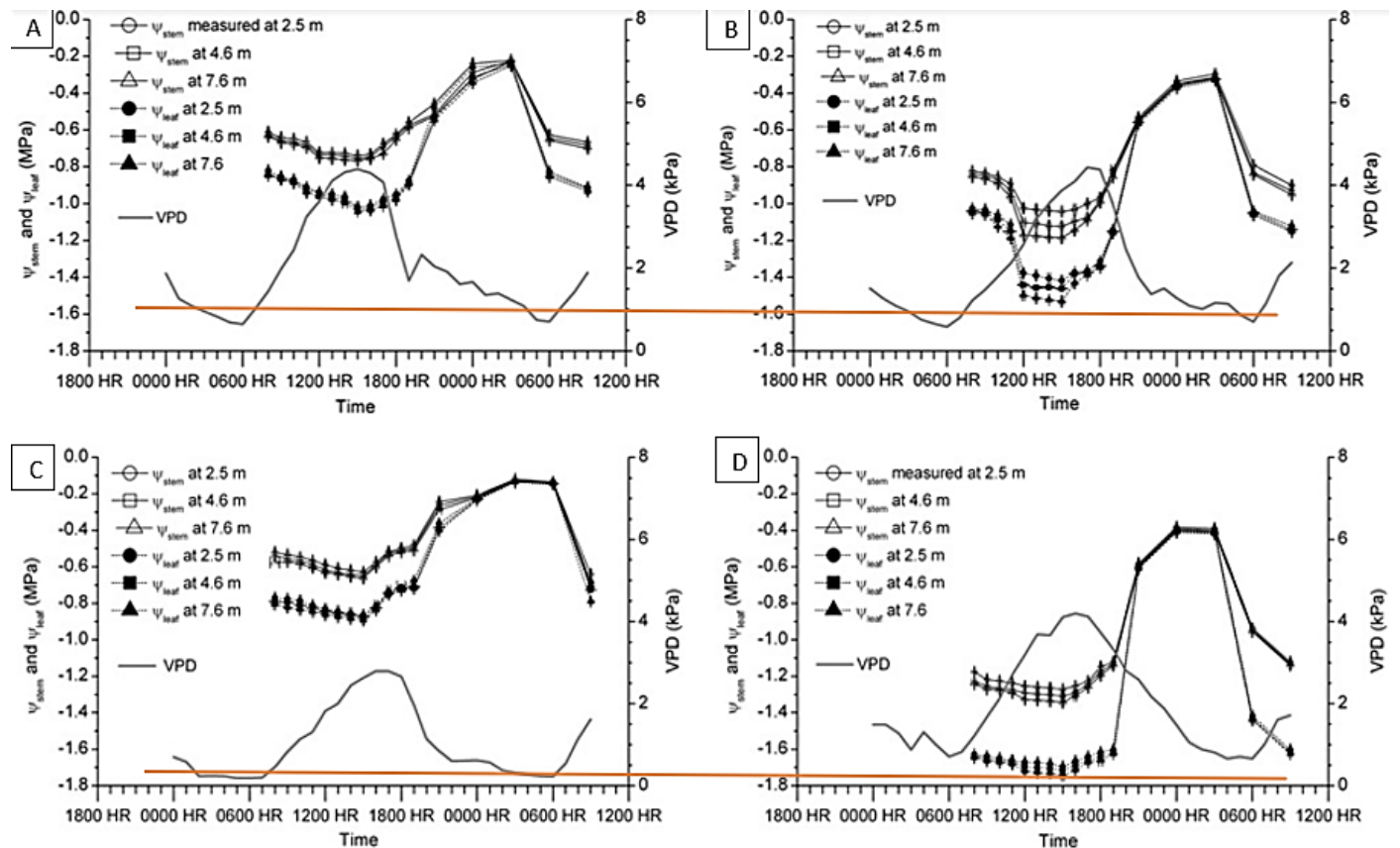


Figure 2.1 Relationship between A) photosynthesis, B) stomatal conductance and C) leaf transpiration and midday stem water potential of trees at two sites just outside Las Cruces, New Mexico. Data was collected during periods when trees were well watered and when they were water stressed during flood irrigation dry down cycles (Othman et al., 2014).

A study by Deb et al., (2012) suggests that pecans may display more of an anisohydric strategy than an isohydric strategy (Figure 2.2). Tardieu and Simonneau (1998) define typical anisohydric behavior as plants displaying approximately constant differences in  $\Psi_{leaf}$  over the course of a day, which is very similar to the differences in pre-dawn  $\Psi_{leaf}$  caused as a result of contrasting soil water availabilities. In contrast to this pattern, isohydric behavior occurs when plants display similar midday  $\Psi_{stem}$  and  $\Psi_{leaf}$  between the well-watered and dry periods (indicated by the red lines in Figure 2.2), therefore suggests more of an anisohydric behavior and suggests that transpiration rates will remain quite high even under high VPDs. Importantly, this behavior could be cultivar dependent, as studies in apple (Massonnet et al., 2007) and grapevines (Pou et al., 2012; Schultz, 2003) indicate that not all cultivars behave the same, with some exhibiting different strategies.



**Figure 2.2** Diurnal variation of stem water potential ( $\Psi_{stem}$ ) and leaf water potential ( $\Psi_{leaf}$ ) at tree heights of 2.5 m (lower canopy), 4.6 m (mid canopy) and 7.6 m (upper canopy) and vapor pressure deficit for A) and C) well-watered conditions and B) and D) a dry soil. A) and B) are at site with a sandy loam soil and C) and D) are at a site with silty clay loam soil, both outside Las Cruces in New Mexico (Deb et al., 2012).

### 2.1.2 The influence of weather variables on transpiration

The study conducted by Ibraimo (2018) determined the influence of individual environmental factors on pecan  $T_c$  by means of quantile regression analysis, specifically to determine which factor bears more weight and establish the upper limit of these variables before transpiration starts to decline as a result of the imposed factor. From Figure 2.3 can this influence be observed for wind speed ( $u_2$ ) ( $\text{m s}^{-1}$ ), air temperature ( $T_a$ ) ( $^{\circ}\text{C}$ ), solar radiation ( $R_s$ ) ( $\text{MJ m}^{-2} \text{d}^{-1}$ ), and vapor pressure deficit (VPD) (kPa). The imposed upper limit on  $T_c$  as a result of climatic variables are  $0.8 \text{ m.s}^{-1}$  for  $u_2$ ,  $21 \text{ MJ m}^{-2} \text{ day}^{-1}$  for  $R_s$ ,  $1.4 \text{ kPa}$  for VPD and  $37 \text{ }^{\circ}\text{C}$  for  $T_a$  (Ibraimo, 2018). The study concluded that VPD is the most significant atmospheric variable driving  $T_c$  followed by  $R_s$ . By assessing the response of  $T_c$  to  $ET_o$ , was it possible to determine the combined impact of all these variables on  $T_c$ . Ibraimo (2018) further found that when  $ET_o$  remained below  $4 \text{ mm day}^{-1}$   $T_c$  increased from  $2.3$  to  $5.4 \text{ mm day}^{-1}$  but once  $ET_o$  exceeded  $4 \text{ mm day}^{-1}$   $T_c$  remained fairly constant (Ibraimo, 2018). This indicates that pecan trees have some degree of control over gas exchange that is contradictory to previous findings of Deb at al., (2012) which suggested an anisohydric water use tendency, whereby little stomatal control is induced during periods of high evaporative demand. It would be beneficial to conduct similar studies under hotter and drier conditions, such as in the Northern Cape where most of the pecans are planted in South Africa, to observe if the statement holds true.



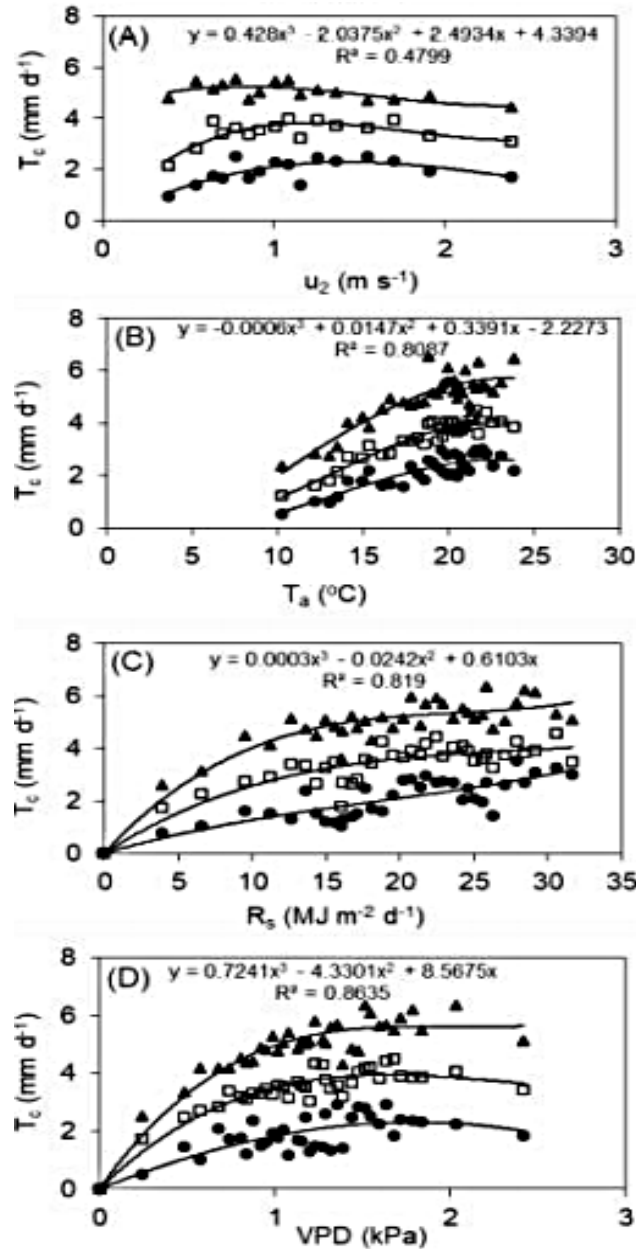


**Figure 2.3** Daily pecan transpiration ( $T_c$ ) as influenced by A) wind speed ( $u_2$ ), B) air temperature ( $T_a$ ), C) solar radiation ( $R_s$ ), and D) vapor pressure deficit (VPD). The black circles represents 0.1 of the regression quantiles, the open squares 0.5 and the black triangles 0.9 (Ibraimo, 2018).

As with many other woody tree crops, photosynthesis (A), stomatal conductance ( $g_s$ ) and  $T_c$  have all been observed to decrease in pecan in response to high vapor pressure deficits and low soil water potential, suggesting stomatal control over  $T_c$  (Kallestad et al., 2012; Mielke, 1981; Rieger and Daniell, 1988). This reaction of pecan to environmental stimulus by stomatal aperture, that influences the water potential gradient and therefore  $T_c$  stream, has been studied by Steinberg et al., (1990) that found a linear relationship between decreased leaf water potential and increased



sap flow rates in pecan trees. However, the degree of  $T_c$  reaction towards prevailing atmospheric conditions as a result of the daily fluctuation of aerodynamic and bulk canopy conductance (also termed decoupling coefficient- $\Omega$ ) could also help to explain the mechanism of crop water use.

Ibraimo (2018) was able to demonstrate that pecan trees exhibit relatively low values for the decoupling coefficient ( $\Omega$ ), which varied between 0.08 and 0.28. This suggests that pecan  $T_c$  is largely coupled to the atmosphere and will respond to bulk VPD, with a fractional change in  $g_s$  leading to an equivalent change in  $T_c$  (Ibraimo, 2018). This is typical of most tall, rough crops, where vigorous mixing of air above the canopy results in high aerodynamic conductance and low  $\Omega$  values (Ibraimo, 2018; Jarvis and McNaughton, 1986).

### 2.1.3 Whole-tree hydraulic flow

The hydraulic flow that exists due to the movement of water from the soil to the plant and then into the atmosphere, as a result of a water potential gradient, can be described as a true continuum (Arora et al., 1992). One of the greatest constraints to the continuum exists in the leaf; through the leaf xylem, as well as the pathway across the mesophyll to the site where evaporation takes place (Goldsmith, 2013 ; Jarvis, 1998; Rodríguez-Gamir, 2016). The amount of resistance within this continuum will vary greatly between various species, as well as within a single species as certain cultural practices dictate the extent of resistance through various rootstocks, root densities and the length of the roots, tree height and branch length, presence of certain pests, persistent waterlogging conditions and unfavorable soil temperatures (Jones et al., 1985; Ryan and Yoder, 1997). These factors all contribute to the hydraulic flow resistance, which impact plant water status and leaf water potential by determining the rate at which water can be transported from the roots to the site of evaporation in the leaves. Stomata play an important role in regulating leaf water potential and ensuring that the hydraulic capabilities of the plant are not exceeded (Sperry, 2000).

A study done by Tsuda and Tyree (2000) in crop plants (soybean, sunflower, kidney bean, tomato, green pepper, eggplant) found that maximum  $T_c$  rates can be attributed to maximum values of whole plant hydraulic conductance. The same tendency was found by Rodríguez-Gamir et al., (2016) in citrus trees where the regulation of  $T_c$  was not solely as a result of stomatal aperture, but also between  $T_c$  and whole-plant hydraulic conductance. The study by Domec et al., (2009) suggested that the hydraulic conductance of different plant organs have the ability to dictate plant water status by influencing stomatal aperture in response to VPD. Therefore, there exists a link between the hydraulic conductance of the leaf, shoot, stems or roots with  $T_c$  (Nardini and Salleo,

2000; Rodríguez-Gamir et al., 2010; Sack et al., 2003; Yang and Tyree, 1993). The studies conducted by Kallestad et al., (2012), Steinberg et al., (1990) and Othman et al., (2014) investigated whole tree water relations and stomatal conductance on an hourly level, providing insights into the diurnal patterns of these parameters on a relatively short time scale. By quantifying sap flow and canopy transpiration (Figure 2.4), Steinberg et al., (1990) was able to show that there was no pronounced lag between sap flow and canopy transpiration, suggesting limited capacitance in a 5-year-old tree and that root uptake was able to match transpiration ( $T_c$ ).

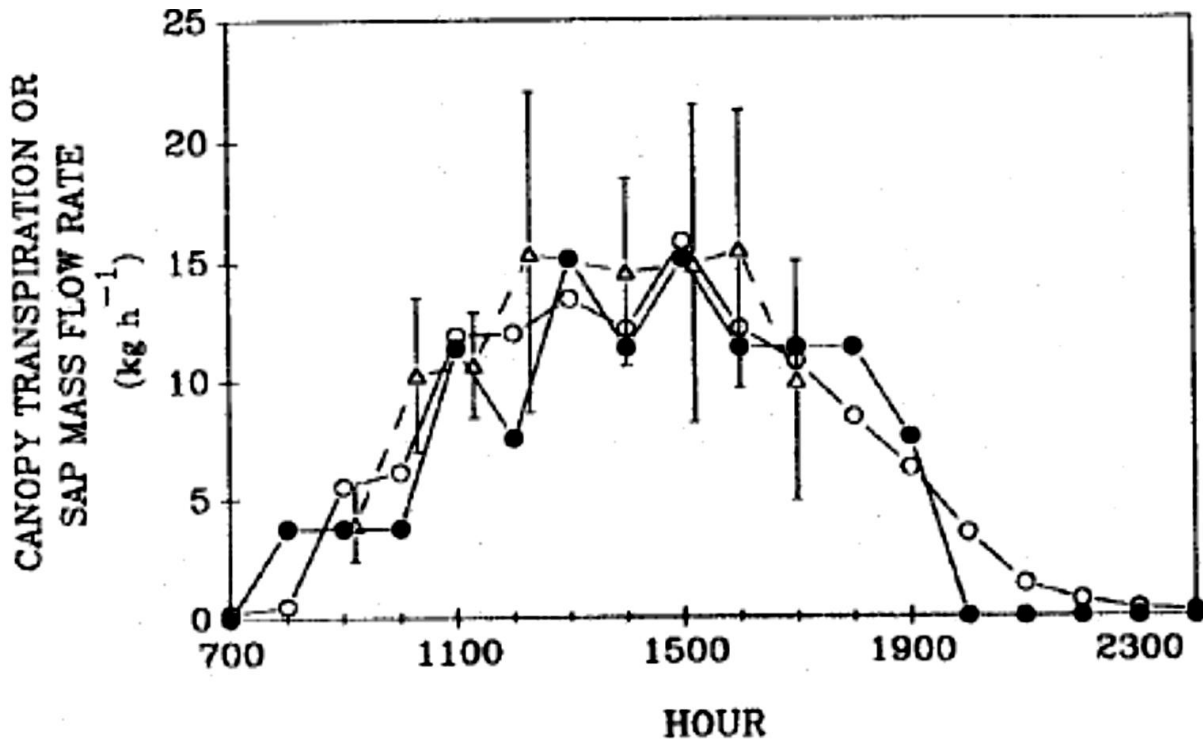


Figure 2.4 Measured (•) and calculated (Δ) canopy transpiration and trunk sap flow (o) from 07hoo until 24hoo (Steinberg et al., 1990).

#### 2.1.4 Pecan tree response to soil water availability

Pecan trees are very sensitive to the soil water content and can have variable responses to irrigation depending on the soil type, which influences the water holding capacity (Deb et al., 2012; Wells, 2015). Pecans are most productive when irrigated on well drained soils, when the water table has dropped beyond the root zone (Sparks, 2005). The study by Sparks (2005) confirmed that trees subjected to no irrigation on well-drained soils, were more productive than trees irrigated whilst the water table was present in the root zone. This phenomenon is quite important to consider when irrigating, as pecan trees have a high-water requirement but do not tolerate waterlogged conditions, stressing the necessity for sensible water application. Results from

Heaton et al., (1982) and Garrot et al., (1993) showed that not only yield per tree was increased by irrigation, but also nut weight, nut fill and oil content. It is therefore important to produce pecans under non-stressed conditions to obtain good quality yields (Kilby, 1980). The study by Smith and Ager (1988) found that net CO<sub>2</sub> assimilation for photosynthesis ( $A$ ) in flooded pecan seedlings was reduced by both stomatal and non-stomatal limitations, whereby this reduction continued for 14 days after waterlogged conditions where alleviated. In mature trees, Kallestad et al., (2012) also reported a decrease in  $A$ ,  $g_s$  and  $T_c$  in response to flooding. These authors also reported an increase in internal CO<sub>2</sub> concentration ( $C_i$ ), which supported depressed photosynthetic rates.

It is therefore favorable to maintain adequate soil water as it allows the maintenance of conducive conditions for hydraulic conductance and prevents a decline in  $A$ ,  $g_s$  and  $T_c$ , provided optimal environmental conditions. Deb et al., (2012) developed a simple model for the prediction of  $\Psi_{stem}$  and  $\Psi_{leaf}$  using soil water content, in combination with midday air temperature. This model, provided good estimates, provided measurements of soil water content combined with air temperature are available, and could be used for irrigation scheduling. This relationship was further evaluated by Wells (2015) who found a positive linear relationship between volumetric soil water content ( $\Theta$ ) and  $\Psi_{stem}$ , except during the kernel filling stage, when high crop loads can induce water stress regardless of adequate soil moisture. Ibraimo (2018) also determined that  $\Theta$  correlates with pecan  $T_c$ , as pecans tree  $T_c$  increased as  $\Theta$  increased, up until 0.32 m m<sup>-3</sup>, whereafter  $T_c$  started to decline with increasing  $\Theta$ .

## 2.2 Pecan water use

The majority of research on water use of pecan orchards has been conducted in the U.S.A (Miyamoto, 1983; Miyamoto, 1989; Samani et al., 2011; Sammis et al., 2004). However, as the climatic conditions of the pecan growing regions in the U.S.A differ to those in South Africa, the latter classified as more arid achieving higher  $ET_o$  values during certain seasons, is it important to conduct water research in South Africa, where only one study has been previously published (Ibraimo et al., 2016). This study was performed near Cullinan, Gauteng, which is cooler than the most important pecan production areas in the Northern Cape province (Hartswater, Prieska, Upington). This has implications for length of the growing season and atmospheric evaporative demand, therefore total seasonal water use of most orchards in South Africa. This section therefore focuses on the available pecan water use literature to highlight the importance of conducting studies in various regions and the validation of an appropriate model able to extrapolate gathered data to other regions.

### 2.2.1 Pecan water use

Water use of orchards can be defined as total evaporation or evapotranspiration (ET) and includes transpiration ( $T_c$ ) from trees and cover crops and evaporation ( $E_s$ ) from the soil. Transpiration from cover crops will not be considered within this study. The determination of water use and irrigation management practices is based on the ET loss of water from the orchard (Miyamoto et al., 1995). The quantification of pecan ET has been done using various techniques such as the soil water balance technique (Miyamoto, 1983), Eddy Covariance and Remote Sensing (Samani et al., 2011), in a range of orchards with different canopy covers, as seen in Table 2.1.

**Table 2.1 Evapotranspiration of pecan orchards reported in literature.  $f_c$  is fractional canopy cover, ET is evapotranspiration and T is transpiration.**

Tree age (years)	$f_{cMax}$ (%)	ET/ T			Measurement method	Irrigation method	Climate	Reference
		Annual <sub>Total</sub> (mm)	Day <sub>Max</sub> (mm)	Day <sub>Max</sub> (L)				
5		ET = 530			Soil water balance	Flood	Arid, desert	Miyamoto (1990)
10		ET = 760			Soil water balance	Flood	Arid, desert	Miyamoto (1990)
15		ET = 920			Soil water balance	Flood	Arid, desert	Miyamoto (1990)
20		ET = 1040			Soil water balance	Flood	Arid, desert	Miyamoto (1990)
25		ET = 1160			Soil water balance	Flood	Arid, desert	Miyamoto (1990)
30	65 – 70	ET = 1420	ET = 9	ET = 800	Eddy covariance	Flood	Arid, desert	Sammis et al., (2004)
40-65 <sup>#</sup>		ET = 1479			Eddy covariance	Flood	Arid, desert	Bawazir and King (2004)
2-35 (16 orchards)	3-70%	*ET=0.5 5-8.4 mm day <sup>-1</sup>			Eddy covariance and Remote sensing	Flood	Arid, desert	Wang et al. (2007b)
Varying (279 orchards)	2.5-80	ET = 413-1095			Remote sensing	Flood	Arid, desert	Samani et al. (2009a)
35		**ET= 1035 T= 846	T= 7.1	T=500	Sap flow and modelled E	Micro-sprinkler	Semi-arid, subtropical	Ibraimo et al., (2016)
36		ET=985 T= 888			Sap flow and modelled E	Micro-sprinkler	Semi-arid, subtropical	Ibraimo et al., (2016)
37		ET= 1050 T= 861			Sap flow and modelled E	Micro-sprinkler	Semi-arid, subtropical	Ibraimo et al., (2016)

#mixed age orchard

\*Annual or seasonal estimates were not reported

\*\*Seasonal ET (only when the trees were in leaf)

Studies conducted in New Mexico report that annual ET of mature, flood-irrigated pecan orchards varied between 1040 and 1448 mm (Bawazir and King, 2004; Miyamoto, 1983; Miyamoto, 1989; Samani et al., 2009b; Sammis et al., 2004), whilst seasonal ET varied between 1170 and 1370 mm (Bawazir and King, 2004; Samani et al., 2009b; Sammis et al., 2004) (Table 2.1). Annual ET includes the period when the trees are leafless in winter, whilst seasonal ET only includes the period when the trees are in leaf, referred to as the growing season. The difference between the two values reflects soil evaporation during the winter months. These orchards were all flood irrigated and situated in an arid desert environment.

The published study of pecan water use in South Africa was conducted by Ibraimo et al., (2016) in Cullinan, South-Africa on the cultivar 'Choctaw' grafted onto 'Barton' rootstocks. The study was conducted over three seasons in a 22-ha commercial orchard of mixed cultivars, which was 34 years old at the start of the study. Trees were planted in a triangular pattern spaced 9 m x 9 m x 9 m apart, along an N-NE to S-SW axis. Seasonal water use varied between 985 mm and 1050 mm over the course of the study, as seen in Table 2.1. The seasonal average ET was 1023 mm season<sup>-1</sup>, which was lower than seasonal ET obtained by Miyamoto (1983), Sammis et al., (2004) and Samani et al., (2011) in New Mexico of between 1170 and 1370 mm. When comparing daily water use over the season between New Mexico and Cullinan, differences were noted at the beginning and end of the season, which were most likely related to the rate of canopy development at the start of the season and rate of senescence at the end of the season, both of which are related to temperature.

The differences in water use between the different studies may be due to various factors including tree age, tree size, cultivar and rootstock differences, planting density, atmospheric evaporative demand and different climatic conditions (Miyamoto, 1983; Wang et al., 2007c). Importantly, none of the studies in New Mexico quantified  $T_c$  and  $E_s$  separately. This becomes increasingly important when modelling water use of orchards, with different irrigation systems and different canopy management strategies (Kool et al., 2014). It also allows the differentiation between beneficial consumptive water use and non-beneficial consumptive use, which is becoming a greater priority as pressure is increasing on the agricultural sector to use water more efficiently. Besides the study of Ibraimo et al., (2016), there are only two other studies where the transpiration of pecan trees was determined (Sorensen et al., 1999; Steinberg et al., 1990). Steinberg et al., (1990) evaluated trunk flow gauges on two 5 year old pecan trees planted on weighing lysimeters in Texas, whilst Sorensen et al., (1999) tested heat pulse needles in 15-20 year old trees in Las Cruces, New Mexico. Very limited data is available from these two studies because only 12 days of data was

collected from the trunk flow gauges, whilst, Sorensen et al., (1999) concluded that the needles did not precisely measure transpiration. Summer transpiration rates (August in the Northern Hemisphere) were between 100 to 150 L tree<sup>-1</sup> day<sup>-1</sup> in the 5-year-old tree. In the study by Taylor and Gush (2014) typical daily average tree transpiration for a 37 year old 'Choctaw' pecan varied during the growing season from a minimum of 100 L day<sup>-1</sup> (1.4 mm day<sup>-1</sup>) to a maximum of between 400 and 500 L day<sup>-1</sup> (5.7 to 7.1 mm day<sup>-1</sup>) (Table 2.1). Transpiration varied throughout the season as affected by changes in canopy size, typical of deciduous species, and ET<sub>o</sub> or evaporative demand. Average daily water use during spring was 217 L day<sup>-1</sup> (3.1 mm day<sup>-1</sup>), in summer 278 L day<sup>-1</sup> (3.97 mm day<sup>-1</sup>) and in autumn 246 L day<sup>-1</sup> (3.51 mm day<sup>-1</sup>). Over the course of season, and even the plants lifespan, the total canopy T<sub>c</sub> is governed by the leaf area (m<sup>2</sup>) that is present per ground area that is covered by the canopy (m<sup>2</sup> ground cover) and is referred to as the leaf area index (LAI) (Granier et al., 2000). Importantly, different amounts of LAI lead to differences in g<sub>c</sub> and T<sub>c</sub> (Ibraimo, 2018). That said, measurement of canopy size becomes a crucial determinant of seasonal T<sub>c</sub>, for instance large canopies (LAI > 6 m<sup>2</sup> m<sup>-2</sup>) have greater contribution of shaded leaves that lowers g<sub>c</sub> and therefore help maintain T<sub>c</sub> even if conditions on the outside of the canopy are not conducive for T<sub>c</sub> to occur (Granier et al., 2000). In small canopies (LAI < 6 m<sup>2</sup> m<sup>-2</sup>) the changes that occur in g<sub>c</sub> and in T<sub>c</sub> are much more pronounced as LAI fluctuates throughout the season (Ayars et al., 1999; Goodwin et al., 2006).

Variation in fractional canopy cover can also be a result of differences in tree spacing and pruning strategy, which causes large variation in reported ET for mature pecans is mostly attributed to differences in tree spacing and pruning strategies, which result in variations in fractional canopy cover (Wang et al., 2007c). The work of Samani et al., (2011) clearly shows the dependency of ET on canopy cover and the large variation in ET for a single production region, as seen in Figure 2.5. Seasonal ET of the 279 orchards measured varied from 413 to 1095 mm, whilst annual ET varied between 771 and 1259 mm. What is clear from the analysis of measurements of pecan ET is that values are highly variable between different orchards and even between years in the same orchard. Therefore, to make this information useful for several different growing areas and even for different years for the same orchard, it is important to model water use.

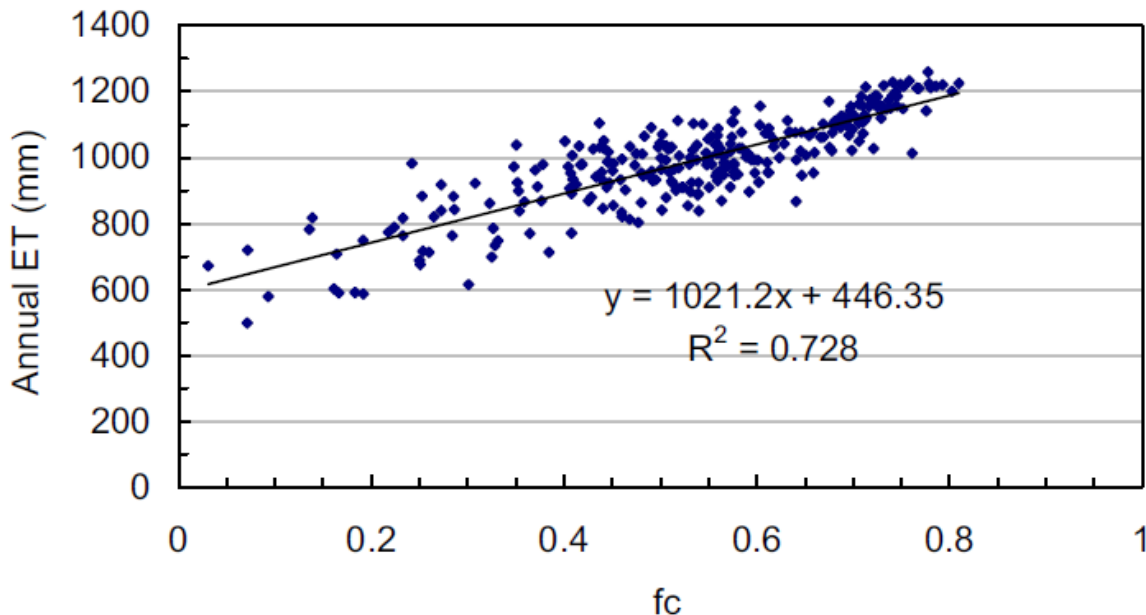


**Figure 2.5 Relationship between annual pecan ET and fractional cover for 279 orchards in New Mexico’s Lower Rio Grande valley. ET was estimated using a regional ET estimation model (Samani et al., 2011).**

### 2.2.2 Soil evaporation

Soil evaporation is a key component in the hydrological cycle with the capacity to consume almost 25% of incoming solar radiation, making its contribution globally significant, as well within orchards where canopy cover is sparse (Trenberth et al., 2009). In general, the evaporative flux that occurs is relatively low, but the amount of change that occurs within the media is more significant and resembles a complex chain of dynamic processes (Or et al., 2013). The complexity of evaporation is as a result of dissimilar drying patterns and the incoherent rearrangement of the remaining water within the soil pores (Or et al., 2013). For evaporation to occur from the soil surface, certain forces or gradients should act upon it in order to drive the process. The atmosphere acts as a continuous and almost unlimited vapor sink leading to the creation of a strong gradient for evaporation to occur (Miyamoto, 1989). The resulting evaporative flux is largely controlled by 1) the amount of energy supplied to facilitate the change of water from the liquid to the vapor phase, which is maintained by internal capillary flow (Figure 2.6), 2) internal restrictions to limit the amount of water in the evaporation zone after considerable amount of mass loss has occurred, marking the onset of the transition period to diffusion-limited vapor transport (Figure 2.7), 3) the degree of vapor movement through the permeable medium into the atmosphere after diffusing through a partly dried permeable medium and the vapor sink, which is the immediate air



boundary layer adjacent to the soil surface (Allen et al., 2005; Lehmann et al., 2008; Schlünder, 1988; Shahraeeni et al., 2012; Suzuki and Maeda, 1968; Yiotis et al., 2010).

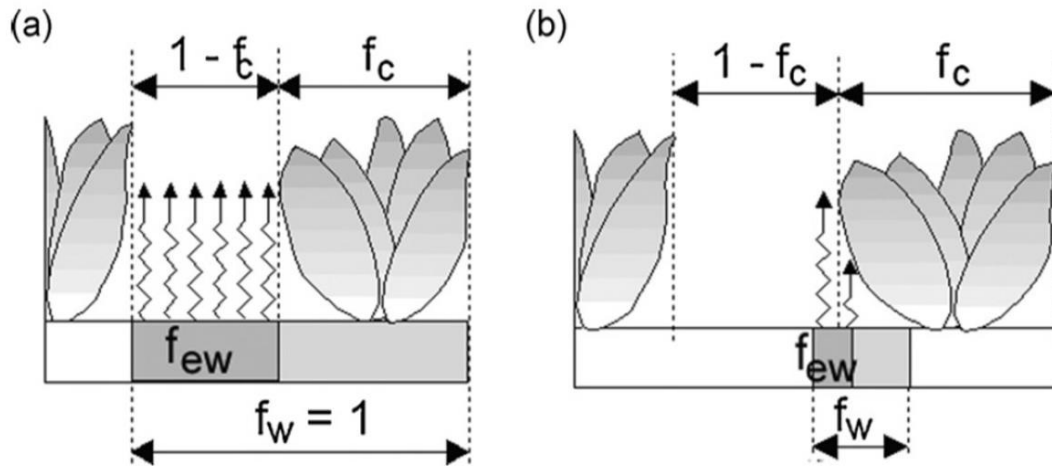


Figure 2.6 Relating the amount of energy available for A) the fractions of soil covered by vegetation, wetted and exposed and wetted (fraction of soil covered by vegetation ( $f_c$ ), fraction of soil wetted by rain or irrigation ( $f_w$ ), fraction of soil that is both exposed and wetted ( $f_{ew}$ ), and exposed soil fraction ( $1-f_c$ )) for a partial cover crop when the wetting results from precipitation or B) from irrigation that only wets a fraction of the soil surface (Allen et al., 2005).

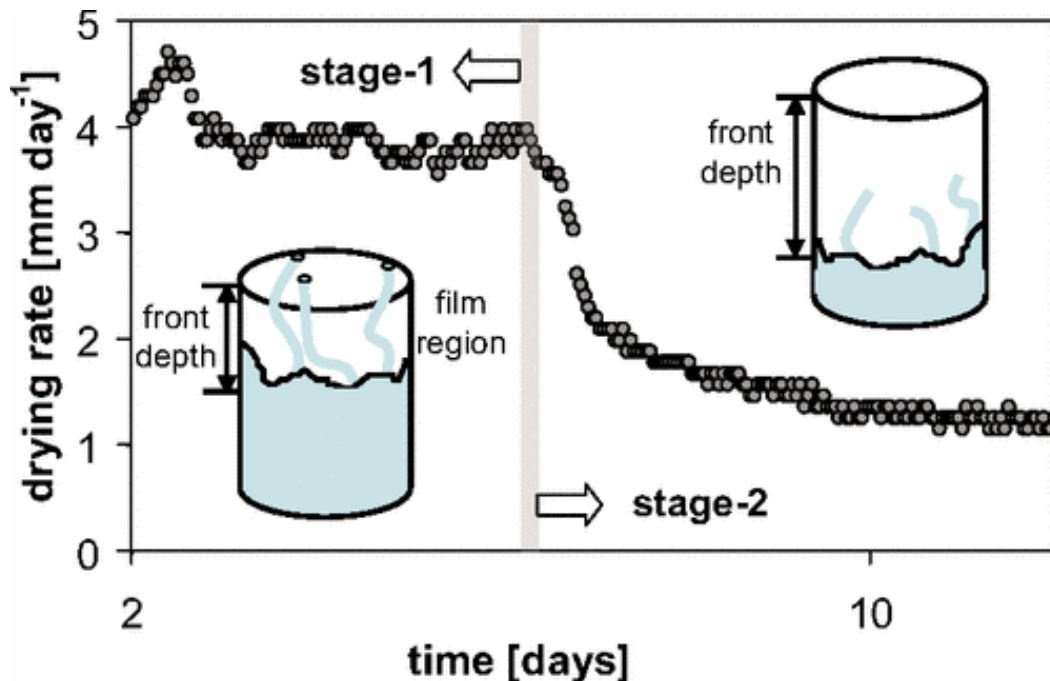


Figure 2.7 Evaporation simulation from a wetted sand column to represent Stage 1 which is governed by capillary flow to the zone of evaporation and Stage 2, which is governed by vapor diffusion (Lehmann et al., 2008).

Inherent soil properties and internal regulation processes have a significant impact on evaporation when energy is not limiting. It is clear that evaporation exists as a result of the concentration gradient created between the surface level of a saturated body of water in the soil and the vapor depleted air. As the water level depletes, air replaces its position according to the pore size and the capillary force needed to occupy the pore space, primarily the larger pores being occupied first (Or et al., 2013). The capillary force at the surface of the declining front, into the previously wetted permeable medium, remains fairly constant as the air enters (Shokri et al., 2010). The rate of evaporation occurs at a very slow pace under most natural conditions, leading to the conclusion that the liquid distribution above the surface of the declining front is near hydrostatic equilibrium (Shokri et al., 2008). For stage 1 evaporation to hold true the declining front should be connected with a continuous supply of water that is able to satisfy evaporative flux demand through viscous flow (Or et al., 2013). As the evaporative flux continues driving the declining front deeper into the soil, the accompanying capillary force has to keep up with the demand by driving capillary flow from a deeper in the pores causing an increasingly negative force, up until a critical value is met where the declining front is replaced by air or the capillary connectivity is interrupted (Lehmann et al., 2008). This series of events will indicate that Stage 1 evaporation is finished.

The invasion of air into capillary pores, marks the onset of Stage 2 evaporation which is diffusion controlled. The receding front, now the second drying front, moves into the permeable medium forming another evaporation plane from which the water can diffuse, across the gradient of drier air at the surface into the atmosphere (Saravanapavan and Salvucci, 2000; Yamanaka et al., 1998; Yamanaka et al., 1997). The two drying fronts exist simultaneously and remain linked hydraulically through capillary-induced liquid flow. During stage 2 the process of capillary flow and evaporation occurs across the gradient into the atmosphere, occurring at the same time, where the liquid movement occurs from the primary to the secondary front where vapor diffusion occurs (Or et al., 2013). From the study by Shokri and Or (2011), it was concluded that the rate of evaporation, after onset of Stage 2, is not dependent on the rate at which stage 1 occurred and remains fairly constant over a range of different permeable media types and boundary layer conditions. Permeable media with different pore size distribution throughout dissimilarly stacked layers will have a pronounced effect on the liquid phase distribution and subsequently on evaporation (Ceaglske and Hougen, 1937; Willis, 1960). The permeable media contains certain transport properties that have a greater role than atmospheric conditions to govern the rate of evaporation at the onset of stage 2, but the atmosphere affects the transition dynamics occurring from stage 1 to stage 2 (Or et al., 2013). In order to limit evaporation, mulches can be used to act as an evaporation suppression mechanism, given that mulches contain pores that are larger than

the underlying layer (Mellouli et al., 2000; Or et al., 2013). The high variability in  $E_s$  in different orchards and across a season suggests the need that  $E_s$  should be modelled separately from transpiration. Through such a model a grower has the opportunity to test the implementation of strategies that would reduce non-beneficial consumptive water losses, for example the application of a mulch within the wetted zone (Ibraimo, 2018). Furthermore, by parametrising an accurate  $E_s$  model a more robust daily ET estimate can be determined, which could lead to improved irrigation scheduling in pecan orchards.

### 2.2.3 Water use efficiency and water use productivity

As previously stated pecans are reported to require a large amount of water, greater than that of other row crops, with ET exceeding 1000 mm for the growing season for mature pecan trees (Bawazir and King, 2004; Ibraimo et al., 2016; Miyamoto, 1983; Samani et al., 2009b; Sammis et al., 2004). This poses a problem in a semi-arid country, such as South-Africa, which is characterized by sporadic and unpredictable rainfall patterns. Therefore, the need exists to conceptualize the WUE of pecan trees in order to utilize the allocated water as efficiently as possible and to allow the benchmarking of growers. There are many definitions of WUE depending on the subject of interest ((Fernández et al., 2020). However, there are four general accepted definitions of WUE;

- 1 Total dry matter per unit evapotranspiration (ET) ( $\text{kg m}^{-3}$ ) (Begg and Turner, 1976).
- 2 Total dry matter per unit of evapotranspiration (ET) ( $\text{t ha}^{-1} \text{m}^{-3}$ ) (Jensen et al., 1980).
- 3 Total photosynthesis per unit transpiration ( $\text{mgCO}_2 \text{gH}_2\text{O}^{-1}$ ) (Sinclair et al., 1984).
- 4 Total yield per unit evapotranspiration ( $\text{kg m}^{-3}$ ) (Evans, 1976a).

For the purpose of this study, the WUE definition; described by Evans (1976b) will be used, as the yield is the economically valuable part of the tree. The WUE will be calculated as;

$$\mathbf{WUE} = \frac{\mathbf{yield}}{\mathbf{ET}} \quad (1)$$

where yield is defined as kg nuts harvested per ha and ET defined as the measured total evapotranspiration of the orchard in  $\text{m}^3$  per ha. The units used will therefore be  $\text{kg m}^{-3}$ . It is important to consider the definition used as WUE estimates can vary by a factor of 10 depending on what portion of the crop is studied (Wang et al., 2007a) and how the denominator is determined.

In ‘Western Schley’ pecans Wang et al., (2007a) found that WUE, using nut dry mass, differed between alternating years, where in “on” years WUE was  $0.262 \text{ kg m}^{-3}$  compared to  $0.149 \text{ kg m}^{-3}$  in “off” years. In “on” years 13.8% of dry matter production was allocated to harvestable fruit compared to only 8% in “off” years (Wang et al., 2007a). Wang et al., (2007a) attempted to estimate WUE based on ET per unit of dry mass produced over the course of a season, which was determined using a physiological model for estimating biomass accumulation of the whole tree. This provides useful insight into how WUE differs during different phenological stages and how it is influenced by VPD (Figure 2.8). Water use efficiency was high at the start and end of the season due mainly to low ET fluxes as a result of low VPD (Figure 2.8A). The influence of VPD on WUE is clearly illustrated in Figure 2.8B and needs to be considered when comparing WUE from different regions. One might have also expected lower water use efficiency near the end of the season during nut filling, as this is a very energy expensive process. These authors also estimate that 25-35% of the total seasonal tree growth was in the roots, which represents a significant sink for carbohydrates.

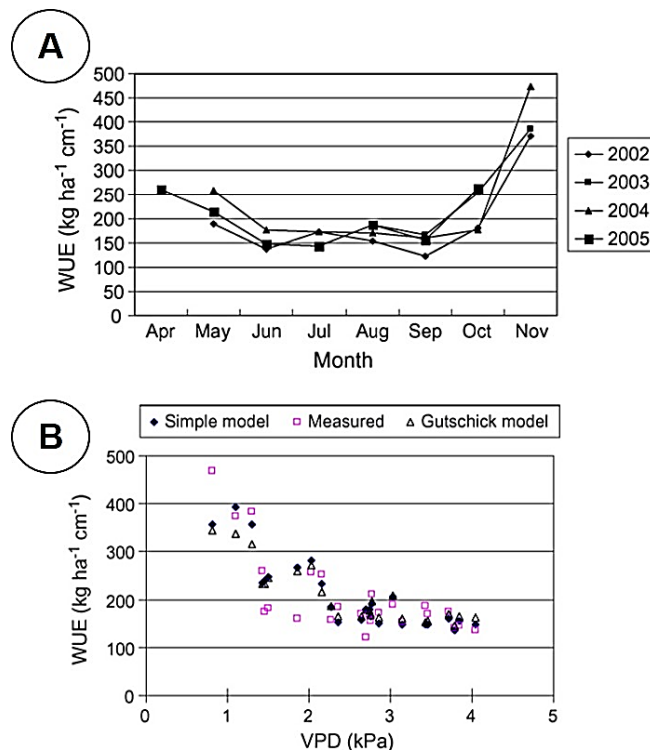


**Figure 2.8 A) Monthly values of water use efficiency (WUE) of pecan trees (Biomass/ET) and B) the impact of VPD on monthly measured and predicted water use efficiency (WUE) for pecan trees near Las Cruces in New Mexico (Wang et al., 2007a).**

Water use efficiency figures for mature pecan orchards were comparable for New Mexico in Texas, USA and Cullinan in South Africa, varying between  $0.15 \text{ kg m}^{-3}$  to  $0.31 \text{ kg m}^{-3}$  (Ibraimo et

al., 2016; Sammis et al., 2004). Miyamoto (1983) suggested WUE (yield/ET) of 'Western Schley' pecans in the El Paso Valley in Texas to be approximately  $0.25 \text{ kg m}^{-3}$  in a wet year and between  $0.27$  and  $0.303 \text{ kg m}^{-3}$  in a moist year. In a two year study by Sammis et al., (2004), a WUE of  $0.18 \text{ kg m}^{-3}$  was determined in an 'off year' and  $0.31 \text{ kg m}^{-3}$  in an 'on year' near Las Cruces, which is comparable to the study by Wang et al., (2007a) as previously mentioned. In the three-year study in Cullinan, WUE was  $0.15 \text{ kg m}^{-3}$  in an 'off year' and  $0.26 \text{ kg m}^{-3}$  in an 'on year' for 'Choctaw'. Water use efficiency needs to be determined for the hotter and drier production regions of South Africa, where higher yields are obtained, but where water use may also be higher. More water will be needed to produce a crop in areas with high evaporative demand.

The accepted WUE definition, mentioned above, differs from the original WUE interpretation where canopy transpiration ( $T_c$ ) was used as primary determinant of crop water use (Begg and Turner, 1976). Its use was limited due to overestimation of WUE values as a result of the T component being less than total ET, skewing the ratio to increase the WUE, especially at the onset of the season when the soil evaporation ( $E_s$ ) component is larger (Begg and Turner, 1976). It could, however, be used as direct comparison for pecan trees at different locations, as it will allow the comparison of the effect of climate on  $T_c$ . It also reduces the impact of variable  $E_s$  rates which are influenced greatly by water availability, for example irrigation method, which will differ across regions depending on grower practices and water conservation techniques (Sinclair et al., 1984). The WUE with T as primary water use component (TWUE) will be determined as;

$$\text{TWUE} = \frac{\text{yield}}{T} \quad (2)$$

where yield is defined as the  $\text{kg ha}^{-1}$  and T defined as the measured transpiration of the orchard in  $\text{m}^3 \text{ ha}^{-1}$ .

It is economically favorable to produce crops with high WUE, especially under conditions of limited water supply (Sammis et al., 2004). Pecan trees have very low WUE, comparable to cotton and fruit tree crops such as apples and citrus, as determined by Sammis et al., (2004) to be  $0.19 \text{ kg ha}^{-1} \text{ m}^{-3}$  based on the total yield per unit evapotranspiration (ET). Water use productivity calculations are very important for a crop such as pecan, as yields are low ( $1500\text{-}4000 \text{ kg ha}^{-1}$ , the nut is rich in oil, low in water content and has a thick, protective shell) and water use is quite high. However, when the economic value of the crop is considered, it may compare much more favorably to these crops. This can be defined as water use productivity (WUP) which will be calculated as;

$$WUP = \frac{R}{m^3} \quad (3)$$

WUP is defined as the monetary value of the crop and will take into consideration the quality of the nuts and how it relates to the price of the product. The units for WUP will be R m<sup>-3</sup>. There are no reports of water use productivity for pecans. This will also vary from year to year based on supply and demand pricing of nuts in 'on' and 'off' years.

As previously stated, areas characterized by low rainfall events require supplemental irrigation to meet the crops high water demand. It is therefore important to also define the irrigation water use efficiency (IWUE) which is the ratio between the harvested crop yield and the total water applied (irrigation + rainfall) (kg m<sup>-3</sup>) (Howell, 1994). Irrigation water use efficiency encompasses a wide range of factors which include; soil characteristics, type of crop, cultural and management practices, canopy interception and drainage water loss (Sammis et al., 2004). It would be beneficial for the farmer to increase IWUE as this will lead to increased profits. This can be accomplished through irrigation scheduling based on a quantitative measures, such as measuring soil water potential or plant based measurements, such as the crop water stress index (Garrot et al., 1993; Sammis et al., 2004). The measured IWUE is higher for irrigation systems that have less surface evaporation, which is a result of the surface wetting pattern of the irrigation system, therefore surface and subsurface systems have higher IWUE (0.235-1.27 kg m<sup>-3</sup> and 0.283-2.27 kg m<sup>-3</sup> respectively) than micro-sprinklers or furrow irrigation (0.044-0.659 kg m<sup>-3</sup> and 0.086-0.56 kg m<sup>-3</sup> respectively) (Sammis, 1980). Irrigation water use efficiency of pecans are also highly dependable on the alternate bearing cycle, where it increases in "on" years, because of higher yields per amount of water used, and decreases in "off" years, because of lower yields for a similar amount of water used as during "on" years (Sammis et al., 2004). Pecan IWUE was estimated at 0.016 kg m<sup>-3</sup> on average and is quite low when compared to other crops (Sammis et al., 2004).

#### 2.2.4 Measurement of crop water use

There are a number of methods available to estimate orchard water use, but the suitability of these methods depends on the crop, as well as the nature of the study. Each method has advantages and disadvantages associated with accuracy, installation and use, equipment availability, data acquisition and analysis, cost, user friendliness, power requirements and upkeep. Some techniques may also be more suited than others for certain situations, e.g. equipment that needs more maintenance should not be used in remote locations or complex equipment should not be used by novice operators as it causes considerable increase in error, as seen for sap flow measurement where user associated error can vary between 40 and 200% (Allen et al., 2011a). Techniques used to measure evapotranspiration (ET) include



micrometeorological methods (Bowen ratio, scintillometry and eddy covariance) or soil water balances (lysimeters or soil water content measurements) (Allen et al., 2011c).

A lysimeter is an apparatus where a representative soil sample is placed within a tank along with the study plant, from which the ET measurement should be made, and suspended above a weighing mechanism that measures the change in weight as water evaporates and is transpired by the plant (Allen et al., 2011c). The change in mass correlates with water loss (ET), after accounting for potential other losses such as drainage and run-off, and gains such as precipitation, and is considered one of the most accurate ET measurements over short periods. However, lysimeter measurements are point measurements (area between 0.05-40 m<sup>2</sup>) and these measurements are often extrapolated to determine ET for large areas. If the vegetative and environmental conditions of the lysimeter do not closely represent those of the larger field, then substantial errors in the estimation of ET of the larger area can result. It is therefore important that the lysimeter must be surrounded by the same vegetation that is in the lysimeter and the lysimeter should not be close to the edge of the field. Another common cause of lysimeter error is termed the 'bloom effect', where the effective area of the lysimeter is exceeded by a larger plant canopy. This method will not be suitable for pecan ET measurement as mature trees are much larger than most other fruit tree crops, meaning that a large lysimeter will be required to maintain representativeness. This could lead to errors in the soil profile (density, structure, layers) as well as rooting characteristics (Allen et al., 2011c; Sparks, 2005) and would therefore be impractical. Other ET measurement methods that are non-destructive would be more appropriate, such as use micrometeorological techniques (Bowen ratio, scintillometers, and Eddy covariance). These techniques vary in their suitability depending on the type and amount of equipment installed, as well as evaluating criteria. For all three of these micrometeorological methods equipment should be installed above the canopy to achieve sufficient fetch and limit the effect of individual trees on roughness elements, which can cause problems with installation and maintenance in tall crops, such as pecan (Allen et al., 2011b).

The Bowen ratio is a sensible, trustworthy and an automated micrometeorological measurement whereby it solves the energy balance equation by determining air temperature and vapor pressure gradients in the surface layer above the evaporating surface and performs best under non-limiting soil water conditions (Bowen, 1926). The method requires adequate upwind fetch to ensure there is an equilibrium boundary layer where air temperature and vapor gradients are constant across the horizontal plane and this often limits where this method can be used (Allen et al., 2011c). It further relies greatly on accurate and representative measurements of solar radiation ( $R_n$ ) and

soil heat flux ( $G$ ) which can be problematic under sparse and dissimilar canopy conditions, which could create potential problems in pecan orchards which have discontinuous canopies and are deciduous in nature (Sparks, 2005). As a result of the sparse canopy conditions multiple net radiometers and soil heat flux locations will be required, which is difficult to maintain in a production orchard which are located far from researchers and where farming equipment needs to routinely move through the orchard rows.

Scintillometry is where an optical apparatus is able to determine variations in air density caused by changes in temperature, humidity and pressure by measuring small fluctuations in the refractive index of air (Allen et al., 2011c). It operates by measuring sensible heat flux ( $H$ ) in the area between the transmitter and receiver (placed on opposite end of the study area). The receiver will determine scintillations, which is the magnitude of the variations in the transmitted signal (Allen et al., 2011c). The advantage of this technique is that it can measure  $H$  fluxes over a large area. However, this technique has the same constraints as the Bowen ratio method, whereby it relies on multiple and representative  $R_n$  and  $H$  measurements and is also quite expensive. Installing the equipment above tall orchards on relatively flat ground can also create problems with proper alignment of the transmitter and receiver.

The Eddy covariance method has the ability to estimate  $ET$ , through separate estimation of  $T_c$  and derived  $E_s$ . It also has a few drawbacks; such as the high amount of corrections that is needed to determine precise values of crop  $ET$ , the extent of error varies between 10 – 30% in energy balance closure determination, it needs a large amount of fetch, continuous changes in wind direction can increase errors, certain parts of the equipment are very fragile and needs experienced personnel to install, work and maintain it (Allen et al., 2011c). However, the eddy covariance system is still an accurate measuring tool of crop  $ET$ , given the elementary requirements of this system is met such as; knowledge and experienced personnel with a proper understanding of turbulence physics, adjusting the flux measurements correctly, obtaining sufficient fetch, placement of instruments above the crop canopies in order to reduce roughness sub-layer distortions and thereby enhancing the eddy size to equal sensor path length (Allen et al., 2011c).

The Eddy covariance method has become a popular method to estimate  $ET$  as it is easy to set up and it is possible to measure  $H$ , latent heat ( $LE$ ) and  $CO_2$  fluxes with high speed and frequency. The method is an atmospheric measurement that works by determining the statistical correlation or covariance between fluxes of vapor or  $H$  within up-and-downward columns of turbulent eddies, and requires high frequency sampling (Allen et al., 2011c). A direct approximation of actual crop



ET can be achieved over a 30 minute or hourly range through the covariance between vertical wind speed ( $w'$ ,  $\text{m s}^{-1}$ ) and vapor density ( $q'$ ,  $\text{g m}^{-3}$ ) (Rana and Katerji, 2000).

$$\lambda E = \lambda \overline{w'q'} \quad (4)$$

Where  $\lambda$  is the latent heat of vaporization ( $\text{J g}^{-1}$ ).

Instantaneous values of  $w'$  and  $q'$  can be measured using a sonic anemometer and an infrared gas analyzer (IRGA). These variables are typically measured at high frequency, between 5-20 Hz, and can be automated over medium sized areas (50-200 m) which is seen as a considerable advantage (Rana and Katerji, 2000). Measurements do, however, need to be conducted over a homogenous surface, where there is continuity between the surface and the instrument height, with accuracy increasing with measurement height, especially for tall canopies (Kool et al. 2014). A number of corrections are required for accurate data, which can be performed during data collection, for example EasyFlux® DL program from Campbell Scientific or PC post-processing software, such as EddyPro software. Whilst trying to obtain LE using the eddy covariance method, the lack of energy balance closure remains problematic and can vary from 10-30% (Allen et al., 2011c). Even in different types of vegetation and climatic environments there was still an average of 20% lack of closure observed (Wilson et al., 2002). It has been reported that the resulting effects lead to under estimation of fluxes occurring between LE and H and overestimation of the available energy  $R_n + G$  (Foken, 2008; Wilson et al., 2002). The problem with the lack of energy balance closure impacts the manner in which data should be interpreted and how the resulting data compares with models (Foken, 2008).

There are several factors contributing to the lack of energy balance closure, which include frequency response of the instrument used, parallel advection, inaccurate measurement of  $R_n$  and  $G$ , energy used to drive the photosynthetic process, separation and misalignment of instrumentation, flux divergence as a result of changes in heat storage in the boundary layer below the instruments, inadequate fetch, effects of long-wave eddies which is not accounted for by the eddy covariance technique and requirement for a number of corrections which leads to greater turbulent flux and interference from the tower (Allen et al., 2011c; Foken, 2008; Howell, 2003; Mahrt, 1998; Twine et al., 2000).

The persisting problem with lack of closure within the eddy covariance method can be solved to a certain extent with various methods; 1) determining LE flux as a residual of surface energy balance, 2) through the assumption that the eddy covariance method can accurately measure the Bowen ratio ( $\beta$ ) leading to modification of LE and H to preserve  $\beta$  and save energy (Twine et al.,

2000). The first method described is unconvincing where it assumes that all measurements are correct and LE is determined as flux of residual surface energy balance, whilst the second method is more trustworthy as it has been validated by accurately determining the lack of closure in crop ET measurements with the eddy covariance method (Consoli and Papa, 2013).

The eddy covariance system has a distinct advantage of being able to indirectly measure  $E_s$  by calculating the difference between crop ET and  $T_c$  (Holland et al., 2013; Zeggaf et al., 2008). The estimation of  $T_c$  is important for modelling plant water use, as well as providing deeper insight into factors that govern plant water use. Techniques such as sap flow, whole plant gas chambers or deuterium tracer studies have been used to determine  $T_c$ . Sap flow techniques are generally best suited for measuring  $T_c$  without changing the  $T_c$  conditions by altering the microclimate surrounding the plant, which is the case with plant chambers, and can be easily automated to measure over extended periods of time to provide easily interpretable data (Smith and Allen, 1996). Numerous sap flow methods are available for  $T_c$  determination, such as heat pulse (Green and Clothier, 1988; Green et al., 2003), thermal dissipation (Granier, 1985, 1987) and stem steady state heat balance techniques (Baker and Van Bavel, 1987). The use of the heat pulse velocity (HPV) method is specifically appropriate for pecans, as trees with a stem diameter greater than 40 mm are needed for the sensors to be inserted (Allen et al., 2011c). This is a popular method as it is relatively inexpensive, has low power requirements, is easy to install and operate and can be automated, making remote measurements possible for various production regions (Green et al., 2003; Smith and Allen, 1996). When inserting the equipment accurate installation of the thermocouple sensors are crucial for accurate measurements. The HPV system contains a probe set which consists of two thermocouples and a heater probe that are radially inserted into the stem, at a predetermined height from the soil surface (below the first branch), and coupled to a datalogger for autonomous measurements (Green and Clothier, 1988). This method has the distinct advantage of measuring sap flow at different depths in the stem by staggering probe insertion depths, thereby accounting for radial variation of sapwood conductivity (Green et al., 2003).

The installation method is the biggest disadvantage for these techniques, as the holes drilled into tree for the insertion of the sensors causes damage to the xylem vessels within the stem and this leads to underestimates of sap flow velocities (Cohen et al., 1981; Green and Clothier, 1988). This requires the adjustment of HPV data to account for the effect of wounding. This adjustment can either be done empirically or by using numerical analysis that considers the wood physical properties and the extent of wounding (Cohen et al., 1981; Swanson and Whitfield, 1981). If the

crop under consideration has a uniform sapwood, that can be considered thermally homogenous, no calibration is required for the determination of sap flux densities (Marshall, 1958). However, if the xylem vessels are randomly arranged or if the interstitial length between accompanying vessels are too significant, leading to time delays in the conduction of heat between the sap and wood matrix, calibration will be necessary as the assumptions of Swanson and Whitfield (1981) for sap flow theory no longer apply (Swanson and Whitfield, 1981).

The other constituent of ET that can also be measured separately is evaporation. Soil evaporation ( $E_s$ ) can be determined using soil micro-lysimeter as described by (Daamen et al., 1993). There are a few shortcomings with the nature of lysimeters, especially in very arid conditions the metal containers can heat up quite rapidly and cause erroneous predictions due to accelerated  $E_s$  in the micro-lysimeters. The method of installation can potentially alter the natural distribution of soil layers thereby affecting hydraulic conductivity within the cylinder. For use in tree crop research where the trees are quite large, the depth of measurement can be a constraint as it does not account for water flux beneath the top-soil and therefore the closed lysimeters limit natural occurring water movement, such as capillary rise and horizontal redistribution (Allen et al., 2011c). Furthermore the large tree crop canopies influence the aerodynamic and radiation distribution occurring at the lysimeter surface, resulting in an accelerated  $E_s$  rate (Allen et al., 2011c). Regardless of aforementioned shortcomings, the measurement of  $E_s$  can be very accurate and can be used to validate crop models and methods to estimate  $E_s$  (Castel, 1996; Ferreira et al., 1996; Payero and Irmak, 2008).

#### 2.2.5 Modelling pecan water use

Various studies conducted in the U.S.A, and especially in New Mexico, reported annual flood-irrigated pecan evapotranspiration (ET) rates to differ extensively between 500 mm and 1400 mm, as a result of differences in tree size and age, seasonal growth stages, prevailing weather conditions and the extent of rooting (Samani et al., 2011; Wang et al., 2007c). Evapotranspiration can therefore be affected by various factors which should be accounted for when determining orchard specific water use. These factors include the cultivar, length of production season, frequency and method of irrigation, soil type, incidences of water stress, as well as cultivation techniques, such as the presence of cover crops, intercropping and mulch application (Pereira et al., 2015). It is impractical to measure ET under all combinations of the various aforementioned conditions, therefore crop models are used to extrapolate the data collected from field studies to various orchards in different climatic conditions regions and under different management practices (Ibraimo et al., 2016).

Numerous modelling approaches are available to predict ET and/or its partitioning into its constituents; canopy transpiration ( $T_c$ ) and soil evaporation ( $E_s$ ), ranging from basic empirical approaches to complex mechanistic models (Kool et al., 2014; Rana and Katerji, 2000). Empirical approaches are simpler and easily parameterized, but often only yield good results in the region where they were developed, whereas mechanistic approaches are more transferable across different regions. However, mechanistic models require a greater amount of input data that can be difficult to measure accurately (Ibraimo, 2018), such as the models proposed by Andales et al., (2006) and Annandale et al., (1999). The model of Andales et al., (2006) simulates the effects of the climate, irrigation and pruning has on tree growth, alternate bearing intensity, yield and potentially estimate volumes of irrigation and pruning for optimal yields. The model of Annandale et al., (1999) determines ET using a soil water balance. The soil water balance is based on mass conservation, whereby irrigation and precipitation add water to soil water, whilst water is lost through crop transpiration (crop water use), evaporation, runoff from the surface or deep drainage past the root zone of the crop. The latter approach has been refined further whereby the soil is partitioned into various strata enabling the measurement of the water and salt balance at shorter intervals (Annandale et al., 2005). The soil water balance model can be quite accurate as mechanistic models try and explain the processes, whereas empirical models are usually less transferable as they contain artefacts of the region wherein they were developed.

A few models have been developed for estimating pecan ET, which vary in complexity and detail, but few has been tested outside of the area of calibration (Allen et al., 1998a; Andales et al., 2006; Miyamoto, 1983; Samani et al., 2011; Sammis et al., 2004; Wang et al., 2007c). Furthermore, these methods are empirical in nature, with the shape of the crop coefficient curve and absolute values thereof, usually only pertaining to the region in which they were determined. Two such easily adopted empirical models are the FAO-56 model (Allen et al., 1998b) and the pecan monthly water use simulator (Samani et al., 2011). Both of these approaches estimate crop ET with the use of meteorological data and single crop coefficients, where the crop coefficient ( $K_c$ ) is defined as the ratio of ET and reference evapotranspiration ( $ET_o$ ). The single  $K_c$  method is a very popular modeling method and operates under the assumption that the response of crop ET to weather variables are the same, which might not hold true as crops respond differently to various combinations of environmental conditions, also crop coefficients are often orchard specific as they are developed according to that specific tree size, irrigation method, pruning strategy and presence of cover crop (Allen et al., 1998b; Villalobos et al., 2013). This methods suitability for orchard crops must be used with caution as certain inaccuracies can occur; 1) orchard crops possess higher surface roughness and tighter coupling to the environment compared to annual

crops, 2) this approach does not account for a larger evaporation surface under incomplete and sparse ground cover conditions, which is normally the case in orchards, which leads to erroneous ET estimates (Villalobos et al., 2013). This could possibly be exaggerated in pecan orchards, where the trees are large and deciduous (causes variable sun-and shade conditions), and where irrigation wetting patterns can vary depending on the irrigation methods used.

The pecan specific model by Samani et al., (2011) used canopy cover for a specific orchard to adjust the crop coefficient for a mature reference orchard ( $K_{c-ref}$ ) to obtain an orchard specific  $K_c$ , as follows:

$$K_c = (0.6035f_{ceff} + 0.4808) K_{c-ref} \quad (5)$$

This approach was evaluated by Ibraimo et al., (2016) in Cullinan, South Africa and the  $K_{c-ref}$ , determined by Samani et al., (2011), where adjusted by 6 months to account for southern hemisphere growing conditions, as provided in Table 2.2.

**Table 2.2 Measured monthly pecan reference crop coefficients ( $K_{c-ref}$ ) which has been offset by 6 months to account for southern hemisphere conditions (Samani et al., 2011).**

	Month								
	Sep	Oct	Nov	Dec	Jan	Feb	Mar	Apr	May
$K_{c-ref}$	0.39	0.59	0.87	1.02	1.04	1.24	1.26	0.84	0.39

Samani et al., (2011) suggested that these values should be adjusted for regions where the length of the growing season differs. Ibraimo et al., (2016) used the relationship between crop coefficient and GDD (equation 6) determined by Sammis et al., (2004) to adjust the  $K_{c-ref}$  values for Cullinan;

$$K_{c-ref} = 3.9 \times 10^{-12} GDD^4 + 1.1 \times 10^{-8} GDD^3 - 1.1 \times 10^{-5} GDD^2 + 4.3 \times 10^{-3} GDD + 0.33x \quad (6)$$

Whereby GDD was determined with a base temperature of 15.5 °C and weather data for each season, as seen in Equation (7) (Miyamoto, 1983).

$$GDD = \left( \frac{T_{min} + T_{max}}{2} \right) - 15.5 \quad (7)$$

Whereby  $T_{min}$  is the minimum temperature (°C) and  $T_{max}$  is the maximum temperature (°C). The  $K_c$  for pecan where then estimated, with equation 6, using adjusted  $K_{c-ref}$  values according to the climate. The calculated values where compared to actual measurements and it was determined that the method yielded poor monthly ET estimates as the  $K_c$  was underestimated at the onset and end of the season, and overestimated in the middle of the season (Ibraimo et al., 2016). This

was attributed to differences in growing season length and again stresses the importance of adjusting the  $K_{c-ref}$  to the local climatic conditions of the study site (Samani et al., 2011). Despite the good estimates of ET in the Cullinan orchard, when the  $K_{c-ref}$  values were adjusted for climate, Ibraimo et al., (2016) suggested that the relationship of Sammis et al., (2004) would not work well in some of the hotter and drier production regions of South Africa, where seasonal GDD exceeded 1500. The GDD approach is unlikely to fully account for canopy development, as perennial crops exhibit carry over effects between seasons, which is more pronounced in deciduous crops as pecan where carbohydrate reserves can influence the rate of canopy development, thereby influencing the  $K_c$  determination (Wood et al., 2003). Ibraimo et al., (2016) suggested that a potential solution to this problem of adjusting the  $K_{c-ref}$  curve could be to use visual observations of phenological stages, which could account for differences in cultivar and climatic conditions. It was further suggested to validate the use of these visual cues in other growing regions, where ET measurements have not been made, as an accurate method to adjust the  $K_c$  accordingly which will give more accurate estimates of ET, given that  $E_s$  is a minor component of ET (Ibraimo et al., 2016). Another discrepancy in data could occur in orchards where canopy cover is less than 65% as the  $E_s$  component will vary significantly, compared to where the model was developed and calibrated.

The study by Ibraimo et al., (2016) suggested more accurate ET estimates can be obtained in pecans when  $E_s$  and  $T_c$  are modelled separately. Such methods include the Shuttleworth-Wallace (S-W) model, the soil, water, energy and transpiration (SWEAT) model and the FAO-dual  $K_c$  approach (Kool et al., 2014). The S-W model is an analytical model and partitions ET with two Penman-Monteith equations; the first for the crop and the second for the soil (Monteith, 1965; Penman, 1948; Shuttleworth and Wallace, 1985). Several authors have tried to simplify this approach, as it is difficult to parameterize and is mostly used to validate other models (Kool et al., 2014). The soil, water, energy and transpiration (SWEAT) model quantifies the relationship between  $E_s$  and  $T_c$  through a two-layer method without much consideration for canopy structure or soil resistance parameters (Kool et al., 2014). The estimation procedure uses meteorological data, with subroutines for water and heat flow in combination with crop measurements (leaf area index (LAI) and height) (Daamen and Simmonds, 1996). The SWEAT model yields satisfactory results, when LAI is larger than 2, but the estimation of resistances needs refinement (Daamen and Simmonds, 1996; Kool et al., 2014). The dual crop coefficient approach has been validated in other studies and has been shown to be an accurate approach, compared to the single crop coefficient approach (Rosa et al., 2012; Villalobos et al., 2013). Separating  $T_c$  from  $E_s$  is important for water use studies, as it allows for a comprehensive understanding of the factors that govern



the regulation of water use from the crops (Kool et al., 2014), which is essential in modelling plant water use.

The study by Ibraimo et al., (2016) suggested that were canopy cover is sparse the  $E_s$  factor will increase dramatically and play a more significant role in ET determination. It was further suggested that the dual  $K_c$  approach of Allen et al. (1998) would be more transferable to other regions as it can obtain a more accurate determination of pecan ET through the separate estimation of the transpiration crop coefficient ( $K_t$ ) (ratio of  $T_c$  and  $ET_o$ ) and the soil evaporation coefficient ( $K_e$ ), which will compensate for higher  $E_s$  values. These two coefficients are multiplied with the reference evapotranspiration ( $ET_o$ ), which is defined as the potential evapotranspiration from a hypothetical grass reference crop, with assumed height of 0.12 m, fixed surface resistance of  $70 \text{ s m}^{-1}$  and albedo of 0.23 (Allen et al., 1998b), as seen in Equation (8) **Error! Reference source not found.;**

$$ET = (K_t + K_e)ET_o \quad (8)$$

According to Allen et al., (1998b)  $ET_o$  can be determined from weather variables collected by an AWS using Equation (9) **Error! Reference source not found.;**

$$ET_o = \frac{0.408(R_n - G) + \gamma \left( \frac{C_n}{T_a} + 273 \right) u_2 (e_s - e_a)}{\Delta + \gamma (1 + C_d u_2)} \quad (9)$$

Where  $ET_o$  is a standardized reference ET for a short grass reference surface in either  $\text{mm d}^{-1}$  for daily computations or  $\text{mm h}^{-1}$  for hourly time steps;  $R_n$  is estimated from measurements of incoming net solar radiation at the crop surface, either measured in  $\text{MJ m}^{-2} \text{ d}^{-1}$  for daily computations or  $\text{MJ m}^{-2} \text{ h}^{-1}$  for hourly time steps;  $G$  is the soil heat flux density at the soil surface, either measured in  $\text{MJ m}^{-2} \text{ d}^{-1}$  for daily computations or  $\text{MJ m}^{-2} \text{ h}^{-1}$  for hourly time steps;  $T_a$  is the mean hourly or daily air temperature at 2.5 m height in  $^{\circ}\text{C}$ ;  $u_2$  is the mean hourly or daily wind speed at 2.0 m height in  $\text{m s}^{-1}$ ;  $e_s$  is the saturation vapor pressure at 1,5 m height in kPa; calculated for daily time steps as the average between saturation vapor pressure at maximum and minimum air temperature and for hourly computations a hourly average air temperature is used;  $e_a$  is the mean actual vapor pressure at 1,5 m height in kPa;  $\Delta$  is the slope of the saturation vapor pressure-temperature curve in  $\text{kPa } ^{\circ}\text{C}^{-1}$ ;  $\gamma$  is the psychrometric constant in  $\text{kPa } ^{\circ}\text{C}^{-1}$ ;  $C_n$  is the numerator constant that changes with reference type and with the calculation time step in  $\text{K mm s}^3 \text{ Mg}^{-1} \text{ d}^{-1}$  or  $\text{K mm s}^3 \text{ Mg}^{-1} \text{ h}^{-1}$ ;  $C_d$  is the denominator constant that changes with reference type and with the calculation time step,  $\text{s m}^{-1}$  (Pereira et al., 2015). Ideally, values for either  $K_t$  and  $K_e$  should be determined under non-stressed conditions when soil water is not limiting, however, a stress coefficient ( $K_s$ ) can be used for water stressed conditions (water deficit or waterlogged) (Pereira

et al., 2015). Whilst,  $K_e$  accounts for differences in irrigation methods, which encompasses its wetting pattern and the frequency by which the surface is wet by precipitation or irrigation, which are important components in the determination of  $E_s$  (Allen et al., 2005),  $K_t$  allows the determination of  $T_c$ , which is critical in assessing how much water is used by the crop and therefore relates to the crop productivity. Therefore through the use of the dual crop coefficient approach ET can be successfully partitioned into  $T_c$  and  $E_s$  and as a result better decisions can be made regarding irrigation water management (Kool et al., 2014). The high variability in  $E_s$  results suggests the need that  $E_s$  should be modelled separately from  $T_c$ . Through this method has the grower the opportunity to implement strategies that would better water use such as mulch application within the wetted zone (Ibraimo, 2018).

A common occurrence with this model is the overestimation of  $T_c$  when  $ET_o$  is high. This is as a result of the inability of the plant to supply water to the leaves at a rate which matches atmospheric demand, even when soil water content is not limiting (Kool et al., 2014; Taylor et al., 2015). Under these conditions stomatal regulation will be the primary regulator of water loss (Sperry et al. 2000), as has been demonstrated in citrus (Taylor et al., 2015). As the crop coefficient model is an atmospheric demand limited approach, it does not necessarily cater for crops which exhibit significant stomatal control over transpiration, although Allen and Pereira (2009) have developed a method for this purpose. The extent to which pecan  $T_c$  will be limited by supply from the roots to the leaves is largely unknown and will be important to determine for accurate modelling of pecan water use.

To measure and model  $E_s$  via the FAO-56 dual crop coefficient approach requires the estimation of an evaporation crop coefficient ( $K_e$ ) which can be multiplied with  $ET_o$  to estimate  $E_s$  (Allen et al., 1998b; Allen et al., 2005).

$$E_s = ET_o K_e \quad (10)$$

Values for  $K_e$  can be determined as (Equation 11) (Allen et al., 1998b; Allen et al., 2005);

$$K_e = K_r(K_{c \max} - K_{cb}) \leq f_{ew} K_{c \max} \quad (11)$$

Where  $K_r$  is a dimensionless evaporation reduction coefficient that depends on the cumulative depth of water evaporated from the surface,  $K_{c \max}$  is the maximum value of  $K_c$  which occurs after rainfall or irrigation. Importantly, it is energetically impossible to maintain a  $K_c$  above 1.4 (Allen et al., 1998b),  $K_{cb}$  is the basal crop coefficient and can be presumed equal to the transpiration crop coefficient ( $K_t$ ) if transpiration is estimated via sap flow methods (Villalobos et al., 2013), and lastly  $f_{ew}$  is the fraction of soil that is wetted and receives solar radiation.



After a rainfall or irrigation event the assumption can be made that the soil surface is wet resulting in evaporation occurring at a maximum rate from the exposed soil ( $K_r = 1$ ) with the only imposed limitation being the availability of energy at the soil surface. Stage 1 will continue until the cumulative depth of evaporation (termed  $D_e$  in mm) has reached its maximum value and the ability of the soil to transport water to the surface becomes limiting and demand exceeds supply (Allen et al., 1998b). This point is dependent on the hydraulic properties of the surface soil layer. At the end of Stage 1,  $D_e$  is equal to readily available water (REW). As evaporation progresses further stage 2 begins, where less water is available for evaporation to occur and a reduction in  $E_s$  occurs (Equation 12), which is reflected by a reduction in  $K_r$ . **Error! Reference source not found.** (Allen et al., 1998b);

$$K_r = \frac{TEW - D_{e,i-1}}{TEW - REW} \text{ where } D_{e,i-1} < REW \quad (12)$$

Following rain or irrigation, the total evaporable water (TEW) in mm from the soil surface during a complete drying cycle, can be calculated as (Equation 13) **Error! Reference source not found.** (Allen et al., 1998b);

$$TEW = (\theta_{FC} - 0.5\theta_{PWP})Z_e \quad (13)$$

Where,  $\theta_{FC}$  ( $m^3 m^{-3}$ ) is the volumetric soil water content at field capacity, the modelling procedure assumes topsoil  $\theta_{FC}$  conditions following a large wetting event (rainfall amount should be larger than  $0.2 \times ET_o$  to be considered as a large wetting event (Allen et al., 1998b)),  $\theta_{PWP}$  ( $m^3 m^{-3}$ ) is the volumetric soil content at permanent wilting point,  $Z_e$  (mm) represent the thickness of the topsoil layer from which evaporation occurs,  $Z_e$  can be estimated through model calibration using measurements of  $E_s$ . The soil water content at  $\theta_{FC}$  and the  $\theta_{PWP}$  can be calculated with the procedure described by Saxton et al., (1986), which considers soil texture. The subsequent calculated value of TEW can then be used to calculate the reduction cycle of soil evaporation that occurs in two different stages (energy limited and falling rate stage) (Allen et al., 1998b). Further,  $D_{e,i-1}$  is the cumulative depth of evaporation after a large wetting event of the previous day (i-1) (mm), which is determined by a daily water balance computation for the topsoil layer (Equation 14) (Allen et al., 1998b);

$$D_{e,i-1} = D_{e,i} + (P_i - RO_i) + \frac{I_i}{f_w} - \frac{E_{s,i}}{f_{ew}} - T_{ew,i} - DP_{e,i} \quad (14)$$

Where  $D_{e,i}$  is the cumulative depth of evaporation following complete wetting at the end of day i (mm),  $P_i$  is the effective rainfall on day i (mm),  $RO_i$  is the runoff that occurs after a precipitation event on day i (mm),  $I_i$  is the depth of irrigation on day i (mm),  $E_{s,i}$  is the amount of evaporation

occurring on day  $i$  (mm),  $T_{ew,i}$  is the depth of transpiration from the exposed and wetted fraction of the soil surface layer on day  $i$  (mm),  $DP_{e,i}$  is the deep percolation loss from the topsoil if the soil exceeds field capacity conditions on day  $i$  (mm),  $f_w$  is the fraction of the soil surface wetted by irrigation (ranges between 0.01 and 1), and  $f_{ew}$  is the exposed and wetted soil fraction (ranges between 0.01 and 1). In deep rooted crop such as pecan can  $T_{ew,i}$  be presumed as zero as the amount of transpiration occurring from the layer where evaporation occurs is very small and can be deemed negligible (Allen et al., 1998b). When an irrigation event wets the entire soil surface,  $f_{ew}$  was almost equivalent to  $f_w$  during those days. The calculation of  $f_{ew}$  (Equation 15) and  $f_w$  (Equation 16) are as follows;

$$f_{ew} = \min (1 - f_{c \text{ eff}}, 1) \quad (15)$$

$$f_w = \min (1 - f_{c \text{ eff}}, f_w) \quad (16)$$

Where  $f_{c \text{ eff}}$  is the average fraction of soil surface covered by vegetation near solar noon (using a ceptometer and grid method to determine ground shaded area). The maximum of  $K_c$  can therefore not exceed  $f_w K_{c \text{ max}}$  (Allen et al., 1998b). The subsequent value is then compared against  $K_e$  to ensure it is less than the imposed upper limit.

The model performance for estimation of ET and  $E_s$  was assessed using the Willmott index of agreement (D), the root mean square error (RMSE) (Equation 17), mean absolute error (MAE) (Equation 18), the coefficient of residual mass (CRM) (Equation 20) and the coefficient of determination ( $R^2$ ). The D is a measure of the degree to which the model predictions are accurate (measured against estimated) (Willmott, 1981) (Equation 19), whereas MAE, RMSE and CRM are residual based measures that give a quantitative estimate of the deviation of the modelled outcome from the observed data set (Abraha and Savage, 2010; Bellocchi et al., 2011). The  $R^2$  is a correlation measure which describes the goodness-of-fit of the model. The  $R^2$  and D values range between 0 and 1, which is indicative of the worst and best model performance values respectively as described by Bellocchi et al., (2011). The MAE varies between zero and infinity, with zero indicated the best model performance. Acceptable parameters for these statistical indices were that  $R^2$  and D should be greater than 0.8 and MAE (expressed as a percentage) should be less than 20%. The CRM is most accurate at zero, with positive and negative values indicate underestimation and overestimation of the model, respectively.

$$RMSE = \sqrt{\frac{\sum_{i=1}^n (P_i - O_i)^2}{n}} \quad (17)$$

$$MAE = \frac{(\frac{1}{n}) \sum_{i=1}^n |P_i - O_i|}{O} \times 100 \quad (18)$$

$$D = 1 - \frac{\sum_{i=1}^n (P_i - O_i)^2}{\sum_{i=1}^n (|P_i - O_i| + |O_i - O|^2)} \quad (19)$$

$$CRM = 1 - \frac{\sum_{i=1}^n O_i - \sum_{i=1}^n P_i}{\sum_{i=1}^n O_i} \quad (20)$$

Where  $P_i$  and  $O_i$ , respectively are measured and estimated values,  $n$  is number of observations,  $O$  is the mean of measured values.

## CHAPTER 3 GENERAL MATERIALS AND METHODS

### 3.1 Site description and experimental layout

The trial site in Vaalharts was situated approximately 25 km Southwest of Jan Kempdorp, Northern Cape, South-Africa (GPS-Coordinates: 28°4'11.01"S, 24°37'54.79"E). The orchard was roughly 10.37 ha (1037 trees) and consisted of trees that were 12 years old (planted in 2006) at the start of the study. The orchard consisted of 40 rows of full bearing, irrigated pecan trees (cultivars included 'Wichita', 'Choctaw', 'Navaho' and 'Western Schley' all grafted on 'Ukulinga' rootstocks) planted at an industry standard of 10 m x 10 m spacing, totalling 100 trees ha<sup>-1</sup> (Figure 3.). Trees were planted in a North-West – South-East orientation, with an approximate height of 10 m and width of 5.7 m at the start of the study. Trees were pruned on a 4-year cycle according to industry standards, with a mechanical hedger to provide uniformity. Trees were irrigated by the same system throughout which was one 150 L h<sup>-1</sup> Mamkad 16 sprinkler (NaanDanJain Irrigation) placed within the row between two trees, with a wetted radius of 6.5 m that provided full surface irrigation. Irrigation was scheduled according to a cycle determined by readings from an Aquacheck probe installed between a pecan tree and a macro-sprinkler in the orchard. The details of the pecan orchard in this study are provided in

Table 3. The soil type ranged from a sandy loam to loam-clay soil, with clay content increasing with depth.

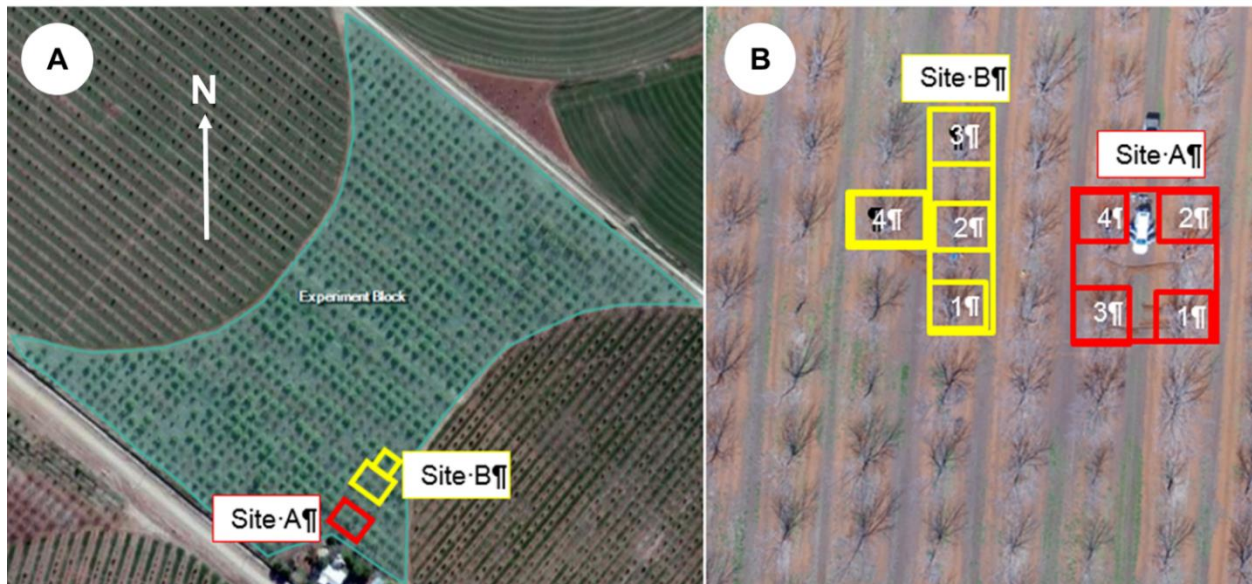


Figure 3.1 A) Orchard layout where the trial took place and the position of the two sites where sap flow was measured, B) At site A four trees were measured, Tree 1 and 2 were 'Choctaw' and Tree 3 and 4 were 'Wichita', at site B four trees were measured, Tree 1 and 4 were 'Choctaw' and Tree 2 and 3 were 'Wichita'.

**Table 3.1 Overview of the mixed cultivar orchard at the trial site in Jan Kempdorp, South-Africa.**

No of experimental trees	Total number of trees = 8. Total number of trees per cultivar = 4.	
Site A Study cultivars	Tree 1 – ‘Choctaw’ Tree 2 – ‘Choctaw’ Tree 3 – ‘Wichita’ Tree 4 – ‘Wichita’	
Site B Study cultivars	Tree 1 – ‘Choctaw’ Tree 2 – ‘Wichita’ Tree 3 – ‘Wichita’ Tree 4 – ‘Choctaw’	
Trunk circumferences of measurement trees (cm)	1 – 84.6 2 – 90.6 3 – 72.2 4 – 74.6	5 – 86.3 6 – 74.6 7 – 80.2 8 – 92.5

### 3.2 Weather data

Weather data was obtained from an Automatic Weather Station (AWS) which was installed within 1 km of the orchard, to the North-west. It was placed within a fenced area for security reasons (Figure 3.). The variables measured included solar radiation (LI-200S, Li-Cor, Lincoln, Nebraska, USA), temperature and relative humidity (HMP50, Vaisala Oyj, Vantaa, Finland), wind speed (cup anemometer, RM Young, Traverse City, Michigan, USA), and rainfall (TE525 tipping bucket rain gauge, Texas Electronics, Dallas, Texas, USA). These sensors were attached to CR1000 data logger (Campbell Scientific Inc. Logan, Utah, USA), with variables logged on an hourly and daily basis. The battery system was connected to a solar panel that continuously charged the 12V battery. Sensors were positioned according to specifications in FAO-56 for calculating reference evapotranspiration ( $ET_o$ ) (Allen et al., 1998b). Quality of the data was assessed according to (Allen, 2008), and the pyranometer was calibrated against an Eppley radiometer (Eppley laboratories, Newport, USA). Data quality on the whole was good throughout the duration of the trial with only an adjustment made to the pyranometer following calibration with the Eppley radiometer.

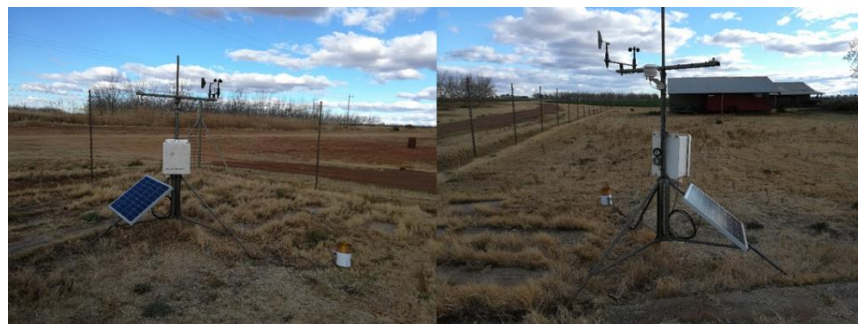


**Figure 3.2 The automatic weather station (AWS) placed within 1 km of the trial site.**

### 3.3 Irrigation and water table monitoring

Irrigation was scheduled by the grower according to a cycle determined by readings from an Aquacheck probe installed between a pecan tree and a macro-sprinkler in Site A tree 2. Two In-line water meters were installed, one at each study site (Figure 3.1), before the sprinklers dedicated to the study area to determine irrigation volumes across the season. The reading of these in-line water meters occurred once a month, from the onset of the season up until harvest when irrigation volumes were determined. Chameleon soil water sensors (Via Farms) were also installed at Site A and B, at depths of 30, 60 and 90 cm, between the macro-sprinkler and the tree and within tree row, to measure soil water potential. The sensor contains two gold-plated electrodes that automatically measures the resistance across a medium, which is encased in a porous gypsum cap that allows water to move through the sensing material whilst dissolving a small amount of water, thus buffering the solution and creating a constant electrical conductivity environment (Stirzaker et al., 2017). The chameleon logger displays either blue, green or red colour depending on the tension observed; blue means the soil is wet (0 to 20 kPa), green means the soil is moist (20 to 50 kPa) and red means the soil is dry (greater than 50 kPa). The sensors were used to determine possible periods where water deficits were experienced due to a lack of irrigation. In water use experiments it is important to measure all inputs of water into the system that might affect total tree water use. The failure to measure all the water inputs into the system can result in an underestimation of actual tree water use. To account for periodic water table fluctuations a piezometer was installed at 2.5 m depth, between study site A and B, and measured every second month during dry period and every month during the wet season.

Irrigation uniformity from the macro-sprinkler was assessed by measuring the volume of irrigation water received at 1 m intervals from the sprinkler into the row until 5m from the sprinkler (Figure 3.3). Irrigation was applied for one hour and the volumes were recorded at each interval with a series of rain gauges inserted into the soil. The sprinkler in the adjacent row was covered during this measurement to limit any drift occurring that might influence results.





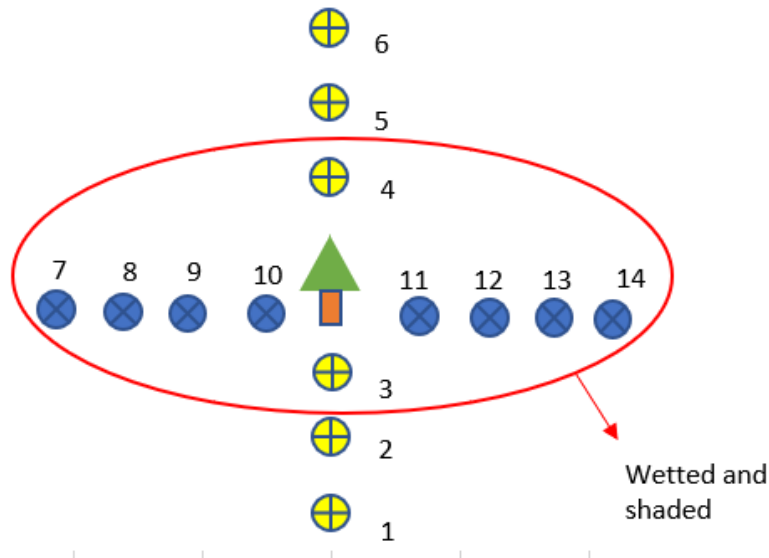
**Figure 3.3 Irrigation uniformity test with a series of rain gauges (▲) placed at 1 m intervals within the row from an uncovered macro-sprinkler (○), whilst opposite sprinkler was covered (●).**



#### 3.4 Ecophysiological measurements

Ecophysiological measurements were used to determine if the trees were experiencing any water stress during the measurement period, as well as correlate it with transpiration measurements to gain further insight into the correlation between sap flow and leaf and stem water potential. Leaf and stem water potential measurements were made at regular intervals throughout the season using a Model 600 Scholander pressure chamber (PMS Instruments Company, USA). The measurements accounted for cultivar variability and trial site and were conducted throughout the day on tree 1 ('Choctaw') and tree 3 ('Wichita') at site A and on tree 2 ('Wichita') and tree 4 ('Choctaw') at site B. The relationship between leaf water potential and its position on the tree was described by Deb et al., (2012), where it was found that the tree experienced water stress earlier at the top of the canopy as a result of its environmental exposure and resistance to liquid water flow in the longer pathway to the peak leaves. The measurement height was kept constant at 1.6 m from the soil to prevent changes in measurement height from influencing the results. Three leaves were sampled from the east and west side in conjunction with a leaf for stem water potential (7 leaves per measurement). Stem water potential was determined by enclosing a leaf on the inside of the canopy in an aluminium covered plastic bag at least 30 minutes before measurements were made (Deb et al., 2012). Hourly measurements were made, with the first measurement (pre-dawn measurement) occurring before sunrise (06:00 am) until the afternoon (17:00 pm).

#### 3.5 Soil evaporation, drainage patterns and root density

Micro-lysimeters were used to determine spatial variability of soil evaporation and to provide data to calibrate and validate a soil evaporation model at tree 4, Site B. The micro-lysimeters were spaced to account for variability, such as shaded or sun exposed soil area and if areas were wet by irrigation or not. Initially, eight micro-lysimeters were placed within the row, four on each side at a spacing of 1.25 m starting at the stem. Six micro-lysimeters were placed perpendicular to the row, three on each side of the tree at a spacing of 1.67 m starting at the stem (Figure 3.). A total of six measurements were made with this setup between 21 and 28 October 2018 ( $f_{c\text{ eff}}$  of 75%) before the layout was changed. The weighing of these cores occurred every hour between 08:00 and 17:00, with new cores being replaced in the morning before the first measurement starts.



**Figure 3.4 Initial Micro-lysimeter placement around the tree,**  represents the micro-lysimeters within the row at a 1.25 m spacing.  Represents the micro-lysimeters perpendicular to the row at a 1.67 m spacing. Micro-lysimeters 1 to 12 represent different wetted and shaded soil surface areas within the ground allocated to the tree.

The second layout achieved a greater coverage of the allocated area surrounding the tree to account for variability in wetting and shading patterns and obtain a better perspective of the interaction between the variables that govern soil evaporation (Figure 3.). The 24 micro-lysimeters were used to measure  $E_s$  between the periods of 4 and 5 December 2018 ( $f_{c\text{ eff}}$  of 80%), 31 January 2019 ( $f_{c\text{ eff}}$  of 80%), 6 to 7 March 2019 ( $f_{c\text{ eff}}$  of 80%), 10 April 2019 ( $f_{c\text{ eff}}$  of 80%), 20 to 22 May 2022 ( $f_{c\text{ eff}}$  of 75%) and 23 until 24 June 2019 ( $f_{c\text{ eff}}$  of 60%). During the measurement period there were no water inputs into the soil water system (precipitation or irrigation), therefore the change in mass of the lysimeter reflected evaporation rates that were indicative of the energy received at that particular point by incoming solar radiation and the soil water content as impacted by previous irrigation and/or precipitation.



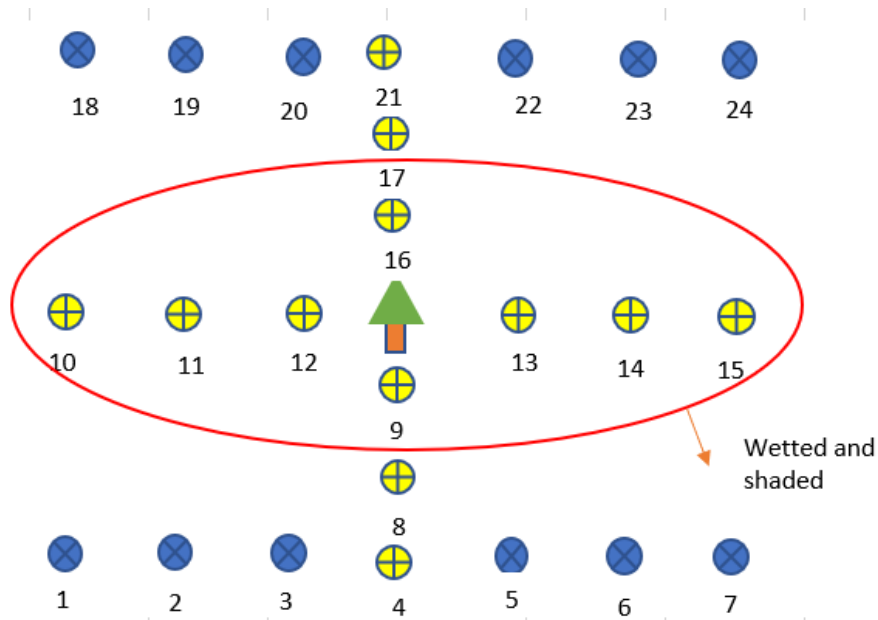


**Figure 3.5 Final placement of micro-lysimeters around the tree,  $\otimes$  represents the micro-lysimeters across the row at 1.25 m spacing.  $\oplus$  Represents the micro-lysimeters perpendicular and parallel to the row at a 1.67 m spacing. Micro-lysimeters 1 to 24 represent different wetted and shaded soil surface areas within the ground allocated to the tree.**

Measurements of the 24 micro-lysimeters occurred daily for certain window periods during the season where the change in mass of the micro-lysimeter over a day was determined by weighing the samples in the morning, at midday and in the afternoon. From the measured mass the volume of water evaporated from the soil in mm was calculated (Flumignan et al., 2012), as described by

$$\text{Equation } E_{ML} = \frac{\Delta M_{ML}}{A_{ML}} + P \quad (21);$$

$$E_{ML} = \frac{\Delta M_{ML}}{A_{ML}} + P \quad (21)$$

Where  $\Delta M_{ML}$  is the change in micro-lysimeter mass (kg),  $A_{ML}$  is the micro-lysimeter surface area and  $P$  is precipitation in mm. For the purpose of this study  $P$  was ignored as measurements were conducted when there was no water input on the day of measurements. On certain occasions measurements were conducted a day after an irrigation event. Total evaporation was determined based on a weighted area that each micro-lysimeter represented within the area occupied by a tree (Sun et al., 2004). Micro-lysimeters represented by the blue symbols, placed across the row, had a radius of 5.25 cm and a height of 14 cm. The micro-lysimeters represented by the yellow symbols, placed perpendicular and parallel to the tree, had a radius of 4 cm and height of 14 cm.

To measure soil water content with the soil profile 15 GS-1 Decagon soil moisture sensors (currently marketed as Teros-10 sensors by Meter Group, Pullman, WA, USA) were installed.

Five GS-1 Decagon soil moisture sensors were placed at three different positions perpendicular to the tree row at tree 2 site B. These positions were within the row at 2.5m from the tree trunk, at the edge of the canopy (2.7 m perpendicular to the tree row) and in the middle of the row (5 m perpendicular to the tree row) at depths of 30 cm, 40 cm, 60 cm, 90 cm and 120 cm, as seen in Figure 3.6. These measurements were used to determine water movement down the soil profile, and water uptake patterns within the soil profile which were compared to rooting patterns within the profile.

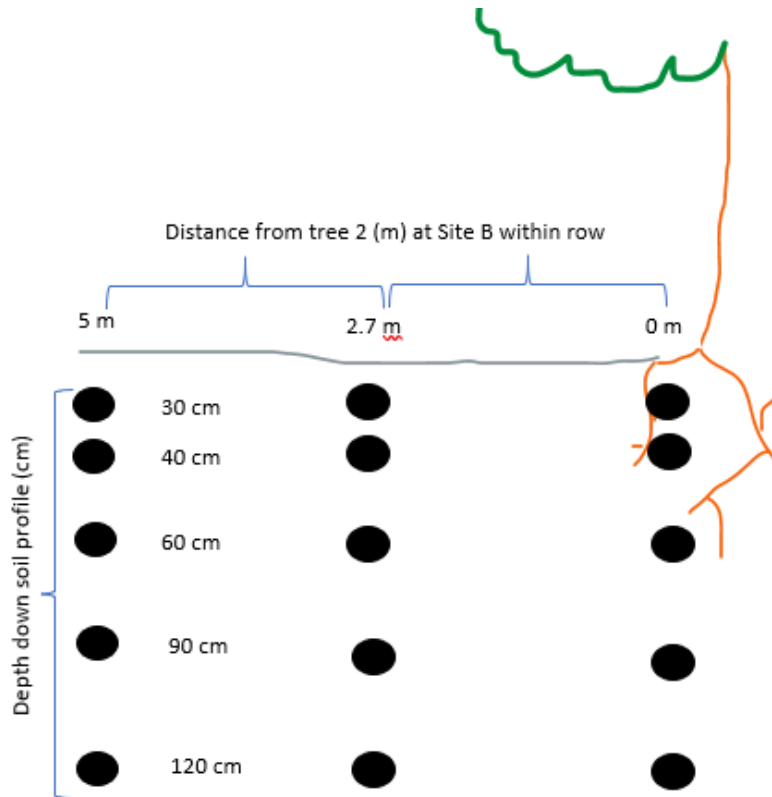


**Figure 3.6 Visual representation of 15 GS-1 Decagon soil water sensor placement at three distances perpendicular to the tree; firstly, within the row at 0 m, secondly at 2.7 m from the tree base and thirdly at 5 m from the tree base at depths of 30 cm, 40 cm, 60 cm, 90 cm and 120 cm at tree 2 site B.**

Soil is inherently very variable in its composition as a result of cultivation practices that disturb the natural occurring deposition and distribution of soil as a result of weathering process from its mother material. At various depths the sand, silt and clay fractions change, which could influence the way water moves down the soil profile, as well as influence root distribution. Soil samples were taken at 10 cm increments, from the soil surface up until a depth of 1 m, from within four profile pits that were dug within the measurement row of Site B at four randomly selected trees, that was not part of the Site B trial. The four samples at each depth were pooled for analysis to

represent the average characteristics of the area between the two study sites in the orchard. Measurements included the bulk density, clay %, sand % and silt % and these measurements were used to account for any large changes in soil texture which could influence water holding capacity.

The rooting pattern of the pecan trees in the orchard was assessed to determine the zones from which maximum water uptake could occur. The rooting pattern was determined using the trench wall and grid method, as described by Achat et al., (2008), at intervals of 1.5 m, 2.5 m, 3.5 m and 4.5 m from the tree trunk perpendicular to the working row. Each profile pit had dimensions of 1 m in breadth and 1 m in depth, with a grid placed on the profile wall to divide the total surface area into 10 cm x 10 cm squares to determine the total number of roots at the various depths, as well as the approximate diameter of the roots at these depths (Figure 3.73.7). It is important to determine both root number and root size as roots of different sizes have different functions. The functionality of small and large roots are attributed to their nature; where larger older roots are multifunctional as its lignified composition contributes to its function as anchorage, storage of reserves, transport solutes and produce lateral roots where fine, unbranched small diameter roots specialize in acquiring water and nutrients (Eissenstat et al., 2000; Ma et al., 2013). The root diameters were measured using Vernier callipers and divided into four classes; roots with a diameter smaller than 2 mm (<2 mm), roots with a diameter between 2 and 5 mm (2-5 mm), roots with a diameter between 5 and 10 mm (5-10 mm) and roots with a diameter larger than 10 mm (>10 mm). According to this classification the first two classes (<2 mm and 2-5 mm) will play an important role in water and nutrient uptake, whereas class 5-10 mm will most likely have impaired water and nutrient uptake and the largest class, >10 mm, was assumed to have very limited to zero water and nutrient uptake.



**Figure 3.7 Grid installed in a 1 m x 1 m soil profile pit wall to determine rooting pattern and root distribution.**

### 3.6 Sap flow measurements

Transpiration was determined using the heat ratio method, which is a heat pulse sap-flux density technique (Vandegehuchte and Steppe, 2013) as described by Burgess et al., (2001) and Ibraimo et al., (2016). This method is appropriate for pecan trees, as these measurements can only be made in woody stems with a diameter larger than 40 mm, which was easily exceeded in this study as seen in

Table 3. It has also been used previously in pecan trees in South Africa (Ibraimo et al., 2016). This method is able to measure sap flow at very low velocities and even reverse flow, this is of interest during the onset and end of the season where leaf area is low. Measurements were made on four 'Choctaw' trees and four 'Wichita' trees. Four heat pulse probe sets were used for each tree (each consisting of a heater probe inserted into a 2.5 mm brass collar and two type-T copper-constantan thermocouples embedded in 2 mm outside-diameter PTFE tubing, placed equidistantly up and down stream of the heater probe at a distance of 0.465 cm), as seen in Figure 3.83.8.

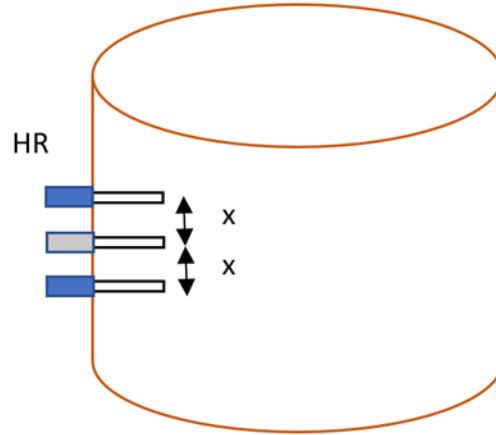


**Figure 3.8 Schematic representation of the HR method proposed by Burgess et al., (2001), with the heater probe in grey and the thermocouples in blue spaced equally apart (indicated by x).**

In order to account for the radial variation in sap flux within the conducting sapwood, thermocouples were inserted at depths of 2, 3, 4 and 6 cm, in the stem in each tree trunk, at 0.5 m above the soil surface and were equally spaced around the trunk. The heat pulse velocity ( $V_h$ ) in  $\text{cm h}^{-1}$  for each probe set was calculated following Marshall (1958) as:

$$V_h = \frac{k}{x} \ln \left( \frac{v_1}{v_2} \right) * 3600 \quad (22)$$

where  $k$  is the thermal diffusivity of green (fresh) wood (assigned a value of  $2.5 \times 10^{-3} \text{ cm}^2 \text{ s}^{-1}$  (Marshall 1958)),  $x$  is distance in cm between the heater and either the upper or lower thermocouple,  $v_1$  and  $v_2$  are increases in temperature after the heat pulse is released (from initial temperatures) as measured by the upstream and downstream thermocouples and 3600 converts seconds to hours. Heat pulse velocities were measured and logged on an hourly basis using a CR1000 datalogger and an AM16/32B multiplexer (Campbell Scientific Ltd, Logan, UT, USA).

The conversion of heat pulse velocities to sap flux densities, taking into account wounding, was performed according to Burgess et al., (2001). Wounding corrections were performed by using wounding coefficients  $b$ ,  $c$ , and  $d$  obtained from a numerical model developed by Burgess et al., (2001) using the following equation:

$$V_c = bV_h + cV_h^2 + dV_h^3 \quad (23)$$

where  $V_c$  is the corrected heat pulse velocity. The functions describing the correction coefficients in relation to wound width ( $w$ ) were as follows:

$$b = 6.6155w^2 + 3.332w + 0.9236 \quad (24)$$

$$c = -0.149w^2 + 0.0381w - 0.0036 \quad (25)$$

$$d = 0.0335w^2 - 0.0095w + 0.0008 \quad (26)$$

Wound widths caused by the insertion of probes was determined by chiselling out a section of wood for a probe set on each tree and measuring the width of the visible wounding. Average wound width for the ‘Wichita’ trees was 1.0 cm, whilst for the ‘Choctaw’ trees it was 0.95 cm. The presence of heartwood, seen as wood discolouration, was determined by taking wood cores with an incremental borer (Figure 3.93.9). This was determined as the width of discolouration that surrounded the point of insertion using electronic Vernier callipers (Figure 3.10). Other wood characteristics, including sapwood moisture content ( $m_c$ ) and density ( $\rho_b$ ) were determined from additional core samples taken during the measurement period.

Following the determination of  $m_c$  and  $\rho_b$ , sap velocity ( $V_s$ ) was calculated from the corrected heat pulse velocity using the equation suggested by Marshall (1958) that was later modified by Barrett et al. (1995):

$$V_s = \frac{V_p P_b (c_w + m_c c_s)}{P_s c_s} \quad (27)$$

where  $c_w$  and  $c_s$  are specific heat capacity of the wood matrix ( $1200 \text{ J kg}^{-1}\text{C}^{-1}$  at  $20 \text{ }^\circ\text{C}$  (Becker and Edwards, 1999) and sap (water,  $4182 \text{ J kg}^{-1}\text{C}^{-1}$ ) at  $20 \text{ }^\circ\text{C}$ , respectively, and  $\rho_s$  is the density of water ( $1000 \text{ kg m}^{-3}$ ). Whole stem flux ( $Q$ ) was calculated, was calculated as the product of  $V_s$  and its cross-sectional area of conducting sapwood and then summed for the entire stem, as applied by Hatton et al. (1990). Integrated volumetric sap flow of the individual trees ( $\text{L day}^{-1}$ ) was converted to transpiration ( $\text{mm day}^{-1}$ ) using the ground area allocated to each tree in the orchard i.e.  $100 \text{ m}^2$ .

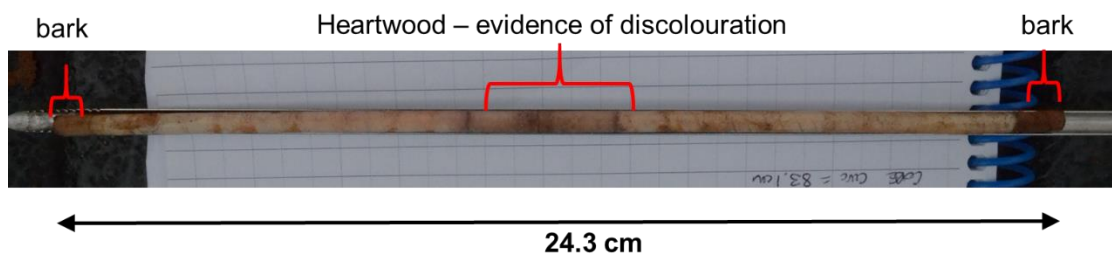


**Figure 3.9 Core taken from a ‘Choctaw’ tree indicating bark thickness and presence of heartwood.**

A single transpiration value was determined for ‘Wichita’ and ‘Choctaw’ trees over the course of the trial. The seasonal transpiration value for each cultivar was determined as a weighted average of the four trees, within each of the two cultivar groups, according to the stem circumference of the individual measurement tree, in comparison to 32 measured stem circumferences within the same orchard, of the same cultivar and age.





**Figure 3.10 Wounding caused as a result of probe insertion into the tree to determine heat pulse velocities and ultimately transpiration.**

### 3.7 Evapotranspiration estimates using the Eddy Covariance technique

An extended Open Path Eddy Covariance (OPEC) system (Campbell Scientific Inc., Logan, UT, USA) was installed within 500m of the trial site to the North-East at a height of 1.2 m above the 8 m trees (Figure 3.193.11). Eddy covariance measurements consists of determination of variable eco-physiological fluxes governing plant responses towards its environment. The basis of measurements correlates vertical wind fluctuations ( $w'$ ) with fluctuating transported admixture ( $q'$ ) varying from the mean at sufficient frequencies (Foken et al., 2012). Variables estimated included latent heat (LE), sensible heat (H) and soil heat fluxes (G). These measurements started at the end of April 2019 and continued until September 2019. The timing of these measurements included full canopy cover, as well as leafless conditions during the over-wintering phase, providing key insights into the fluctuation of LE, H and G over a season.

The OPEC system consisted of a CR3000 datalogger and IRGASON open-path infrared analyser and 3D sonic anemometer (Campbell Scientific Inc., Logan, Utah, USA), which was mounted on a lattice mast. Air temperature and humidity were measured using a HygroClip2 HC2-S(3) thermohygrometer probe (Rotronic Instruments, Bassersdorf, Switzerland). Net radiation ( $R_n$ ) was measured using an NR-Lite net radiometer (Model 240-110 NR-Lite, Kipp & Zonen, Delft, Netherlands) mounted 9.2 m above ground. Four soil heat flux plates (model HFT-S, REBS, Seattle, Washington, USA) were used to estimate G at a depth of 80 mm in the soil under the trees and between the rows, and four TCAV-L soil temperature averaging probes (Campbell Scientific Inc., Logan, Utah, USA) at depths of 20 and 60 mm were used to calculate the heat stored above the plates (Figure 3.1103.12). Plates were placed under a tree and in the middle of

the row to account for variation in solar radiation distribution on the orchard floor throughout the day.

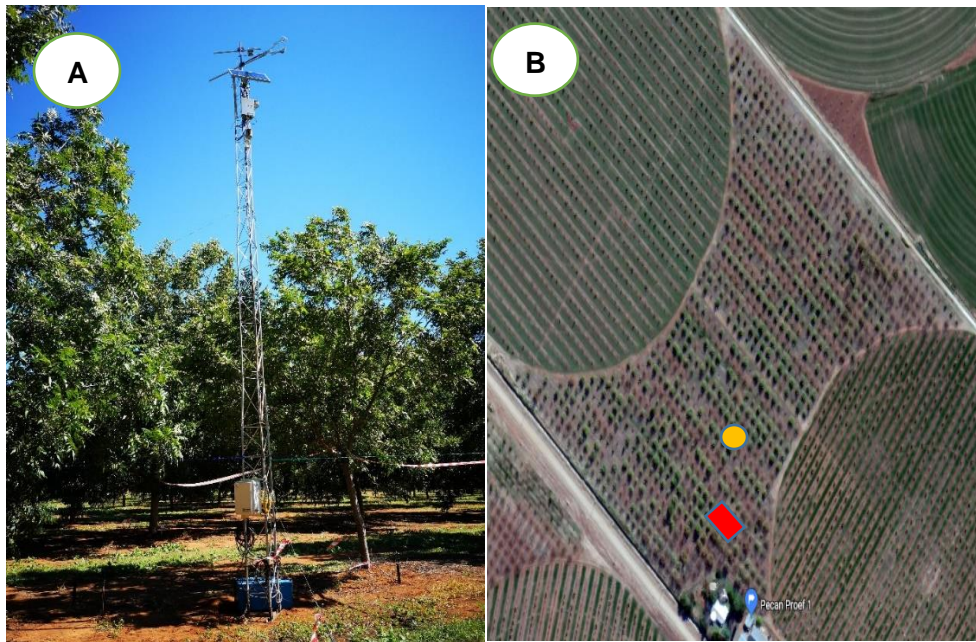


**Figure 3.19** ● A) Position of the Open Path Eddy Covariance system above the tree canopy. ■ B) Position of the Open Path Eddy Covariance system in relation to the sap flow measurements.

Volumetric water content in the first 60 mm of the soil surface was measured using two Time-Domain Reflectometers in the top 30 cm of the soil (CS616, Campbell Scientific Inc., Logan UT, USA). These sensors were connected to the CR3000 datalogger (Campbell Scientific Inc., Logan, UT, USA) and measurements were performed at 10 Hz frequency using the Easyflux-DL software from Campbell Scientific. The program applies the most common open-path EC corrections to fluxes. Averages were also obtained every 30 min.



**Figure 3.110** A Hukseflux HFP01 soil heat flux plate in parallel with two TCAV-L soil temperature averaging probes.



### 3.8 Determination of canopy size

The correlation between  $T_c$  and canopy development is an important consideration when trying to model crop water use as the total  $T_c$  that could potentially occur can be limited by the canopy volume. The fractional interception of photosynthetically active radiation ( $f_{IPAR}$ ) of four trees, two at each trial site, was measured every four to six weeks, from September 2018 up until September 2019, with a Decagon AccuPAR LP-80 ceptometer (Decagon Devices, Pullman, WA, USA) to determine the relationship between canopy cover or leaf area index (LAI) and water use. At trial site A tree 3 ('Wichita') and tree 4 ('Wichita'), and at site B tree 1 ('Choctaw') and tree 4 ('Choctaw') were chosen as representative trees of each cultivar. Measurements were taken under cloudless, full sun conditions between 12 and 2 pm on a predetermined 1 m x 1m grid, starting from the stem, stretching across the row and between the rows. The grid layout accounted for the total area allocated to the tree, as seen in Figure 3.13.13. These ceptometer measurements were used to determine  $f_{c\text{eff}}$ , which is the fraction of soil surface covered by vegetation near solar noon.



**Figure 3.13 Representation of the grid layout for the determination of canopy cover using a Decagon AccuPAR LP-80 ceptometer (Decagon Devices, Pullman, WA, USA).**

## CHAPTER 4 PECAN EVAPOTRANSPIRATION

### 4.1 Introduction

Crop water use or evapotranspiration (ET) consists of a transpiration ( $T_c$ ) and evaporation ( $E_s$ ) component. Crop water use information for pecan orchards is very limited, as most of the research was done in the crops native range within the USA. From pecan ET studies conducted within the US, a large range of water use estimates were found, mainly due to climatic and tree size variation between measurement locations (Miyamoto, 1989; Samani et al., 2011; Sammis et al., 2004; Wells, 2015) (see Table 2.1 in Chapter 2.2.1). As climatic variation also occurs between South African pecan production regions, it is important to quantify seasonal crop water use in the various regions to ensure that water use models developed in cooler regions apply to hotter regions.

Most pecan crop water use studies have focused on quantifying total crop water use, or ET, without partitioning into its main constituents. It is, however, more advantageous to measure the individual components separately, granting the ability to obtain a better understanding of the dominant factor's contribution to total ET, as well as what causes the variation in both portions. By learning what causes fluctuations in  $T_c$  and  $E_s$  it is possible to gain a deeper understanding of what factors determine ET, which is invaluable for assessing the accuracy of potential modeling approaches of orchard water use. Further, by separating measurements better estimation can be obtained of beneficial and non-beneficial consumptive water use (Reinders, 2010). Beneficial crop water use includes the  $T_c$  component, as it relates directly to dry matter production and therefore crop yield. Non-beneficial consumptive water use includes  $E_s$ , as it does not directly relate to processes involved in maintaining optimal crop water status and therefore production (Miyamoto, 1983; Reinders, 2010). Pecan ET was estimated in an orchard in Cullinan, South Africa by Ibraimo (2018), who reported variable seasonal  $T_c$  volumes for 'Choctaw' trees of 846 mm, 888 mm and 861 mm for the respective 2016 to 2018 production seasons. From the same study measured  $E_s$  varied between 97 mm and 189 mm for the three production seasons. Throughout each season there was large variation in these measurements, which was attributed to differences in weather between the three seasons and slight changes in canopy size as a result of pruning.

Soil evaporation is a key and integral part of ET, especially in deciduous orchards where sparse canopy cover conditions govern the amount of solar radiation received at the surface of the soil at the beginning and end of each season, which often receives high-frequency irrigation. These conditions are conducive for  $E_s$  to occur, as proven in two studies whereby in a sprinkler irrigated mature olive orchard (canopy cover of 36%),  $E_s$  accounted for approximately 30% of the total ET, compared to a young olive orchard (5% canopy cover),  $E_s$  constituted 43% of total ET with drip

irrigation (Bonachela et al., 1999; Bonachela et al., 2001). A number of factors therefore influence  $E_s$  in an orchard, which include soil texture, irrigation type and scheduling, crop type, crop age and physiological stage, weather variables and planting pattern (Wang and Liu, 2007).

When considering pecan ET and its constituents, it is suggested that pecans have a high-water demand, which is higher than other row crops (Sparks, 2005). This water demand cannot be satisfied by rainfall alone under conditions where pecans are typically grown in South Africa (semi-arid conditions), as rainfall is too sparsely distributed, and its sporadic nature does not always coincide with crop demand. Supplemental irrigation is therefore required to maintain a viable crop. In South Africa water scarcity is an ever-growing concern to production, therefore it is important to assess the water requirements of pecan grown in these areas to ensure future cultivation is a feasible option. The competition for water resources is ever increasing and without the introduction of new water sources, few options remain for crop cultivation, unless growers become more efficient in the way they manage the amount of water they have, or the choice of crop which they choose to cultivate. One method of quantifying how effectively a crop uses water is water use efficiency (WUE) (total yield per unit ET) ( $\text{kg m}^{-3}$ ), whilst economic considerations include water use productivity (WUP) (crop monetary value (Rand) per unit ET) ( $\text{R m}^{-3}$ ) and irrigation water use efficiency (IWUE), which is the ratio between the harvested crop yield and the total water applied (irrigation + rainfall) ( $\text{kg m}^{-3}$ ) (Howell, 1994). The WUE and WUP allows benchmarking within the industry between growers in various regions to aid in improving their efficiencies and will further assist in crop choice in certain areas, as well as possible practices that improve WUE and WUP.

The aim of this chapter was to quantify  $T_c$  of both 'Wichita' and 'Choctaw' cultivars to determine if  $T_c$  will differ daily in accordance to canopy development, crop load and the prevailing weather conditions that will possibly lead to different seasonal crop water use values. Furthermore, pecan ET values obtained at Vaalharts were compared to measured values in Cullinan, as it was hypothesized that ET in Vaalharts would be higher than previous measurements in Cullinan, due to a longer growing season and hotter conditions. The main contributors to ET were determined, as well when the contribution of each component was greatest. Lastly the viability of growing this high-water demanding crop was determined under semi-arid conditions and was compared to other horticultural crops for justification considering the ratio of yield to water use, as well as the monetary value of the yield.

## 4.2 Materials and Methods

Materials and methods pertaining to Chapter 4 can be found in Chapter 3.2, Chapter 3.3, Chapter 3.5, Chapter 3.6, Chapter 3.7 and Chapter 3.8.

## 4.3 Results

### 4.3.1. Weather conditions

To define the conditions under which measurements were made, weather data was recorded by an automatic weather station (AWS) for the duration of the trial. As seen in Figure 4.1,  $R_s$  demonstrated typical seasonal variation, reflecting long days in summer and shorter days in winter. Temperatures steadily increased from the initial installation in September 2018 up to the end of January 2019, and then started to gradually decrease to the minimum at the end of May. The minimum temperature for the measurement period was  $-4.08\text{ }^{\circ}\text{C}$  on 15 June 2019 and the maximum temperature was  $40.28\text{ }^{\circ}\text{C}$  on 17 January 2019. Out of the 365 days measurement period, 83 days experienced temperatures exceeding  $35\text{ }^{\circ}\text{C}$  (23% of the season). The total seasonal (Sept 2018 – Sept 2019) rainfall was 359 mm. Rainfall events with highest amounts of precipitation were widely distributed between December 2019 and April 2019. The daily maximum VPD for the season was 4.05 kPa and the minimum was 0.4 kPa, with a daily average of 2.11 kPa for the 2018-2019 season. For the measurement season VPD exceeded 2.5 kPa for 109 days (30% of the season). The total reference evapotranspiration ( $ET_o$ ) for the season was 1597 mm, which is indicative of the hot, dry growing conditions (semi-arid) of Vaalharts as it greatly exceeded precipitation. Total growing degree days (GDD) for the 2018/19 season amounted to 1861 days.

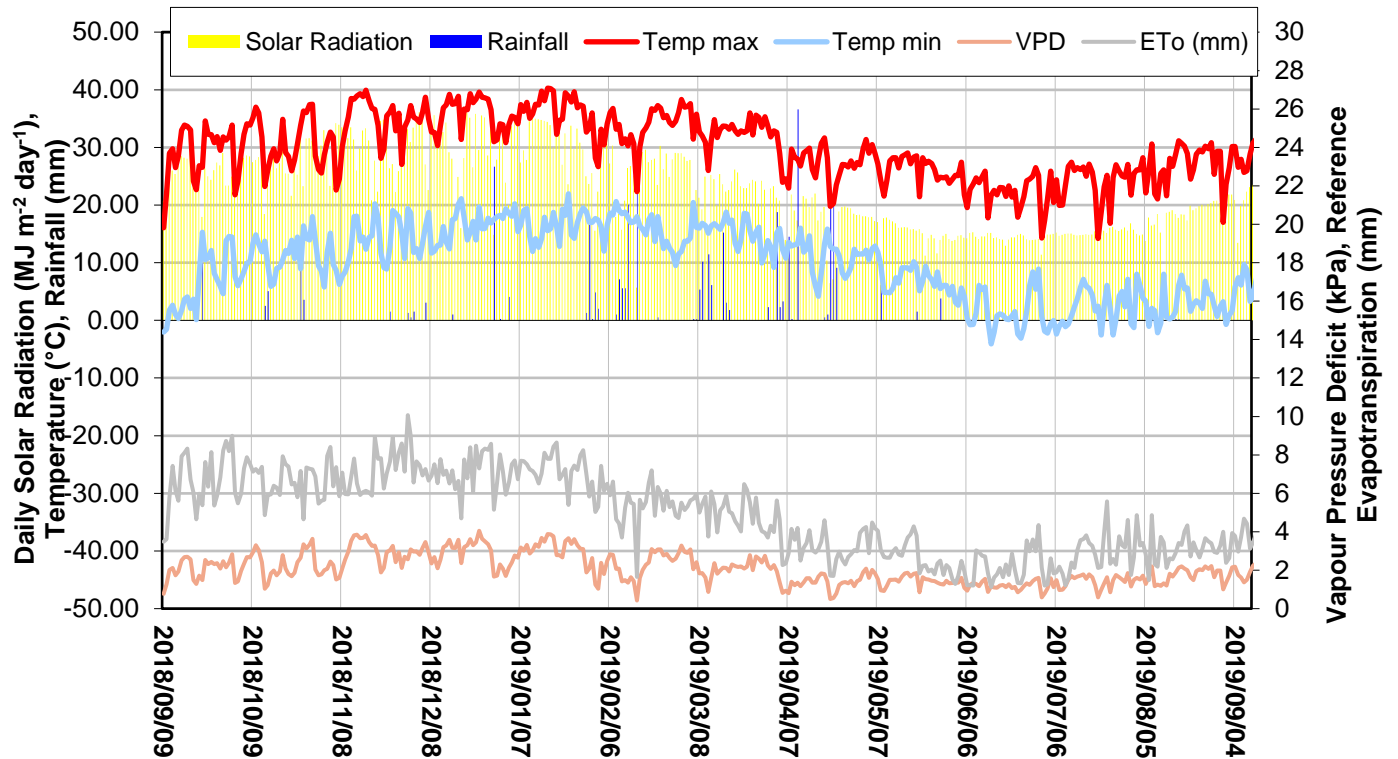


**Figure 4.1** Weather data from the automatic weather station from 09 September 2018 until 09 September 2019, which included solar radiation ( $\text{MJ m}^{-2} \text{ day}^{-1}$ ), minimum (Temp min) and maximum (Temp max) temperature ( $^{\circ}\text{C}$ ), seasonal rainfall (mm), vapor pressure deficit (VPD) (kPa) and reference evapotranspiration ( $\text{ET}_o$ ) (mm).

#### 4.3.2. Pecan transpiration and Canopy Development

Canopy transpiration ( $T_c$ ) of both ‘Wichita’ and ‘Choctaw’ cultivars were measured to determine estimates of  $T_c$  under semi-arid conditions. The  $T_c$  measurements differed between the two measurement cultivars; whereby ‘Wichita’ trees used less water throughout the season (887 mm) than ‘Choctaw’ trees (925 mm). Maximum daily  $T_c$  also differed between the two cultivars, for ‘Wichita’ trees it was  $425 \text{ L tree}^{-1} \text{ day}^{-1}$  ( $4.25 \text{ mm day}^{-1}$ ), whilst for the ‘Choctaw’ trees the maximum  $T_c$  was  $508 \text{ L tree}^{-1} \text{ day}^{-1}$  ( $5.1 \text{ mm day}^{-1}$ ) (Figure 4.11). Average daily  $T_c$  for the middle of the season (December to March) was  $356 \text{ L day}^{-1}$  for the ‘Wichita’ trees, whilst average daily  $T_c$  for the ‘Choctaw’ trees for this period was  $408 \text{ L day}^{-1}$ .

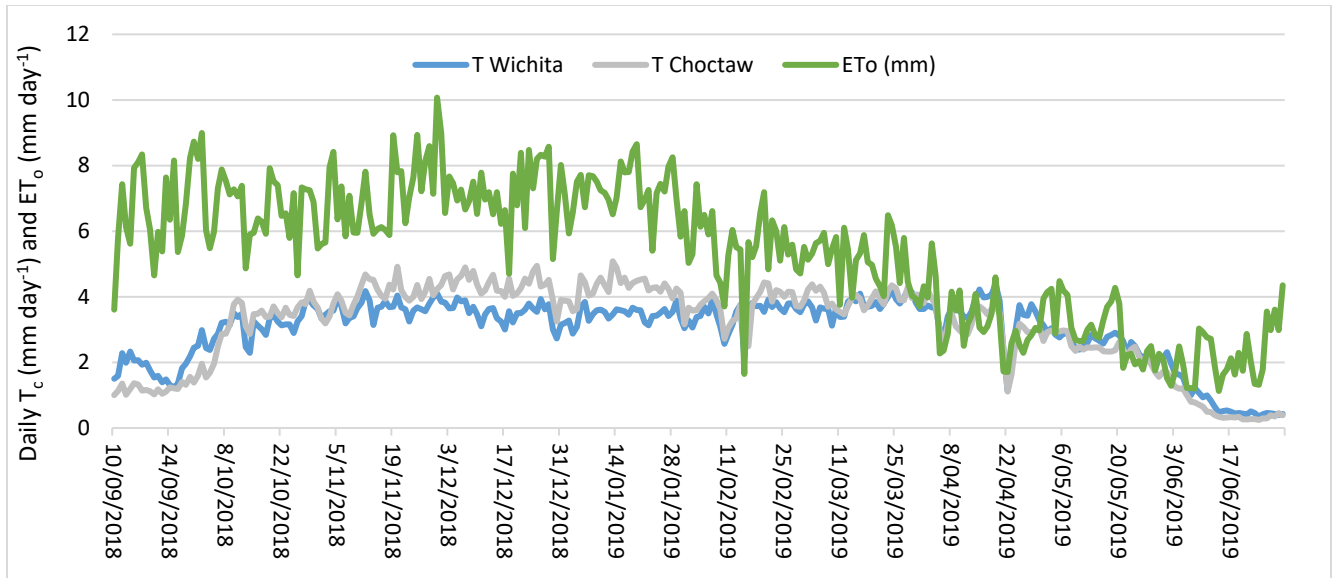


**Figure 4.11 Measured daily transpiration rates ( $T_c$ ) of ‘Wichita’ (Blue line) and ‘Choctaw’ (Grey line) cultivars and corresponding reference evapotranspiration ( $ET_o$ ) (mm) (Green line) measurements during the 2018-2019 production season.**

Seasonal  $T_c$  is linked to the leaf area of a tree which is able to evaporate water from its surface, as this will dictate possible maximum  $T_c$  for a given atmospheric evaporative demand when soil water is not a limiting factor. For deciduous species, such as pecans, the leaf area index (LAI) changes throughout the season. When assessing changes in canopy size (leaf area index-LAI) over the season it was evident that there was a rapid increase in LAI as the trees came into leaf at the start of the season, with ‘Choctaw’ having a greater increase in LAI compared to ‘Wichita’ (Figure 4.3). There was a steady increase in LAI throughout the season, until a peak was reached for ‘Choctaw’, on 21 May 2019, and for ‘Wichita’, on 5 March 2019, whereafter LAI of both cultivars decreased, with senescence starting shortly after each cultivar reached their respective peaks. Whilst canopy size was very similar between the two cultivars at the start of the season, the LAI varied from the end of May, where ‘Choctaw’ trees had higher LAI than the ‘Wichita’ trees, as a result of a larger second seasonal flush.



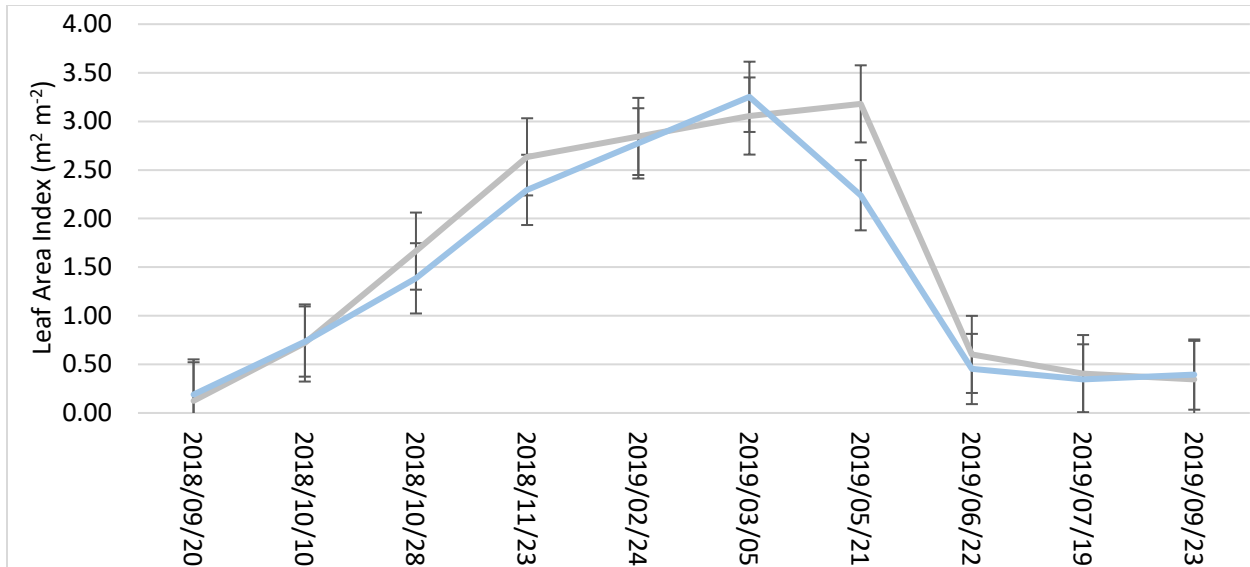


**Figure 4.3 Average leaf area index (LAI) of 'Choctaw' (tree 1 and 2) (Grey line) and 'Wichita' (tree 3 and 4) (Blue line) pecan trees in Vaalharts over the 2018-2019 production season. Error bars indicate the standard error of the two trees.**

The change in LAI of the 'Wichita' trees at site A closely mimicked the same seasonal change in  $T_c$ . The 'Choctaw' trees, that had the higher LAI, maintained higher  $T_c$  rates and used more water throughout the measurement period. The LAI increased as the trees come into leaf, reaching a maximum LAI causing the  $T_c$  to be at its highest, but the LAI decreased at a greater rate compared to the  $T_c$  rates that decreased at a more constant rate. As mentioned, there was a more pronounced second flush in 'Choctaw' trees which could have resulted in the trees staying in leaf longer.

To eliminate some of the variability caused by weather conditions, transpiration crop coefficients ( $K_t$ ) were determined **Error! Reference source not found.** for 'Wichita' and 'Choctaw' trees (Figure 4.44.4). It can be seen that  $K_t$  follows the same initial trend as measured  $T_c$  as a result of increased LAI for both cultivars, whereby it increased at a rapid rate at the beginning of the season, up until 10 October 2018, where after the increase was more gradual and the difference between the two cultivars became more apparent. During this period high rates of  $T_c$  were observed with high  $ET_o$ , suggesting the relationship stayed constant, along with a constant LAI causing the plateau of  $K_t$  during the period between 11 October 2018 and 9 February 2019. The biggest difference was from 10 February 2019 until 6 June 2019 whereby the  $K_t$  increased. This increase occurred at the same time as the increase in LAI towards the end of the season. During this period the pecan trees-maintained  $T_c$  rates similar to rates in the middle of the season, whilst  $ET_o$  was decreasing as a result of cooler temperatures and lower solar radiation. This resulted in



an increase in  $K_t$  values at this time. During the period of 9 May 2019 until 15 June 2019, the  $T_c$  of both measurement cultivars declined rapidly, but within that period the  $K_t$  value was still high between 9 May 2019 and 2 June 2019, which again is attributed to lower  $ET_o$  values relative to  $T_c$ . At the onset of leaf senescence (28 May 2019),  $T_c$  rates of both cultivars dropped dramatically, and the  $K_t$  values decreased significantly.

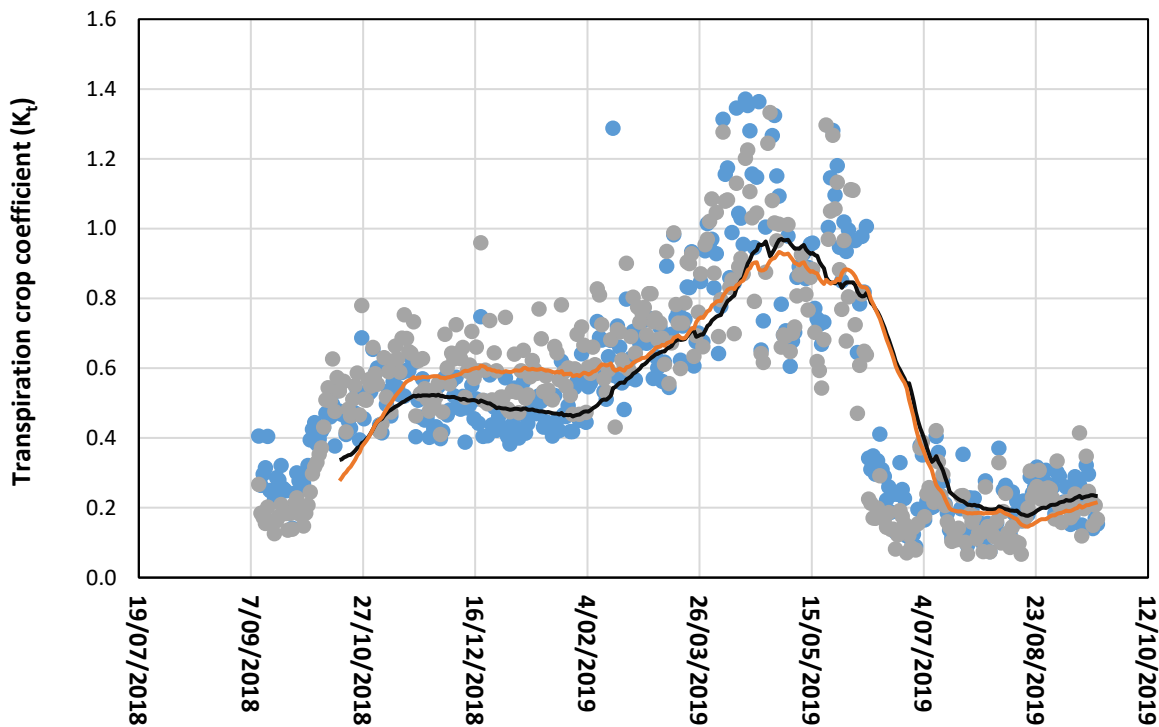


**Figure 4.4** Seasonal transpiration crop coefficient ( $K_t$ ) of 'Wichita' (blue dots) and 'Choctaw' (grey dots) and the daily average (across three days) of each respective cultivar represented by the black line for 'Wichita' and the orange line for 'Choctaw' through the course of the 2018-2019 production season.

#### 4.3.3. Soil Evaporation

Measurements of daily soil evaporation ( $E_s$ ) were conducted to assess spatial and temporal variability of  $E_s$  within the area allocated to each tree, on a daily and seasonal basis (Figure 4.5). Measurements were conducted using micro-lysimeters. The first five measurements between the 21 and 28 October 2018 were done with the initial layout, indicated with patterned bars (Figure 3.). The second layout (Figure 3.) was used for the remainder of micro-lysimeter measurements. When comparing the two micro-lysimeter layouts it was evident that the second layout (Figure 3.) provided useful additional information regarding the spatial assessment of  $E_s$  in the area allocated to a tree. When considering the temporal variation of total  $E_s$  throughout the season it can be

seen that the  $E_s$  increased at the beginning of the season, reaching a maximum daily  $E_s$  of  $1.67 \text{ mm day}^{-1}$  on the 4 December 2018, where after it gradually declined until 10 April 2019 where there was a small increase in  $E_s$  as a result of rainfall, and further declines to reach the lowest value of 2019 on 22 May 2019 of  $0.45 \text{ mm day}^{-1}$ , where after  $E_s$  starts to increase nearing the end of the measurement period. The wetted areas constituted of both irrigation and rainfall, and dry areas only considered rainfall. Considering the spatial variation, it is evident that the highest evaporation rates were recorded in the area that was wetted and exposed to radiation, followed by the wetted and shaded and dry and radiation exposed, and lastly the area that was dry and shaded.

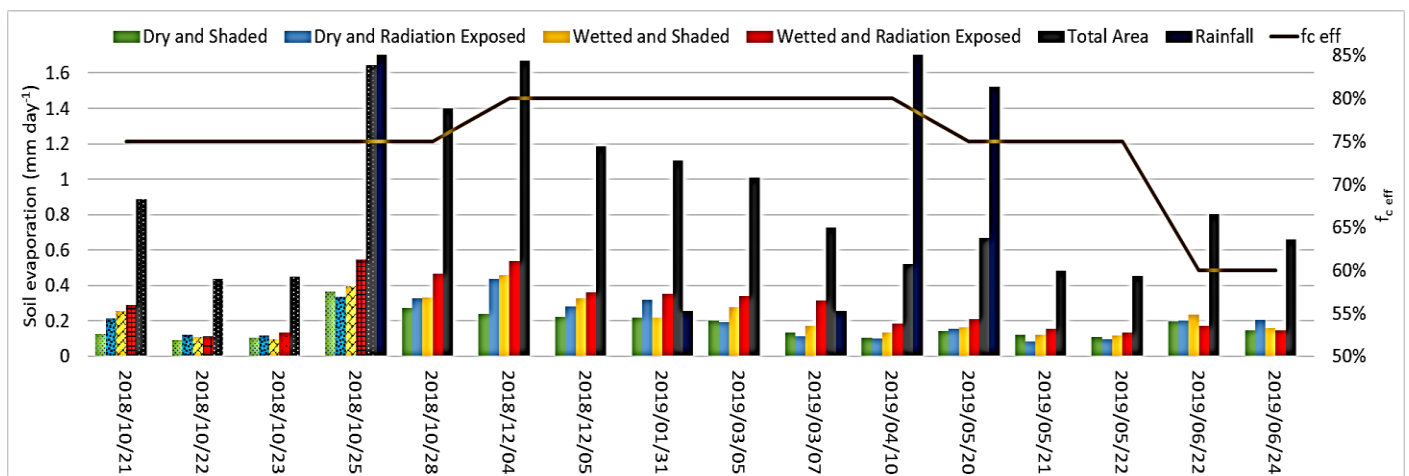


**Figure 4.5 Spatial and temporal variation of average daily soil evaporation ( $E_s$ ) ( $\text{mm day}^{-1}$ ) from micro-lysimeters throughout the 2018/19 season. Rainfall (mm) and the corresponding  $f_c$  eff (%) are plotted on the secondary y-axis. The first four measurement days represent measurements from the initial micro-lysimeter layout (Figure 3.), whilst the bars with no patterns represent micro-lysimeter measurements from the second layout (Figure 3.).**

To determine the cause of the spatial and temporal variation in  $E_s$  the two-stage function of  $E_s$  was explored, as discussed in Chapter 2.2.2. During stage 1 (energy limited phase) PAR was measured at the soil surface to indicate if solar radiation would be a factor limiting evaporation. Photosynthetic active radiation (PAR) received at the soil surface where the micro-lysimeters were placed was evaluated, in relation to the LAI of the 'Wichita' tree under which the micro-lysimeters were placed (Figure 4.6). Photosynthetically active radiation received at the soil surface varied according to the position of the micro-lysimeter, as well as the date of measurement, which was influenced by the LAI of the tree. On the first measurement date when LAI was fairly low areas exposed to radiation had the highest PAR followed by the shaded areas. The amount of measured PAR at the surface was the highest for all measurements at this point, as canopy cover was still sparse and there was high incident  $R_s$  on that day. When LAI was at a

maximum, the area exposed to radiation, and within the wetted zone of the sprinklers, received the highest amount of PAR as compared to the area exposed to radiation without being wetted. The micro-lysimeters under the tree (shaded areas) had the lowest PAR measurements up until the last measurement (22 June 2019), whereby leaf senescence was complete and the PAR received by the microlysimeters underneath the canopy was higher than measurements in 21 May 2019 and would have influenced evaporation rates as seen in Figure 4.5.

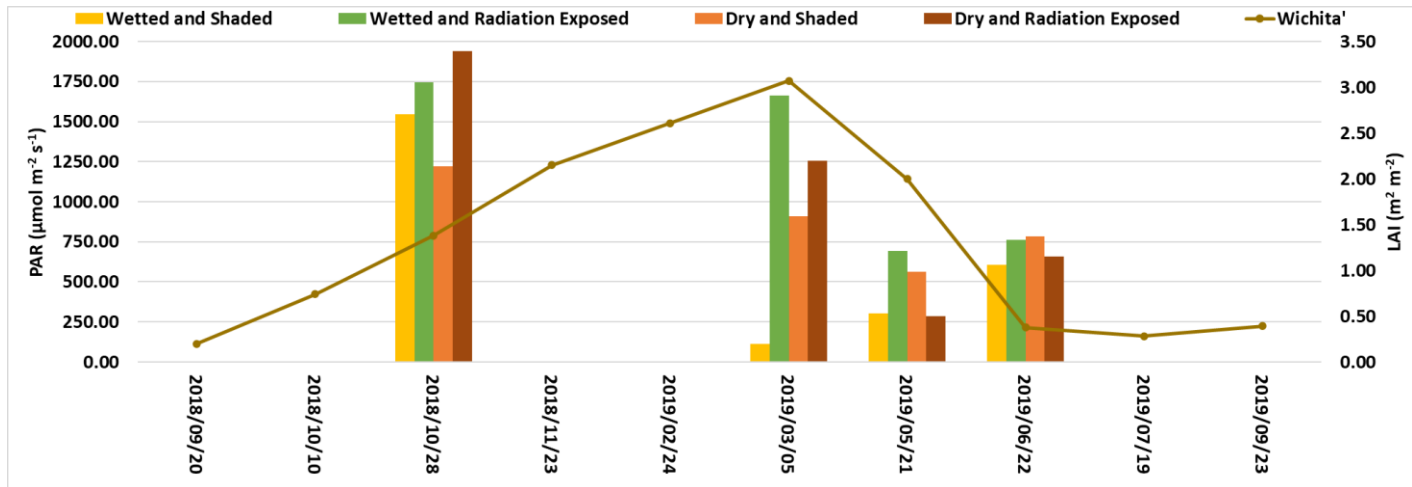


**Figure 4.6** Photosynthetic active radiation (PAR) ( $\mu\text{mol m}^{-2} \text{s}^{-1}$ ) at the received at the soil surface where the soil-micro-lysimeters were placed on selected days in relation to the leaf area index (LAI) of 'Wichita' tree 4 at Site B (brown line).

As evaporation is also limited by the volume of water present in the soil (falling rate stage), the irrigation uniformity was tested to determine the wetting pattern as a result of irrigation (Chapter 3.3). There was considerable variation in irrigation distribution across the orchard floor (Figure 4.7). The highest amount of irrigation was recorded within a distance of 2 m from the macro-sprinkler (therefore 3 m from the tree trunk), decreasing as the distance from the sprinkler head increased. From these results it is evident that the area under the tree received the least amount of irrigation water (between 3 and 5 m from the sprinkler), followed by the area 2 m from the sprinkler which had the highest amount of irrigation and lastly the area 1 m from the sprinkler had the second highest amount of irrigation. If the area under the tree receives sufficient irrigation, the potential rate for evaporation is mainly determined by the energy supply received at the surface, but the frequency of irrigation would affect how much water is available to evaporate between irrigation events. The pattern of radiation received on the orchard floor was quite variable during the season and therefore influenced the evaporation rates underneath the canopy during times when the trees were in leaf (shaded). It can be seen that the areas receiving the least amount of irrigation had the highest rates of  $E_s$  as a result of the high amount of radiation received at these

areas in the orchard (positions 1, 7, 18 and 24 were wetted and were exposed to radiation), compared to the area underneath the canopy where high amounts of irrigation water were received but solar radiation levels were low.

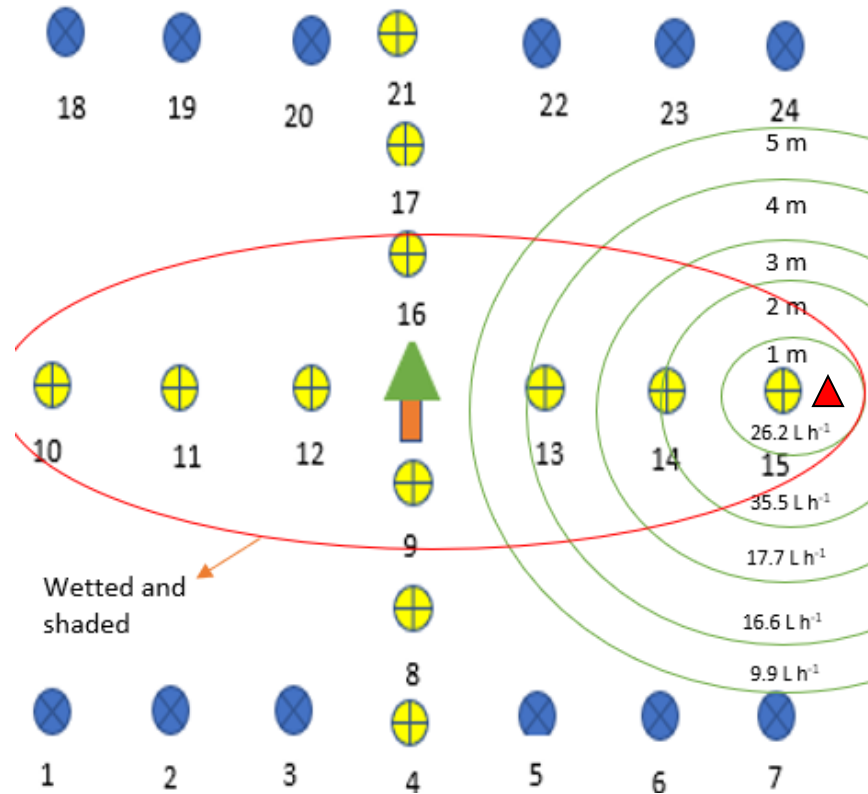
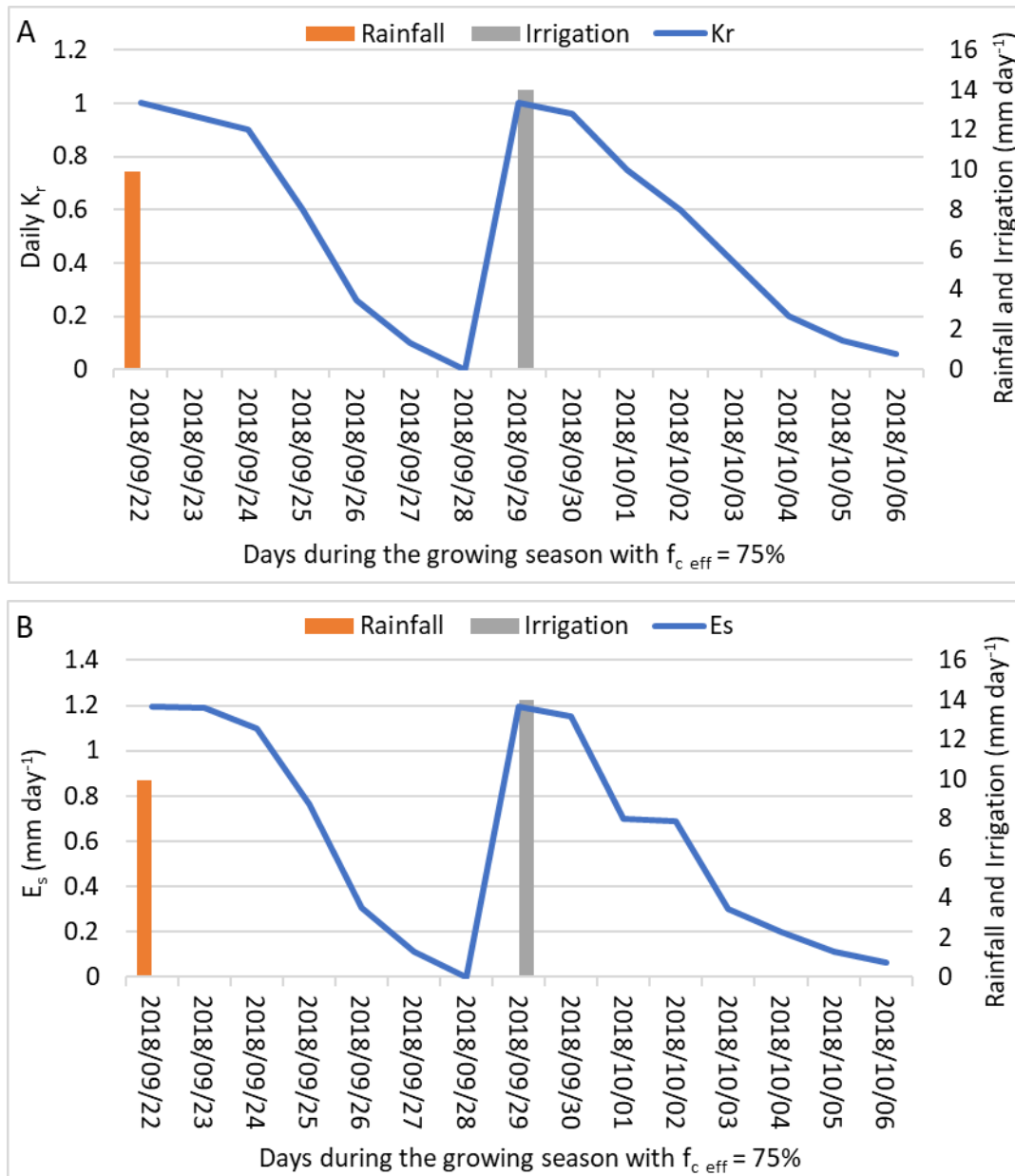


Figure 4.7 Irrigation uniformity test ( $L h^{-1}$ ) at set 1 m intervals from macro-sprinkler (represented by red triangle) on the second micro-lysimeter layout for reference (numbered 1 to 24).

In order to determine the accuracy of  $E_s$  estimation, derived from the FAO-56 method, the reaction of the  $K_r$  function was evaluated, which is the dimensionless evaporation reduction coefficient, after a rainfall and irrigation event, along with the accompanying estimated  $E_s$  for the same period (Figure 4.8). The dates considered were after a rainfall event (9 mm) and irrigation (14 mm), and it can be seen that  $K_r$  reached its maximum of 1 after each event, whereafter there was a slight decrease a day after the wetting event, followed by a rapid decrease thereafter until the next wetting event (Figure 4.8A). The resultant estimated  $E_s$  followed a similar pattern whereby the daily  $E_s$  rate increased after the wetting event, but the  $E_s$  rate only reached its maximum a day after the rainfall event, with a similar decreasing pattern.



**Figure 4.8 A) Estimates of the soil evaporation reduction cycle ( $K_r$ ) and B) soil evaporation ( $E_s$ ) (mm day<sup>-1</sup>), after a respective rainfall (mm day<sup>-1</sup>) and irrigation (mm day<sup>-1</sup>) event, measured on a daily basis during a period when the effective canopy cover ( $f_{c\text{ eff}}$ ) was 75% in Vaalharts.**

The accuracy of the  $E_s$  model modelling approach was assessed using both parameterization and validation data sets, with eight micro-lysimeter measurements used for each phase of model assessment (Figure 4.9). The performance of the model was good with  $R^2$  varying between 0.84 for parameterization and 0.8 for validation phase, which is within the acceptable standards. Parameterization (Figure 4.9A) performance had a D value of 0.97, RMSE of 0.17, MAE of 11% and crm of 0.95, whilst the validation (Figure 4.9B) had D value of 0.97, RMSE of 0.14, MAE of 10% and crm of 0.85. The MAE is below the threshold of 20% for both parameterization and

validation which indicates that the slight deviation is still within acceptable limits. Based on the positive CRM value the deviation is attributed to an underestimation of estimated  $E_s$  values.

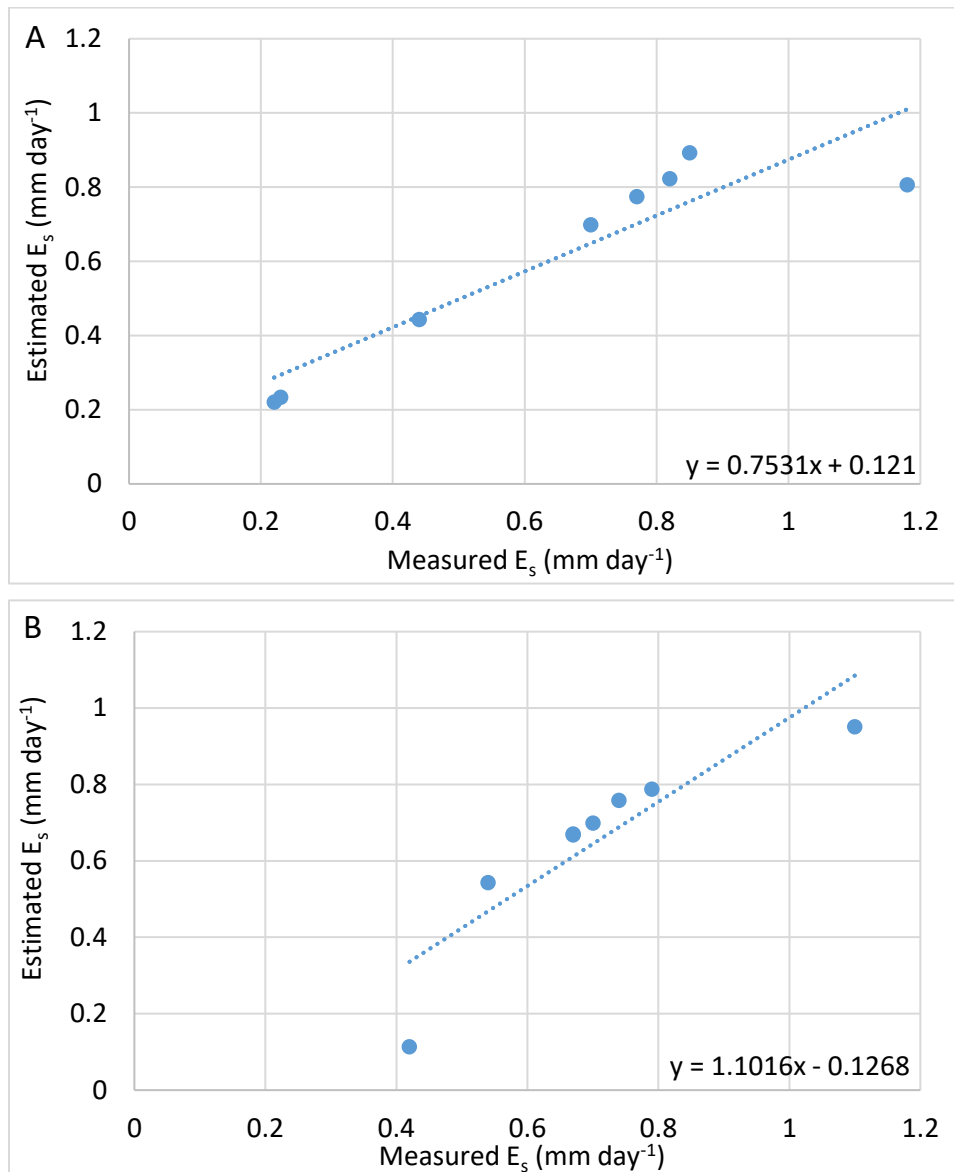


**Figure 4.9 (A) Parameterization (n=8) and (B) validation (n=8) of  $E_s$  estimates using the FAO-56 dual  $K_c$  model for a sandy loam soil in the mature pecan orchard in Vaalharts.**

Evaluating the estimated  $E_s$  trend, derived from the FAO-56 method, over the course of the season (300.75 mm evaporated across the season), along with accompanying LAI and  $ET_o$ . It can be seen that at the beginning of the season, when LAI was starting to increase, the rate of  $E_s$  fluctuated quite significantly on a daily basis according to fluctuating  $ET_o$  patterns (Figure 4.10). When LAI was at its maximum,  $ET_o$  started to gradually decline, but  $E_s$  continued to fluctuate. Once LAI started to decline the  $ET_o$  also decreased along with the  $E_s$  rate. The  $E_s$  only decreased

for a short period whereafter there were large fluctuations in  $E_s$  rates until 10 June 2019. Hereafter  $E_s$  started to increase, as during this latter time there was plant available moisture as rainfall was prevalent and irrigation practices prevented soil dry down from occurring.

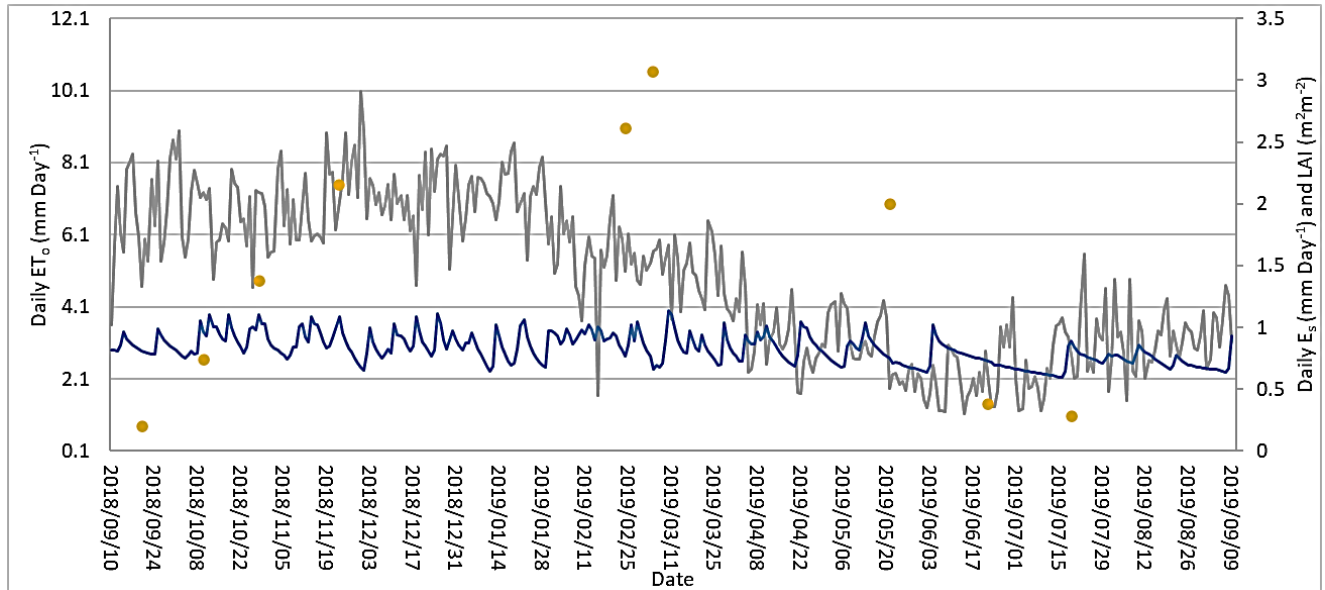


**Figure 4.10 Seasonal estimated  $E_s$  ( $\text{mm day}^{-1}$ ) (blue line) with the varying LAI ( $\text{m}^2 \text{m}^{-2}$ ) (yellow dots) and the accompanying  $ET_0$  ( $\text{mm day}^{-1}$ ) (grey line) for the 2018-2019 measurement period.**

#### 4.3.4. Pecan evapotranspiration and partitioning

For the 2018/19 season ET was determined as the sum of  $T_c$  (average of the four ‘Choctaw’ and ‘Wichita’ trees respectively), determined using the heat ratio method and soil evaporation ( $E_s$ ), determined using the FAO-56 evaporation model. The average seasonal ET (September 2018 until August 2019) for ‘Choctaw’ and ‘Wichita’ trees for this study site was 1136 mm and 1233 mm respectively. There was good correlation between ET, determined as the sum of  $T_c$  and  $E_s$ , and ET from the tower, for the months of June and July 2019, but ET measurements from the tower was lower in May 2019 and higher in August 2019 (Figure 4.11). At the onset of the growing season, between the months of September and November 2018 the increase in monthly total ET and monthly average  $K_c$  values reflected the increase in canopy cover at this time (Figure 4.11). From January onwards,  $ET_0$  typically started to decline at a rapid rate, which was accompanied by a gradual decline of ET. The sudden increase in  $K_c$  values during the period of April and May, was as a result of ET exceeding  $ET_0$ , which could be attributed to the second growth flush that occurs in pecans at this time. After May ET,  $ET_0$  and  $K_c$  declined rapidly as leaf senescence and leaf drop began.



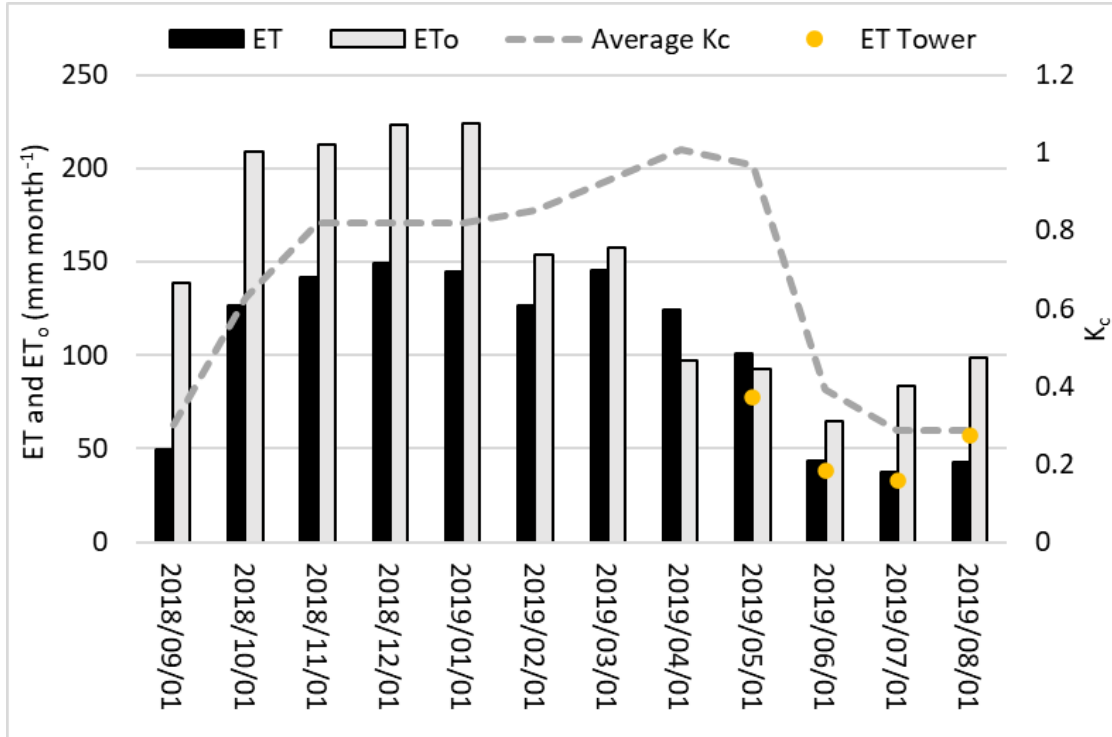


**Figure 4.11 Monthly measured evapotranspiration (ET), ET from Eddy covariance tower and reference evapotranspiration (ET<sub>0</sub>) with crop coefficients (K<sub>c</sub>) of a 14-year-old pecan orchard during the 2018/19 production season.**

In order to improve irrigation scheduling techniques and modelling of water use, an accurate estimate of ET, partitioned into T<sub>c</sub> and E<sub>s</sub>, is required in order to better understand beneficial and non-beneficial consumptive water use (Figure 4.12). In the 14-year-old pecan orchard, T<sub>c</sub> accounted for 78% of total ET, with E<sub>s</sub> accounting for the remaining 22% of the total ET in the 2018/19 production season when the trees were in leaf (October-May). Evaporation was highest at the onset and conclusion of the season when canopy cover was sparse, contributing between 36 and 52% to total ET in the months of September 2018 and June 2019, respectively.

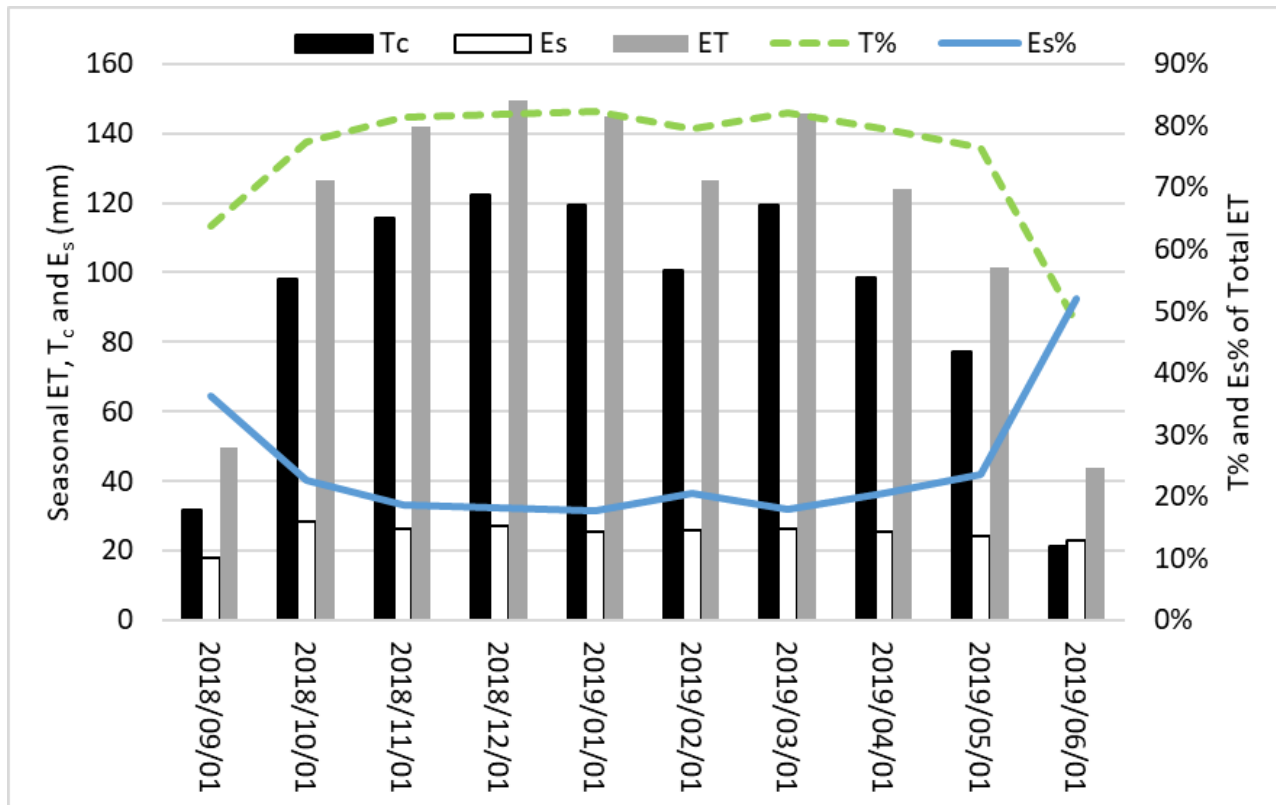


**Figure 4.12** Partitioning of pecan evapotranspiration (ET) into total monthly transpiration ( $T_c$ ) and modelled soil evaporation ( $E_s$ ) in the 14-year-old mixed cultivar pecan orchard during the 2018-2019 production season in Vaalharts, South Africa, as well as the percentage contribution of  $T_c$  and  $E_s$  to total ET.

#### 4.3.5. Pecan water use efficiency and productivity

The water use efficiency (as described in Section 2.2.3) of pecan trees was calculated as the ratio between yield (nut in shell) and ET, with ET estimates derived as the sum of average  $T_c$  for each cultivar (average of the four trees of each measurement cultivar) and  $E_s$  estimates from the FAO-56 evaporation model. In this study it varied between  $0.24 \text{ kg m}^{-3}$  for ‘Choctaw’ trees during an ‘off-year’ and  $0.40 \text{ kg m}^{-3}$  for ‘Wichita’ trees during an ‘on-year’ (Table 4). When comparing these results with published estimates, WUE for the ‘Wichita’ trees in an ‘on-year’ at Vaalharts was higher than other reported values for pecans. In Cullinan estimates varied between  $0.14 \text{ kg m}^{-3}$  in an ‘off-year’ to  $0.23 \text{ kg m}^{-3}$  in an ‘on-year’ (Ibraimo, 2018), with similar results in Las Cruces, where WUE varied between  $0.24 \text{ kg m}^{-3}$  (Sammis et al., 2004) and  $0.19 \text{ kg m}^{-3}$  (Miyamoto, 1983). The difference could possibly be attributed to the higher yield obtained in Vaalharts in comparison to Cullinan, whereas the differences between Vaalharts and Las Cruces could be attributed to a lower seasonal ET in Vaalharts as compared to Las Cruces. Water use efficiency of ‘Wichita’ trees at Vaalharts was comparable to the WUE of macadamias (average WUE of  $0.42 \text{ kg m}^{-3}$  (Ibraimo, 2018)) or other oil bearing crops such as olives (average WUE of  $0.19 \text{ kg m}^{-3}$

(Fernandes-Silva et al., 2010)). However, WUE of 'Choctaw' trees was lower than these crops, as a result of the off year. When compared against high yielding crops such as table grapes (between 1.69 and 7.71 kg m<sup>-3</sup> depending on irrigation method) (Du et al., 2008) or citrus (1.97 kg m<sup>-3</sup>) (García-Sánchez et al., 2007), WUE is much lower in pecan trees as a result of its lower yields, indicating the carbohydrate expense of producing oil bearing crops, and its high water use as a result of the large canopies of pecans trees.

The estimation of water use productivity (WUP) is very important for low yielding but high value crops, such as pecans, as it assigns a monetary value to the water used to cultivate the crop, which governs if the crop justifies its water use to cultivate. There are numerous factors that can cause WUP to fluctuate within a season, prices can fluctuate according to the demand and supply function for that season, the weather will influence water use as it's dictated by ET<sub>o</sub>, alternate bearing pattern of certain cultivars, as well as for the quality of the crop under consideration. It is therefore important to compare data over a few seasons to determine accurate and fair values for pecans. This study provides the first estimates of WUP for pecans in South Africa, but only for the 2018/19 season. The WUP differed between 'Choctaw' (R18.44 m<sup>-3</sup> in an 'off-year') and 'Wichita' (R26.59 m<sup>-3</sup> in an 'on-year') trees, as both yield and quality were higher for 'Wichita' trees, which resulted in higher income (Table 4.1). Pecan irrigation water use efficiency (IWUE) varied between 0.019 kg m<sup>-3</sup> for 'Choctaw' ('off-year) and 0.031 kg m<sup>-3</sup> for 'Wichita' ('on-year') trees in Vaalharts. The IWUE of the 'Choctaw' trees in this study were comparable to the study by Sammis et al., (2004) as the yield obtained was similar to the yield used to derive IWUE for micro-sprinklers (2800 kg ha<sup>-1</sup>) and furrow irrigation (2500 kg ha<sup>-1</sup>). This was higher than the average reported for pecans (0.016 kg m<sup>-3</sup> (Sammis, 1980)), but was lower than values reported specifically for micro-sprinkler (0.044-0.659 kg m<sup>-3</sup>) and furrow irrigation (0.086-0.56 kg m<sup>-3</sup>) in pecans (Sammis et al., 2004; Sammis, 1980). This could be attributed to the high surface area covered by macro-sprinkler irrigation used within this study. As these results were only based on a single season, and pecans exhibit alternate bearing patterns, the WUE and WUP will differ across seasons and warrants further measurement. The transpiration water use efficiency (TWUE) was greater than the measured WUE as the T<sub>c</sub> component is lower than ET (creates inverse effect to increase WUE).

**Table 4.1 Crop yield, seasonal water use (ET), total income, total water applied, water use efficiency (WUE), water use productivity (WUP), irrigation water use efficiency (IWUE) and transpiration water use efficiency (TWUE) for two pecan cultivars under non-limiting soil water conditions for the 2018/19 production season.**

Cultivar	Crop Yield (kg ha <sup>-1</sup> nut in-shell)	Seasonal ET (m <sup>3</sup> )	Income (R ha <sup>-1</sup> )	Total Applied Water (m <sup>3</sup> ) (Irrigation + Rainfall)	WUE (kg m <sup>-3</sup> )	WUP (R m <sup>-3</sup> )	IWUE (kg m <sup>-3</sup> )	TWUE (kg m <sup>-3</sup> )
'Choctaw'	2800	11595	213850	14730	0.24	18.44	0.019	0.30
'Wichita'	4550	11130	296000	14730	0.40	26.59	0.031	0.51

#### 4.4 Discussion and Conclusion

When considering the constituents of ET ( $T_c$  and  $E_s$ ) separately, a more profound understanding can be achieved of crop water use. The importance of irrigation in this region is demonstrated by comparing total seasonal  $T_c$  (925 mm for 'Choctaw' and 887 mm for 'Wichita') and measured rainfall (359 mm) for the same period, as seasonal rainfall events are too erratic and limited to meet tree water demand and to sustain optimal crop production. The climatic conditions for the measurement period can be described as hot, dry growing conditions as the total  $ET_o$  for the season was 1597 mm and greatly exceeded precipitation. Transpiration in the pecan orchard at Vaalharts varied throughout the season, with the lowest values at the onset and end of the season. This was due to the deciduous nature of pecan trees with the low  $T_c$  rates reflecting the relatively low LAI at the start and end of the season. This study further indicated that  $T_c$  is linked to canopy size, as the higher leaf area for the 'Choctaw' trees led to a higher seasonal  $T_c$  of 925 mm and achieved a higher maximum daily  $T_c$  rate of 508 L tree<sup>-1</sup> day<sup>-1</sup> (during peak conditions) compared to 'Wichita' trees which transpired 887 mm over the season with a maximum daily  $T_c$  rate of 425 L tree<sup>-1</sup> day<sup>-1</sup>. The 'Wichita' trees experienced an 'on' year (higher yields than 'Choctaw') in the Vaalharts region in the 2018-2019 production season and exhibited a less pronounced second flush during the oil accumulation phase, further studies should be performed to indicate if it is due to the low yield of the 'Choctaw' trees or if it relates to other factors. This second seasonal flush of 'Choctaw' trees was probably caused by a surplus of carbohydrate reserves as a result of lower crop load for the 2018-2019 production season, typical of alternate bearing trees, leading to a larger amount of carbohydrates able to act as source to supply a developing flush (Andersen and Brodbeck, 1988; Kozlowski, 1992; Wood et al., 2002). The

second flush was suggested by Ibraimo et al., (2016) to contribute to a six stage crop coefficient as opposed to the traditional four stage crop coefficient curve (Allen et al., 2005).

To eliminate some of the variability caused by weather conditions, were transpiration crop coefficient ( $K_t$ ) determined **Error! Reference source not found.** for 'Wichita' and 'Choctaw' trees. Throughout most of the season,  $K_t$  values were slightly higher for the 'Choctaw' trees than the 'Wichita' trees, reflecting the slightly higher transpiration rates and greater leaf area index (LAI) of these trees. The difference in the rate of increase or decline between  $ET_o$  and  $T_c$  resulted in a 6 stage crop coefficient curve as observed by Sammis et al., (2004) and described by Ibraimo et al., (2016) for pecans. All the measured values were smaller than 1.4 as it is not energetically possible for the  $K_t$  to exceed 1.4 for tall, rough tree crops (Allen et al., 2011c). As suggested by Ibraimo et al., (2016), the key to applying this curve to other regions, is the adjustment for canopy cover and local climate conditions. Estimates of canopy size would therefore be important when modelling  $T_c$  in order to allow for orchard specific estimates of water use.

The rate of  $E_s$  was relatively constant through most of the season but was highest at the onset and end of the season when canopy cover was sparse and frequent irrigation was applied (onset) and higher amount of rainfall occurred (end of season), contributing 36 and 52% to ET in the months of September 2018 and June 2019 respectively. Soil evaporation is dependent on numerous factors that fluctuate on a daily and seasonal basis. This is as a result of spatial and temporal variability of  $E_s$ , which is a function of supply (soil water) and demand (atmospheric variables driving evaporation). Both factors vary as water application is not evenly distributed across the surface and atmospheric variables differ across a day, and weather conditions change daily. From the study by Ibraimo (2018), it was confirmed that  $R_s$  had the greatest impact in determining  $E_s$  rates under non-limiting soil water conditions, which was also observed within current study, whereby soil micro-lysimeters wetted and exposed to radiation had the highest  $E_s$  rates. Similar observations were made by Ibraimo (2018) whereby spatial variation of  $E_s$  was observed as solarimeters underneath the pecan canopy showed lower values close to the trunk due to shading, but at 3 to 4.5 m from the trunk more solar radiation reached the surface. It was also observed that the area having the second highest  $E_s$  received irrigation but was shaded, this could possibly be attributed to canopy porosity which allows for diffuse light to penetrate through the canopy and cause higher  $E_s$  rates to occur. After a wetting event, the  $E_s$  is governed by two stages, with stage 2 (falling rate stage) dominating in this study, as irrigation events were scheduled on average once a week, but for longer periods of time to fill the soil profile to field capacity. This resulted in significant drying of the topsoil in between irrigation events if no rainfall

was received. Although the topsoil was dry, it was unlikely to adversely affect the crop as it is deep rooted and able to access water from deeper in the soil profile. Soil evaporation was successfully estimated with the FAO-56 method, as confirmed by parameterization and validation studies, with seasonal estimates amounting to 301 mm for the season. It was also able to demonstrate temporal variation of  $E_s$ , whereby higher rates were achieved at the onset and conclusion of the season when canopy cover was sparse. The measured  $T_c$ , along with the estimated  $E_s$ , was used to derive ET estimated for the entire season.

Seasonal ET of the mature pecan orchard in Vaalharts, grown under predominant semi-arid conditions in a subtropical climate, was lower (1136 mm) than the ET measured for mature orchards in Las Cruces, New Mexico, grown under arid conditions (between 1215 and 1300 mm) (Miyamoto, 1983; Sammis et al., 2004). The variation in ET between Las Cruces and Vaalharts is attributed to the large difference in annual  $ET_o$  between the two study sites (1941 mm for Las Cruces and 1536 mm in Vaalharts), and in Las Cruces the area is characterized by dry and arid conditions with sparse annual rainfall varying between 203 and 228 mm (compared to 301 mm in Vaalharts), high amounts of solar radiation and high summer temperatures (Malm, 2003). The higher ET values could also be attributed to the difference in irrigation system, as the orchards were flood irrigated in New Mexico that increases the amount of  $E_s$  occurring as the wetted area is much larger. The irrigation system used plays a very important role as the more surface area is wetted by irrigation the more area is available for  $E_s$  to occur from, which is illustrated in the study by Sammis et al., (2004) whereby subsurface drip and drip irrigation had the highest IWUE compared to micro-sprinklers or furrow irrigation. However, as the total  $E_s$  is also determined by the frequency of irrigation which was not reported in this study nor from Sammis et al., (2004) or Miyamoto (1983), is it not possible to conclude that the variation in ET between the two study sites are solely driven by different irrigation practices.

Similar differences existed between the orchard in Vaalharts and the one in Cullinan, with the orchard in Cullinan having lower ET (1023 mm averaged over three seasons) (Ibraimo, 2018). The  $ET_o$  between the two South-African trial sites, Cullinan (1583 mm) (Ibraimo, 2018) and Vaalharts (1756 mm) (current study), differed by 173 mm. The difference in ET values between study sites could be attributed to Vaalharts being hotter and drier than Cullinan. In addition, the larger tree size in Cullinan and lower  $E_s$ , as a result of irrigation by micro-sprinklers (wetting diameter of 7 m and discharge of 90 L h<sup>-1</sup>) and more shading from the larger canopy (90% canopy cover) compared to Vaalharts which had macro sprinklers (wetting diameter of 9 m and discharge of 150 L h<sup>-1</sup>) with canopy cover of 82%, could also have contributed to differences, as a higher  $T_c$ .

and lower  $E_s$  rates were expected. The resulting  $E_s$  differed between the two sites whereby Vaalharts had higher  $E_s$  (estimated 300.75 mm) compared to Cullinan (average 147.67 between 2009 and 2011).

It was further found that  $T_c$  was the main contributor (78%) to seasonal ET in the orchard in Vaalharts, with  $E_s$  accounting for 22%. As  $T_c$  was the main contributor to ET through the majority of the season, is it important to try and maximize transpiration through judicious irrigation, as water stress, caused by either a water deficit or waterlogging, can severely impact yield and quality of pecan orchards (Garrot et al., 1993). The biggest water saving can be achieved by limiting  $E_s$  (non-beneficial water use), such as limiting the area exposed to both irrigation and radiation, as seen with  $E_s$  measurements, whereby the highest  $E_s$  rates were experienced in area that were both wet and exposed to solar radiation. This statement was confirmed by evaluation IWUE between different irrigation techniques, whereby IWUE was lowest for irrigation techniques covering more surface area (Sammis et al., 2004). If savings are to be made growers should consider changing to drip irrigation systems in the shaded area of the tree canopy, in areas closest to the tree stem as the highest concentration of fine roots were found in that area. Another consideration to limit  $E_s$  is through mulch application, as seen in in young pecan orchards with sparse canopy cover whereby the  $E_s$  component of ET will be much greater (Ibraimo, 2018). A mulch could also be applied to mature orchards whereby canopy cover is sparse at the onset and conclusion of the season when  $E_s$  rates are high.

The irrigation practice used in this study is not the most efficient, as was confirmed with IWUE benchmarking results where macro-sprinklers with a large wetting diameter had poor IWUE of  $0.019 \text{ kg m}^{-3}$  for 'Choctaw', which could be attributed to higher  $E_s$  occurring as a result of a larger wetting surface compared to micro-sprinklers and furrow irrigation ( $0.086$  and  $0.056 \text{ kg m}^{-3}$  respectively) (Sammis et al., 2004; Sammis, 1980). Only IWUE of the 'Choctaw' trees in this study was used for comparison as the yield obtained was similar to the yield used to derive IWUE for micro-sprinklers ( $2800 \text{ kg ha}^{-1}$ ) and furrow irrigation ( $2500 \text{ kg ha}^{-1}$ ) in the Sammis et al. (2004) study. As yield is a primary determinant of IWUE, and varies between seasons in this alternate bearing crop, differences in IWUE are not only attributed to amount of irrigation applied but the interactive relationship that exists between yield obtained per amount of irrigation used.

After the seasonal ET was considered with its constituents, it is necessary to assess the yield per unit water used by the crop to allow for benchmarking of producers across key regions by assessing the water use efficiency (WUE) and water use productivity (WUP). Further it is a vital comparison to make as it quantifies the amount of water used per unit of economical harvested



crop, which is important in low bearing crops with high water demands, such as pecan. The WUE of pecans in Vaalharts differed between cultivars due to differences in yield and ET, with 'Choctaw' experiencing an 'off-year' with a WUE of  $0.25 \text{ kg m}^{-3}$ , whereas 'Wichita' experienced an 'on-year' with a WUE value of  $0.40 \text{ kg m}^{-3}$ . For growers it is important to try and increase WUE, as it would indicate either an increase in yield with an equivalent ET as previous seasons, or lower ET with a constant yield, which is becoming increasingly important as farmers are under pressure to use water sources more sparingly in semi-arid conditions with erratic and sparsely distributed rainfall patterns. Both scenarios are favorable for a higher economical production per unit water used. As it is often not in the growers' control to maintain a constant high yield for successive seasons, it is important for growers to consider how they can improve WUE by limiting total ET. This can be achieved by viewing the ET constituents separately to determine where water saving techniques can be implemented. The transpiration water use efficiency (TWUE) was greater than the measured WUE as the  $T_c$  component is lower than ET (creates inverse effect to increase WUE), this effect has been described by Begg and Turner (1976) whereby the  $E_s$  component of ET results in unproductive water loss and does not directly equate to a higher yield, which will result in lower WUE. The second indicator growers can use for benchmarking is WUP and this can aid in determining the economic value of the water used to produce the crop. The 'Wichita' cultivar obtained a higher WUP in this study as it had higher yield, quality and lower water use than 'Choctaw' trees. Additional data of various cultivars across a number of years is needed to make allow for more accurate estimations of WUE and WUP as yields fluctuate, water use varies, and market prices are determined seasonally based on the supply and demand of pecan nuts in the local and international market which governs prices.

## CHAPTER 5 KEY FACTORS INFLUENCING PECAN EVAPOTRANSPIRATION

### 5.1. Introduction

The seasonal evapotranspiration (ET) of pecan orchards varies across different production regions (Ibraimo, 2018; Miyamoto, 1989; Samani et al., 2011; Sammis et al., 2004; Wells, 2015). A better understanding of how pecan water use is influenced by the environment in which they are grown might help explain these observed differences. The variation in pecan ET between production regions can be attributed to a number of factors. Atmospheric conditions, especially vapor pressure deficit (VPD), determine the water loss demand, by acting as a continuous and never satisfied water vapor sink that drives water loss from leaf surface. This atmospheric evaporative demand is the result of a number of weather variables, which together with the condition of the boundary layer surrounding a leaf, determines the rate of water loss from the leaf surface into the atmosphere. The degree to which crops can control transpiration rates via stomatal conductance can be described through a decoupling coefficient ( $\Omega$ ) (Jarvis, 1986). A study in a pecan orchard in Cullinan found that pecan trees have a relatively low  $\Omega$  of 0.16, which suggests that pecan trees are well-coupled to the atmosphere (Ibraimo, 2018). Pecan transpiration will therefore be sensitive to changes in stomatal conductance and any factor which influences stomatal conductance will influence transpiration rates. The study by Ibraimo (2018) found that transpiration reached a plateau at VPD above 1.4 kPa, suggesting that pecan stomata start to close in response to high atmospheric evaporative demands and that VPD was the primary determinant of water loss from the leaf surface in pecans followed by solar radiation ( $R_s$ ). It has also been reported that transpiration rate can be decreased as a result of hydraulic limitation together with stomatal regulation (Rodriguez-Gamir et al., 2016). This has implications for transpiration rates of pecan trees under hot and dry conditions, such as those experienced in the Northern Cape Province.

Trees regulate their stomatal aperture in response to constantly changing weather conditions in order to maintain a specific leaf water potential threshold (Jarvis, 1998). This response characterizes their behavioral traits as either isohydric or anisohydric (Roman et al., 2015). Isohydric plants regulate stomatal closure to maintain a constant midday leaf water potential, regardless of environmental demands or soil water deficits (Sade et al., 2012). In contrast, anisohydric plants take more risks, lacking strong stomatal control, leading to fluctuating leaf water potentials with changing atmospheric demand, striving to sustain high photosynthetic rates even when soil water declines (Pou et al., 2012; Sade et al., 2012). For anisohydric species like pecan trees, leaf water potential correlates with plant available soil water (Sade et al., 2012). A

study by Deb et al. (2012) demonstrated a good correlation between midday leaf water potential and soil water content in pecans, suggesting anisohydric tendencies. However, differences between cultivars warrant further investigation. The same study revealed a linear relationship between plant available soil water and stem water potential.

Pecans are known to have a strong correlation between available soil water and plant water status (Deb et al., 2012; Steinberg et al., 1990; Wells, 2015). Nevertheless, the impact of various soil water levels on canopy transpiration ( $T_c$ ) under similar environmental conditions requires further exploration. Wells (2015) recommended measuring these factors during budbreak until nut sizing, excluding kernel filling, as moderate crop load induces water stress irrespective of soil water content. Further to the current study in Vaalharts will it be determined if there exists a correlation between root pattern distribution and water uptake, therefore  $T_c$  rates, as it will validate pecan response to irrigation. It has been determined that not only is the amount of roots available for water uptake important, but also the type of roots within the vicinity of plant available water (PAW) (White Jr and Edwards, 1978). This has been seen in the distribution of fine roots between well-watered and water-stressed trees, where finer roots with lower tissue density occur as a result of high water stress (-200 kPa) (White Jr and Edwards, 1978). In addition, the study by Green and Clothier (1999) illustrated that transpiration rates and sap flow of deeper rooted, well-watered apple trees had a less significant response to irrigation, whereas stressed trees with fine roots, mostly in the top 5 – 10 cm, increased sap flow up to five times as high following irrigation. In the same study the importance of soil water potential was highlighted, as it influences water uptake rate by the roots as well as the water status of the tree. It was shown that the highest root densities occur nearest to the surface, as temperatures are more favorable, and it is in this zone where most of the water application occurs (White Jr and Edwards, 1978).

The aim of this chapter was to determine the influence of key factors on pecan  $T_c$  and ET which might help explain the measured values obtained in Chapter 4. It was hypothesized that transpiration rates within the same cultivar, as well as between the study cultivars 'Wichita' and 'Choctaw', will differ on a daily basis in accordance with canopy development and prevailing weather conditions, leading to different seasonal crop water use values. Pecans exhibit anisohydric tendencies as minimum diurnal leaf water potentials depend largely on prevailing weather conditions, with leaf water potential falling more on days with high midday vapor pressure deficit than days with a low vapor pressure deficit. Therefore by understanding the underlying factors regulating pecan water use it will be possible to select the correct modelling approach for pecan orchard water use.

## 5.2. Materials and Methods

Materials and methods pertaining to Chapter 5 can be found in Chapter 3.2, Chapter 3.3 Chapter 3.4, Chapter 3.5, Chapter 3.6 and Chapter 3.8.

## 5.3. Results

### 5.3.1. Factors influencing transpiration

Scatter plots were used to determine the relationship between hourly atmospheric variables and  $T_c$  for 'Choctaw' and 'Wichita' cultivars (Figure 5.1), giving valuable insight into how  $T_c$  was regulated at a whole tree level in response to its environment. Only the period between November 2018 and April 2019 (when canopy cover was at a maximum), and the hours from 06:00 until 18:00 during the day, were used for the analysis to avoid the confounding effect of limited leaf area and lack of transpiration during the night on the results. It can be seen that when assessing each weather variable individually, and as a whole, there was less scatter in the data for 'Wichita' than the 'Choctaw', but the trend in the response of  $T_c$  to each variable was very similar. From Figure 5.1A and B it can be seen that pecan  $T_c$  had a very good correlation with temperature ( $T_a$ ), as  $T_c$  increased as temperature increased, up until  $T_c$  started to plateau when temperatures started to exceed 30 °C and there was no further increase in  $T_c$  at higher temperatures. Solar radiation had variable effects on  $T_c$ , whereby it initially increased with increasing  $R_s$  but not in a linear fashion and expressed more scattered results at low  $R_s$ , until it reached a plateau at higher levels of incident solar radiation (between 2 – 3 MJ m<sup>-2</sup> h<sup>-1</sup>) (Figure 5.1C and D). Vapor pressure deficit (VPD) had a fairly good correlation with  $T_c$  whereby it initially increased linearly, up until higher VPD levels when a plateau was reached at approximately 1.5 kPa (Figure 5.1E and F). The response of  $T_c$  to reference evapotranspiration ( $ET_o$ ), which is used as an indicator of atmospheric evaporative demand, had a similar response to VPD, whereby it increased in linear fashion at low  $ET_o$ , up until higher values were reached when more scatter in the response was evident and  $T_c$  reached a plateau (Figure 5.1G and H).

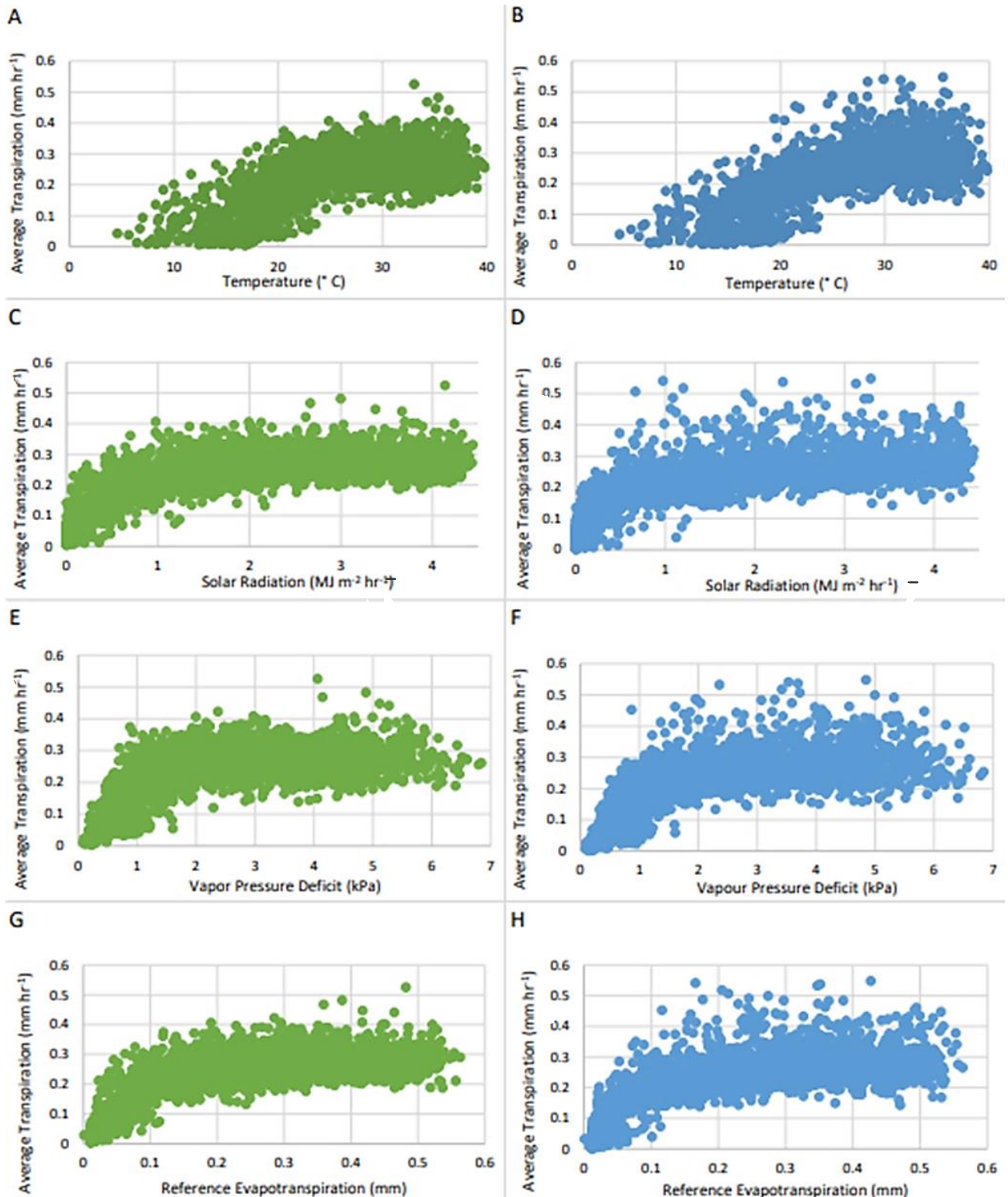
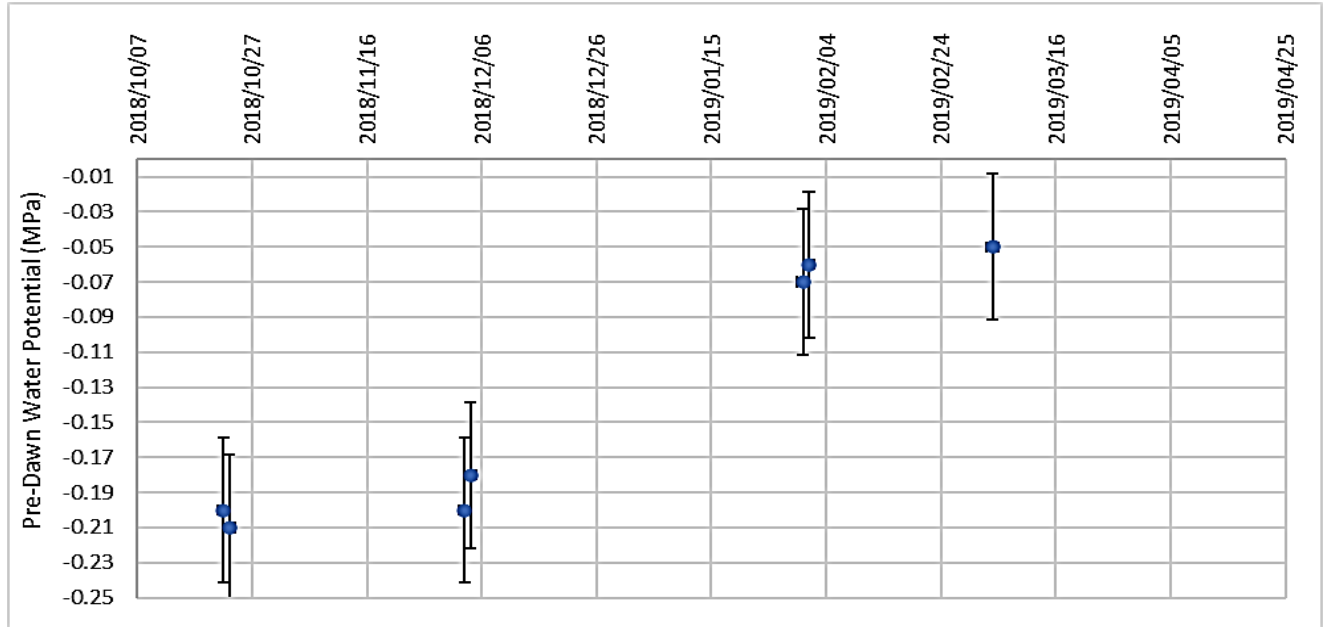


Figure 5.1 The response of hourly transpiration (mm h<sup>-1</sup>) of 'Wichita' (left hand panel) and 'Choctaw' (right hand panel) to atmospheric variables, which included (A & B) air temperature (°C), (C & D) solar radiation (MJ m<sup>-2</sup> h<sup>-1</sup>), (E & F) vapor pressure deficit (kPa) and (G & H) reference evapotranspiration (mm) for the measurement period of November 2018 until April 2019 and during daylight hours (06:00 to 18:00).

### 5.3.2. Pecan ecophysiology

From pre-dawn leaf water potential measurements (Figure .2) was there no evidence of water stress as all the values were higher than the minimum threshold of -0.42 MPa (Taylor, 2020).



**Figure 5.2 Average pre-dawn leaf water potential (MPa) measurements of all four selected measurement trees for transpiration throughout the season.**

Diurnal hourly measurements of water potential ( $\Psi$ ) were also done on three occasions (22 October 2018, 4 December 2018 and 11 April 2019) to determine how pecans react to weather variables which determine the gradient for transpiration. Both sun and shade leaves contribute to whole tree transpiration and thus the water potential of both types of leaves were determined when considering whole tree transpiration as suggested by Cohen et al., (2007). For this study, the fraction of sunlit leaves was estimated to be 60% and the fraction of shaded leaves to be 40%, as a result of the dense canopy of the trees which is influenced by pruning practices. The diurnal variation in  $\Psi$ , as a result of leaf exposure to sun or shade, can be seen in Figure , as well as the resultant hourly  $T_c$  rate and measured VPD. From Figure it is evident that the minimum value for  $\Psi_{sun}$ ,  $\Psi_{shade}$  and  $\Psi_{stem}$  was achieved at the same time on each measurement date but the time of the minimum values varied for the measurement dates. Whilst a minimum was reached at 12:00 in October and December, in April this minimum was only realised at 13:00. It is also clear that sun leaves consistently had the lowest  $\Psi$ . The highest values were found for  $\Psi_{stem}$ , except on 22 October 2018 where it was lower than  $\Psi_{shade}$  from 07:00 until 10:30. Changes in  $\Psi$  and  $T_c$  were not consistent with changes in VPD. This is evident in the April measurement (Figure C), as VPD was lowest on this day yet  $\Psi$  was also lowest and the highest  $T_c$  rate was realised. This is in



contrast to December when VPD was highest, yet the highest  $\Psi$  were measured together with the highest  $T_c$  rate of all the measurement periods. It can be seen that when VPD reaches the threshold of 1.5 kPa, the  $T_c$  rate starts declining and  $\Psi_{\text{sun}}$ ,  $\Psi_{\text{shade}}$  and  $\Psi_{\text{stem}}$  starts increasing.

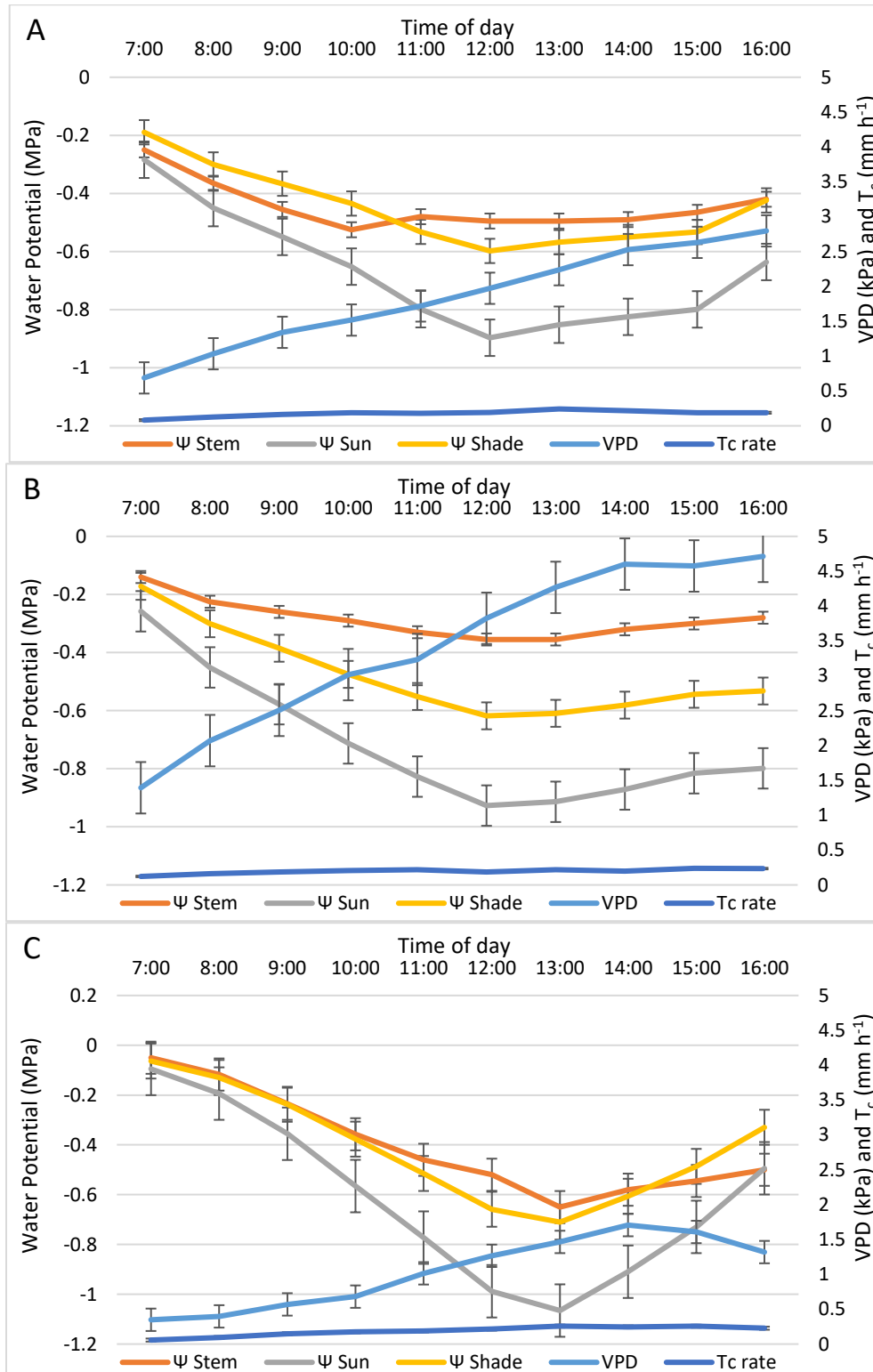




**Figure 5.3 Hourly change in stem water potential ( $\Psi_{\text{Stem}}$ ) (MPa), sun leaf water potential ( $\Psi_{\text{Sun}}$ ) (MPa) and shade leaf water potential ( $\Psi_{\text{Shade}}$ ) (MPa) measurements compared to the vapor pressure deficit (VPD, kPa) and transpiration ( $T_c$ ,  $\text{mm h}^{-1}$ ) for A) 22 October 2018, B) 04 December 2018 and C) 11 April 2019 with standard error indications averaged for four measurement trees.**

The leaf (sun and shade exposed) and  $\Psi_{\text{Stem}}$  in relation to changing VPD was determined on three days (22 October 2018, 04 December 2018 and 11 April 2019, Figure ). With regards to the fluctuation in  $\Psi$  with changing VPD (Figure A, B and C), it can be seen that  $\Psi$  of sun and shade leaves and the stem decreased with the initial increase in VPD at the start of a day, but then at a certain point it no longer decreased with increasing VPD and in some instances  $\Psi$  increased as VPD increased later in the day. The extent and rate of decline of  $\Psi$  differed between measurements depending on the level of VPD reached and whether it was a sun or shade leaf or a measure of  $\Psi_{\text{stem}}$ . The shaded leaves had a good correlation with changing VPD, seen in Figure A, and maintained a higher  $\Psi$  than  $\Psi_{\text{sun}}$  with increasing VPD, but lower than  $\Psi_{\text{stem}}$ . From Figure B can be seen that the sun exposed leaves had the lowest  $\Psi$  of all measurements at corresponding VPD values, and also exhibited the fastest rate of  $\Psi$  decline with increasing VPD values. The correlation between VPD and  $\Psi_{\text{Stem}}$  found a good correlation whereby an increase in VPD resulted in the lowest and slowest decrease in  $\Psi_{\text{Stem}}$  (Figure C).

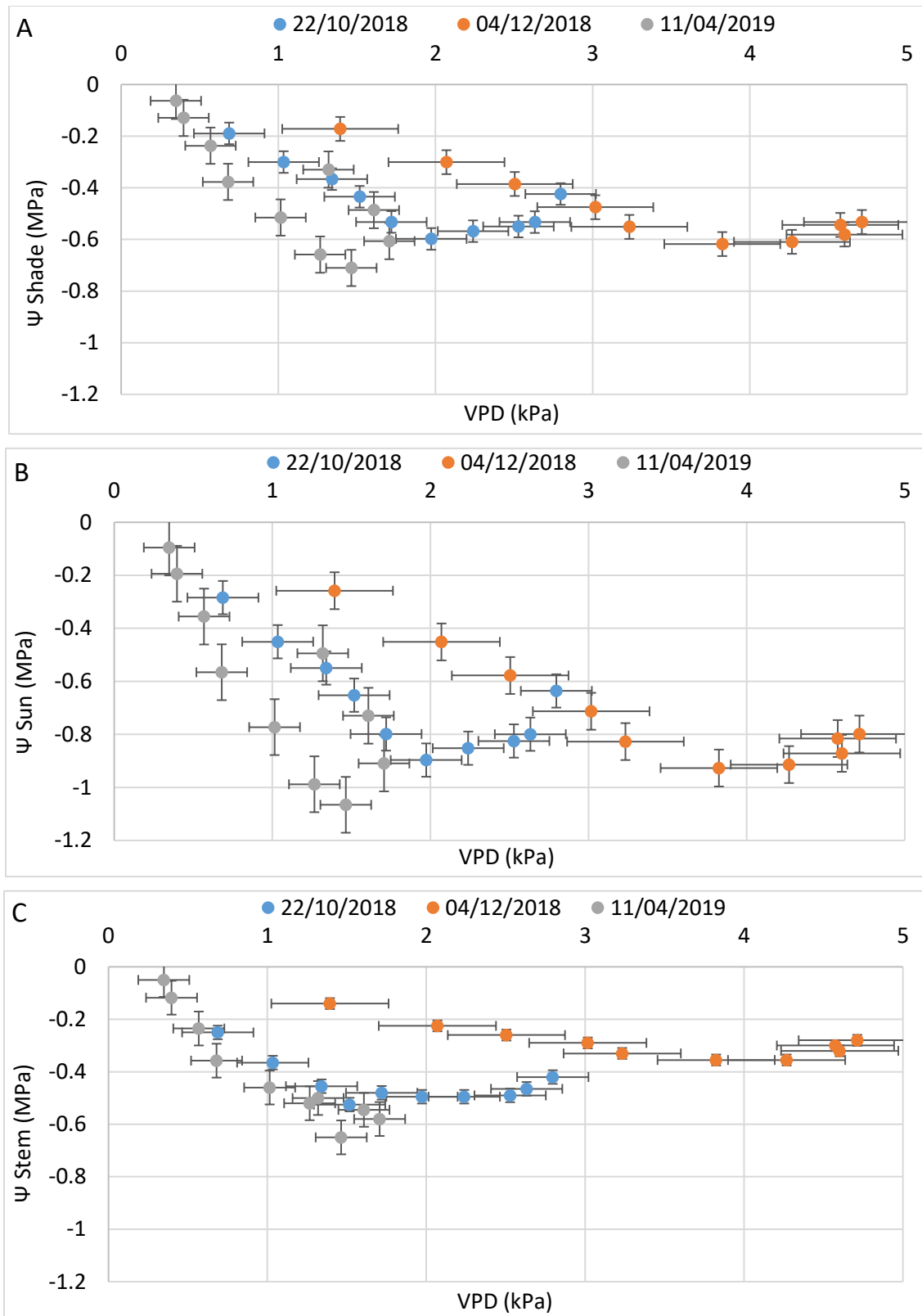
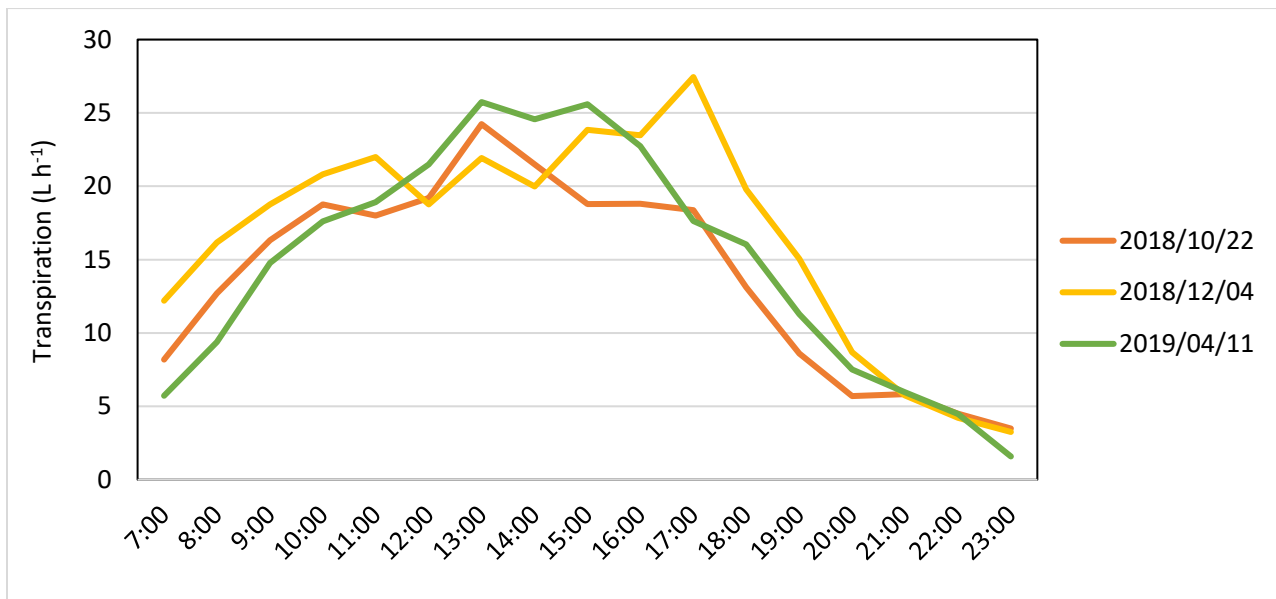


Figure 5.4 A) The relationship between hourly leaf water potential measurements of A) shaded leaves ( $\Psi_{\text{Shaded}}$  (MPa)), B) sun leaves ( $\Psi_{\text{Sun}}$  (MPa)) and C) stem water potential ( $\Psi_{\text{Stem}}$  (MPa)) against

**average VPD (kPa) for three selected days (22 October 2018, 04 December 2018 and 11 April 2019) for four measurement trees, between 07:00 and 16:00.**

Despite the similarity in  $T_c$  across the three measurements dates,  $ET_o$  for these days varied quite considerably, with recording 6.5 mm on 22 October 2018, 7.5 mm on 4 December 2018 and 2.5 mm on 11 April 2019 (Figure ). From Figure can be seen that on 04 December 2018 (highest  $ET_o$  measurements) also achieved the highest rate of transpiration ( $257 \text{ L day}^{-1}$ ), and 11 April 2019 (lowest  $ET_o$  measurement) achieved the second highest transpiration rate ( $243 \text{ L day}^{-1}$ ), lastly 22 October 2018 had the lowest transpiration rate ( $236 \text{ L day}^{-1}$ ) but had the second highest  $ET_o$ . Although  $T_c$  rates did not compare well with  $ET_o$ , there was a good relationship between  $T_c$  and  $\Psi_{Sun}$  when considering data from all three measurement dates (Figure ).



**Figure 5.5 Average hourly measured canopy transpiration rate ( $\text{L h}^{-1}$ ) throughout the day corresponding to dates of water potential measurements as well as measurement trees used for  $\Psi$  measurements.**

The measured hourly  $T_c$  rates correlated with measured  $\Psi_{Sun}$  and followed the typical trend where the transpiration rate increased during the morning, reaching a maximum at midday (between 12:00 and 14:00) where-after it decreased in the afternoon, except for 4 December 2018 where the maximum  $T_c$  rate was reached at 17:00, with the highest hourly  $T_c$  across measurements dates of  $27 \text{ L h}^{-1}$  (Figure ).

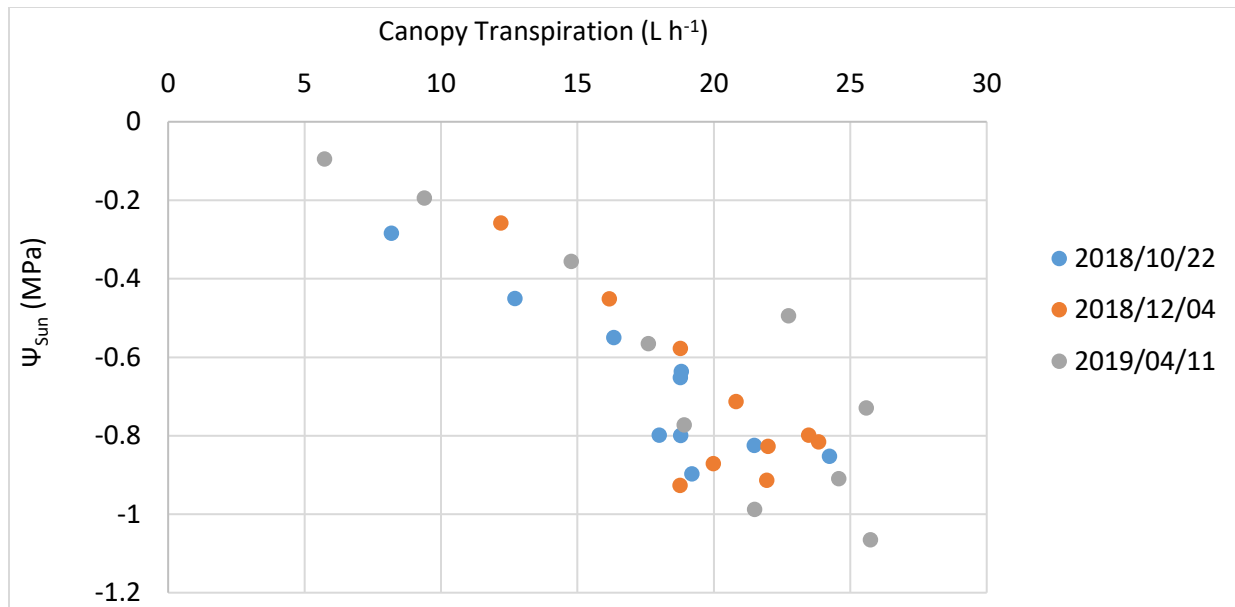


**Figure 5.6** The relationship between  $\Psi_{\text{Sun}}$  (MPa) and canopy transpiration ( $\text{L h}^{-1}$ ) for three measurement days corresponding to dates of water potential measurements for the measurement trees.

### 5.3.3. Root distribution and tree water status in relation to soil water content

When conducting water use studies it is important to capture maximum  $T_c$  rates and in order to do this it is important to ensure that no water deficits occurred. This was achieved in this study by measuring volumetric soil water content ( $\Theta$ ) in combination with root distribution of the pecan trees. Any possible influence of soil evaporation ( $E_s$ ) on  $\Theta$  was not considered as the shallowest sensors were placed at 15 cm from the soil surface, which is too deep in the soil to be impacted by soil surface evaporation. This was also the case for the sparse cover crop present that had a shallow root system, with its transpiration deemed to be negligible. Soil temperature, measured at 30 cm depth with chameleon sensors, ranged between 17 and 23 °C (Figure 5.7C) during the periods when the trees were in leaf and most of the rainfall occurred. Chameleon sensors were also used to assess if sufficient soil water was available at different depths within the soil profile. From Figure 5.7, it can be seen that the soil profile was kept relatively wet, except for a small period in December 2018. The blue represents a wet soil (0 to -20 kPa), green means the soil is moist (-20 to -50 kPa) and red represents a dry soil (<-50 kPa), the change from blue status to green indicates water uptake by roots up to at least 90 cm. Although the Chameleon sensor indicated a possible water deficit in December 2018, irrigation was scheduled by the grower using an Aquacheck probe and data from this probe did not indicate that irrigation was necessary.

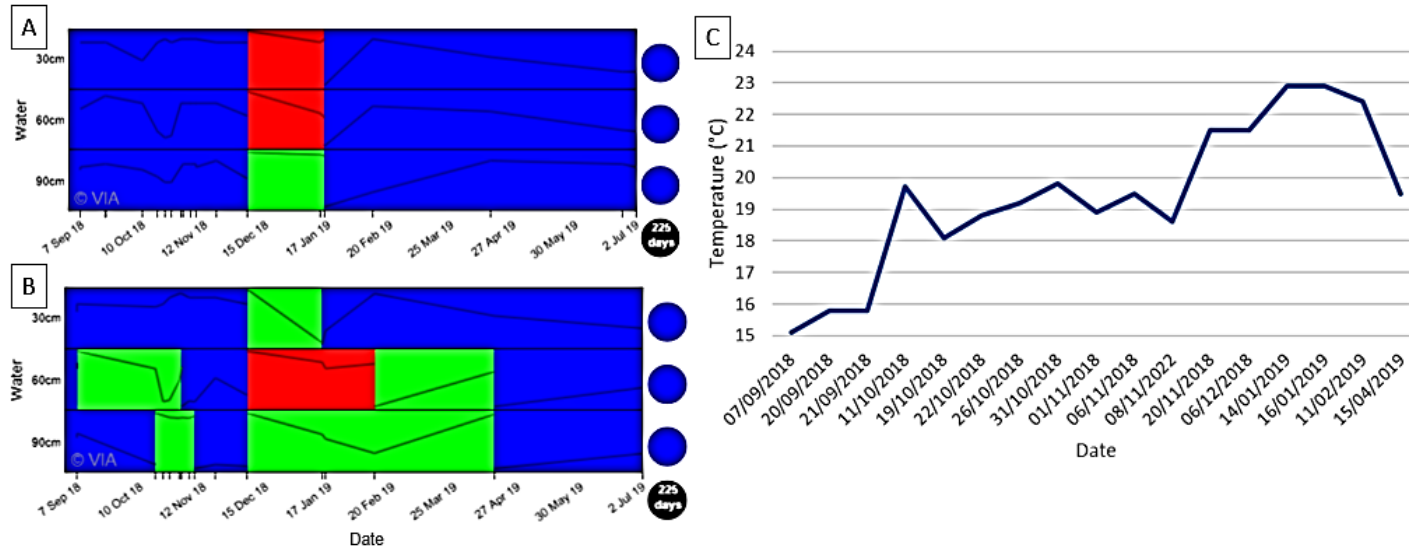


**Figure 5.7** Matric potential data from Chameleon sensors at A) trial site A at depths of 30, 60 and 90 cm throughout the season and B) trial site B at depths of 30, 60 and 90 cm. C) Average soil temperature (°C) of both sites at 30 cm depth for the period of 7 September 2018 until 15 April 2019.

To determine if sufficient of water was received by the pecan trees the irrigation (I) (mm) and rainfall (R) (mm) volumes were considered in relation to  $ET_o$  (mm),  $T_c$  (mm) and estimated ET (mm) (Figure 5.8). Although the possibility of short periods of stress cannot be ignored, it is evident from Figure 5.8 that the combined I and R exceeded ET for much of the season, except on 6 May 2019 when cumulative ET was higher than I+R for a short period of time. As ET exceeded I for long periods, in the absence of R, it is unlikely that water stress occurred in the orchard during the trial. In addition, cumulative  $T_c$  was a lot lower than applied I. It can further be seen that R during this season would have been insufficient to meet the water requirements of the orchard. The total average applied irrigation per tree over the season was 1200 mm per tree over the study period. The area is prone to high-water tables which could impact transpiration, as a result of waterlogged conditions for extended periods of time. However, data from a piezometer suggested that this was not the case for the duration of the study. At its shallowest the water table was at 1.87 m below the surface which occurred during the dormancy period (data not shown). Root depth reached a maximum of 1.1 m below the surface, as determined by root distribution studies.

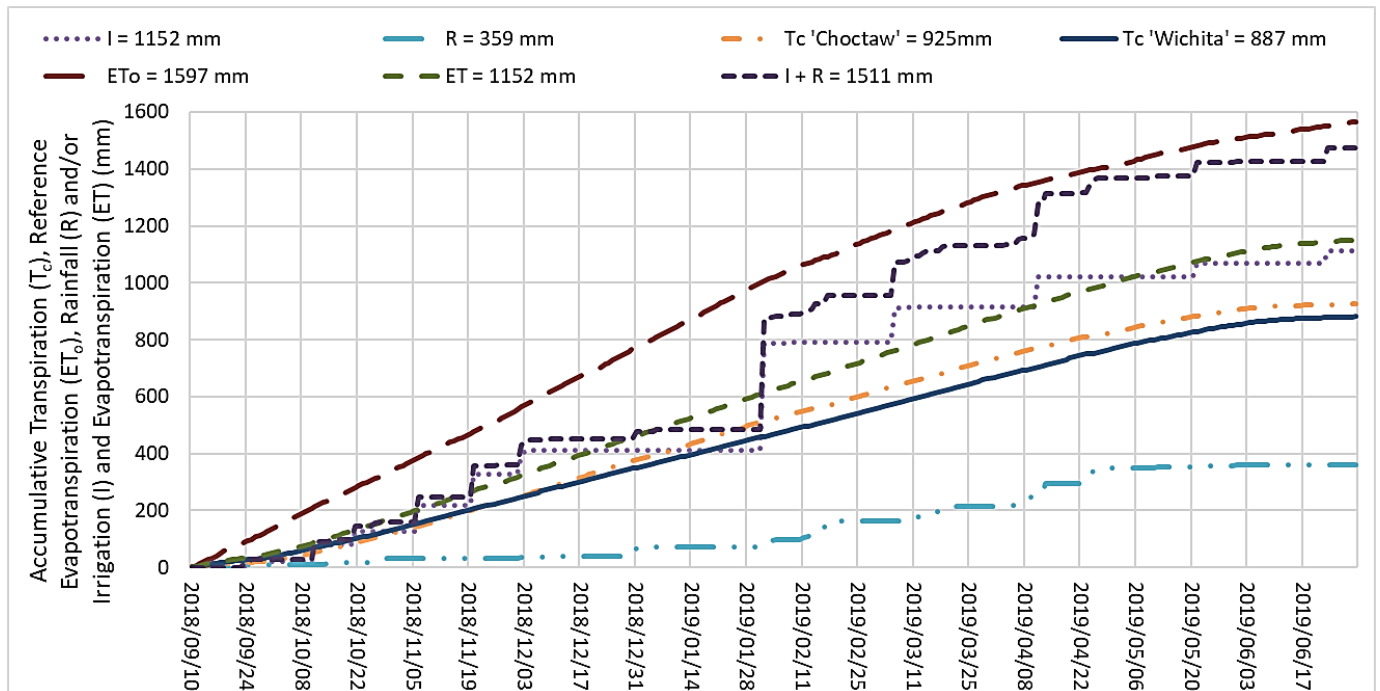


**Figure 5.8 Accumulative Irrigation and/or Rainfall (mm), Reference Evapotranspiration (mm), Evapotranspiration (mm) and Transpiration (mm) for ‘Choctaw’ and ‘Wichita’ trees during the period of 10 September 2018 until 30 June 2019.**

From the results in Table 5, it can be seen that the soil properties remained relatively constant with increased depth, with only a slight increase in silt % and a small decrease in sand %, with clay and bulk density remaining relatively constant. The soil texture was classified as a sandy loam for all analysed depths, which typically suggests a well-drained soil. Further can be seen that there were no large fluctuations in permanent wilting point (PWP), field capacity (FC) or plant available water (PAW) down the soil profile.

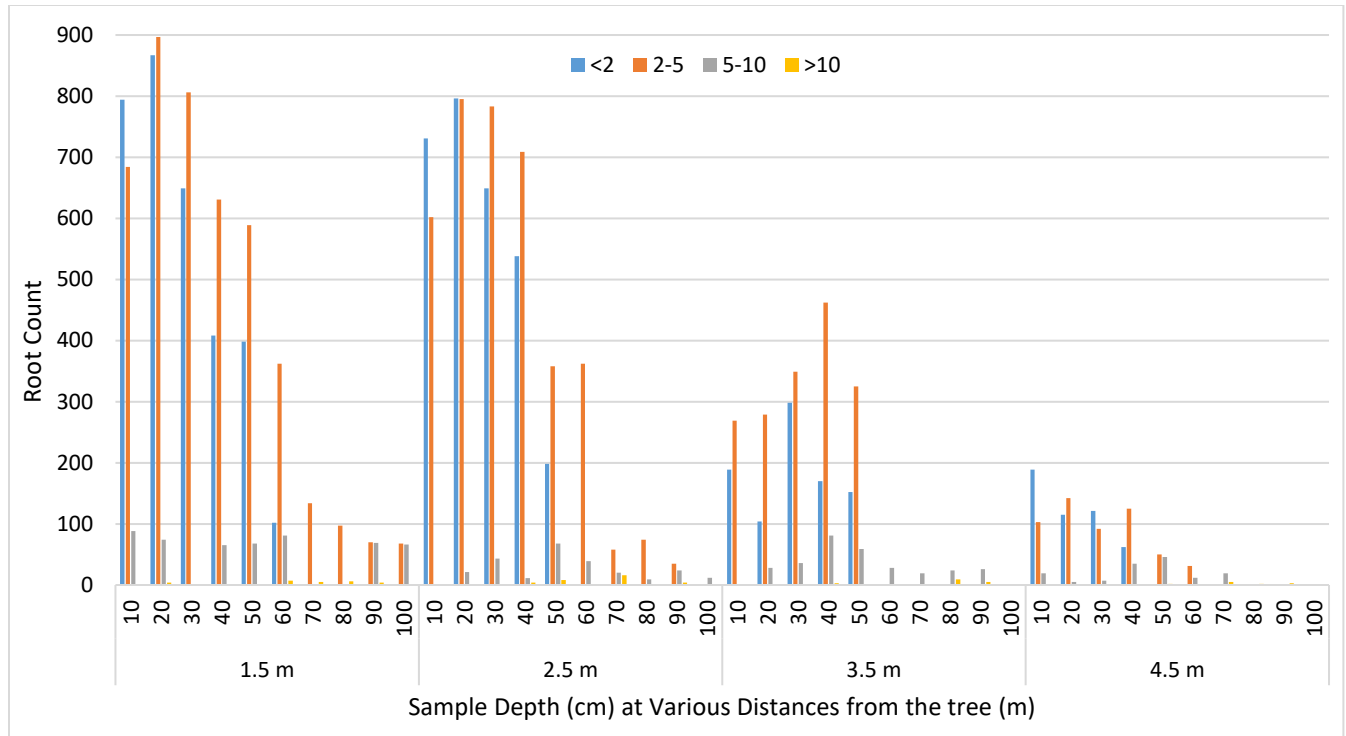
**Table 5.1 Soil sample results of bulk density ( $\text{kg m}^{-3}$ ), clay (%), sand (%), silt (%), permanent wilting point ( $\text{cm}^3 \text{ water cm}^{-3} \text{ soil}$ ), field capacity ( $\text{cm}^3 \text{ water cm}^{-3} \text{ soil}$ ), plant available water ( $\text{cm}^3 \text{ water cm}^{-3} \text{ soil}$ ) and texture at various depths (cm) down the soil profile with accompanying soil texture classes, taken from random points within site A and B.**

Depth (cm)	Bulk Density ( $\text{kg m}^{-3}$ )	Clay (%)	Sand (%)	Silt (%)	Soil Texture	Permanent Wilting Point ( $\text{cm}^3 \text{ water cm}^{-3} \text{ soil}$ )	Field Capacity ( $\text{cm}^3 \text{ water cm}^{-3} \text{ soil}$ )	Plant Available Water ( $\text{cm}^3 \text{ water cm}^{-3} \text{ soil}$ )
10	1480	12	66	22	Sandy loam	0.096	0.199	0.102
20	1405	14	65	21	Sandy loam	0.105	0.206	0.101
30	1475	12	69	19	Sandy loam	0.097	0.194	0.098
40	1440	14	63	23	Sandy loam	0.105	0.210	0.104
50	1485	10	71	19	Sandy loam	0.088	0.185	0.097
60	1460	12	65	23	Sandy loam	0.097	0.201	0.104
70	1395	8	72	20	Sandy loam	0.079	0.177	0.098
80	1365	10	65	25	Sandy loam	0.089	0.196	0.107
90	1390	14	62	24	Sandy loam	0.105	0.211	0.106
100	1490	8	71	21	Sandy loam	0.080	0.180	0.100

Results of root distribution analyses from the trench and wall method will be evaluated firstly at 1.5 m, 2.5 m, 3.5 m and lastly at 4.5 m perpendicular to the tree row (Figure 5.9). The highest total number of roots counted for a profile (total root count = 8093) was from the trench dug at 1.5 m perpendicular to the tree row. Most of the roots were concentrated between 0 to 30 cm from

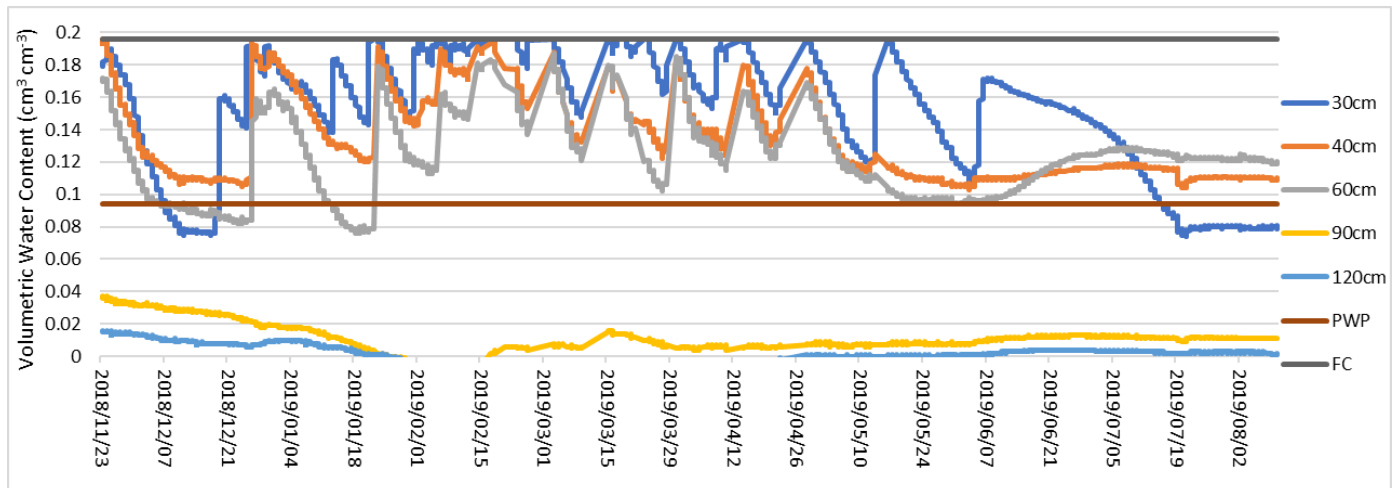


the soil surface, with most of these roots having a small diameter (Figure 5.9). Root counts declined rapidly below 50 cm and most of these roots had a diameter of between 5 and 10 mm. A slight change in root distribution with the soil profile was noted at 2.5 m from the tree perpendicular to the tree row (total root count = 6967), when compared to 1.5 m from the tree (Figure 5.9). In comparison to 1.5 m from the trunk, there were less roots between 10 and 20 cm but more roots at 40 cm (1262), with most of these roots had 40 cm having diameters of <2 mm and between 2-5 mm. At 1.5 m from the trunk, the predominant root size was between 2-5 mm followed by roots having diameter less than 2 mm and more roots of between 5–10 mm than at 2.5 m. At 2.5 m from the tree trunk some roots with a diameter larger than 10 mm were found between 40 cm and 90 cm. At 3.5 m from the tree trunk (total root count = 2915), root density increased from 20 to 50 cm from the soil surface, with no roots found at 10 cm, which is in contrast to root distribution at 1.5 and 2.5 m from the tree trunk (Figure 5.9). Less roots were found in the top 40 cm (1015) and a lower proportion of roots had a diameter < 2 mm. At a distance of 4.5 m from the tree trunk, perpendicular to the tree within the working row, the fewest number of roots were found regardless of diameter with a total number of 1185. As at 3.5 m from the trunk, no roots were found in the top 10 cm. The highest root densities occurred between 20 and 50 cm, which was dominated by roots with diameters from <2 mm to 5 mm. Roots with the largest diameter occurred more frequently at a shallower depth (Figure 5.9). The number of roots decreased as the depth increased.



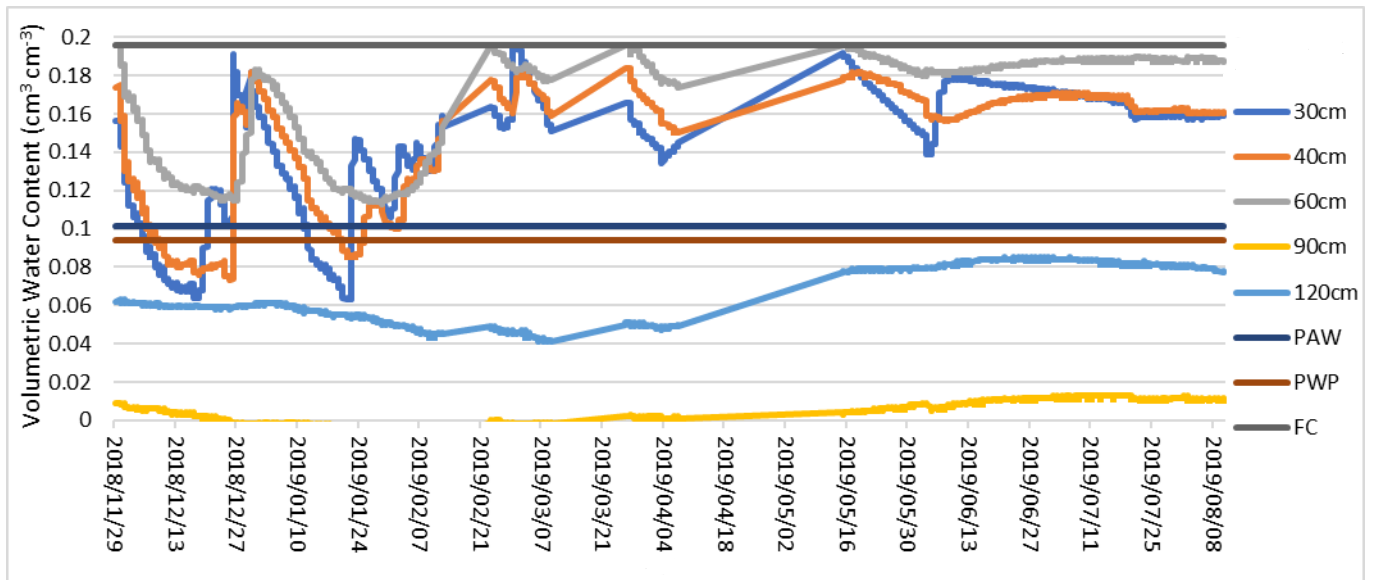
**Figure 5.9 The number and diameter of roots found at 1.5 m (n=8093), 2.5 m (n=6967), 3.5 m (n=2915) and 4.5 m (n=1185) from the trunk perpendicular to the tree row.**

After determining zones of high root distribution, is it important to understand PAW in the different rooting zones. The  $\Theta$  ( $\text{cm}^3 \text{cm}^{-3}$ ) was determined at different depths down the soil profile at 2.5 m from the tree within the tree row (Figure 5.10). The results were determined using hourly measurements with the GS-1 Decagon soil sensors, excluding rainfall and irrigation events, and only considering data below FC, as drainage would be negligible at that time and the fluctuating pattern would give a better representation of plant water uptake and if it corresponds to root densities depicted in Figure 5.9. From Figure 5.10 can be seen that  $\Theta$  content at 2.5 m from the tree trunk varied predominantly between depths of 30, 40 and 60 cm, with  $\Theta$  dropping below PWP on one occasion at 30 cm and twice at a depth of 60 cm for short periods of time. The  $\Theta$  was managed predominantly between FC and PWP, which is PAW, except at the two deepest measurement depths (90 and 120 cm), whereby it was constantly below PWP for the entire measurement period with no fluctuation in  $\Theta$  observed.



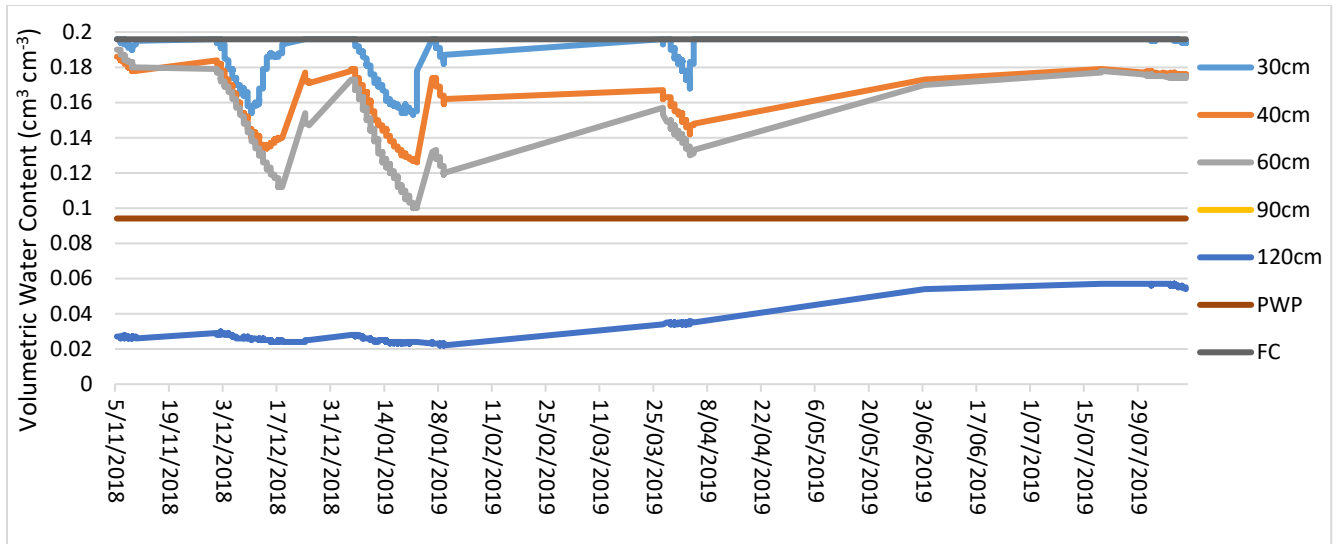
**Figure 5.10 Seasonal fluctuating hourly measurements of volumetric water content at various depths and indications of Field Capacity (FC) and Permanent Wilting Point (PWP) at 2.5 m from the tree within the tree row.**

Soil water content fluctuated to a lesser extent at 2.5 from the tree trunk within the working row (Figure 5.11) than at the same distance from the trunk within the tree row especially towards the end of the season in February 2019. The  $\Theta$  was also maintained within PAW except on two occasions whereby  $\Theta$  was below PWP at depths of 30 and 40 cm, on 28 November 2018 and again 16<sup>th</sup> January 2019. The  $\Theta$  at depths of 90 and 120 cm never increased above PWP for the measurement period, compared to depths of 30, 40 and 60 cm which was maintained within the PAW zone. However, at this position a higher  $\Theta$  was maintained at a depth of 120 cm, compared to the same position within the tree row, which could potentially indicate water influx from another source, such as a water table. When comparing the occurrence of roots with fluctuating patterns of  $\Theta$  at the same distance from the tree, within the working row, a definite pattern between the changes in  $\Theta$  (Figure 5.11) and the presence of roots (Figure 5.9) can be seen where an increase in roots results in a greater flux in  $\Theta$ .



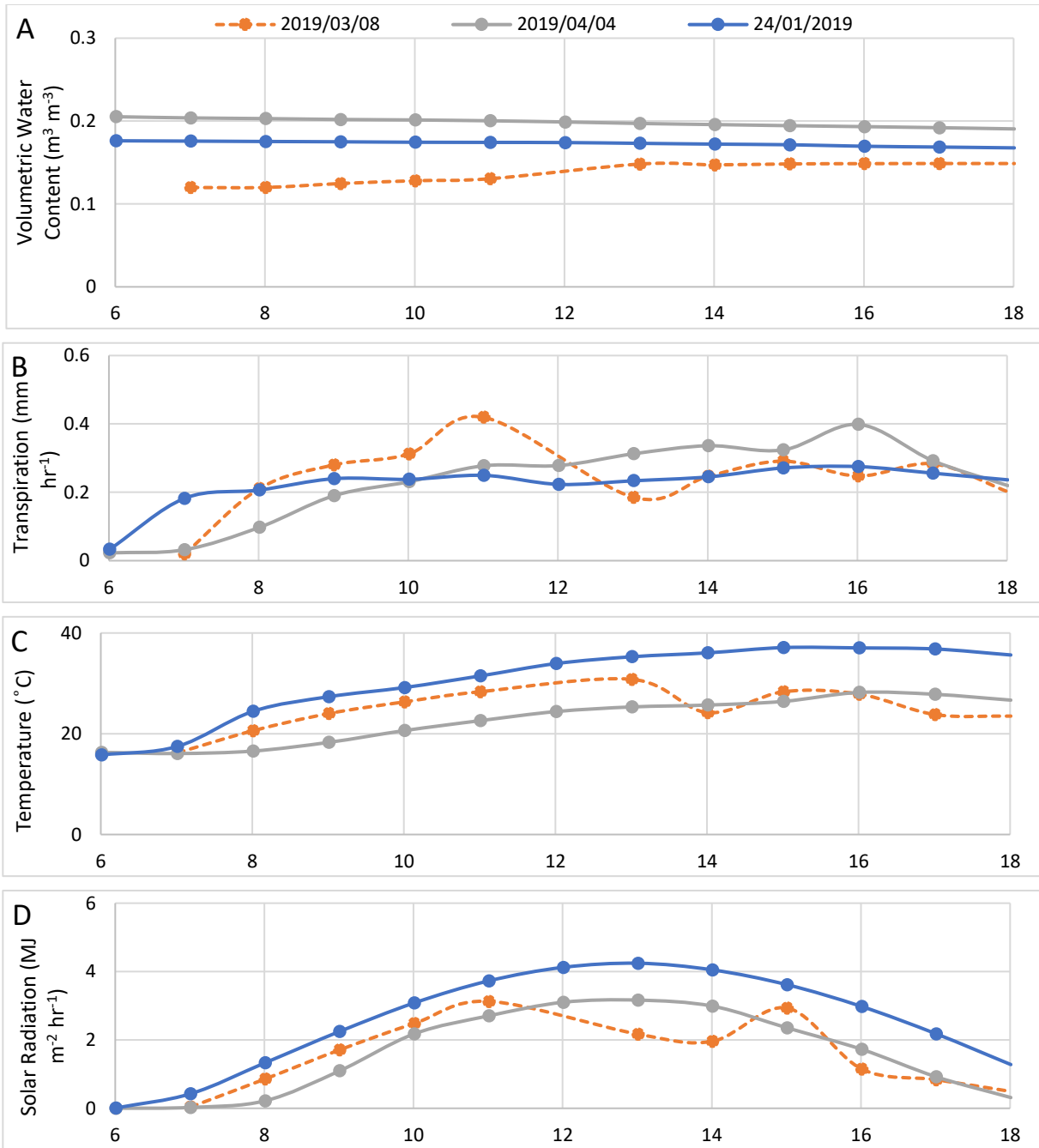
**Figure 5.11 Seasonal fluctuating hourly measurements of volumetric water content at various depths and indications of Field Capacity (FC) and Permanent Wilting Point (PWP) at 2.5 m from the tree within the working row**

At a distance of 5 m perpendicular to the tree trunk, within the working row, there was the least amount of  $\Theta$  flux at 30, 40 and 60 cm depths, with the 30 cm sensor reaching a higher volumetric water content compared to 40 cm, which had the second highest water content and lastly 60 cm (Figure 5.12). Soil water content at the three top measuring positions had the lowest amount of fluctuation and it all occurred in unison, which is likely attributed to the low number of roots found at that distance that leads to less water uptake at that point (Figure 5.9), that could cause variable rates of  $\Theta$  flux. At this position within the row  $\Theta$  stayed above PWP for the entire season for all measurement depths, except at 120 cm and at 90 cm. The lack of fluctuation at 120 cm is also attributed to sparsely distributed fine roots, with the increase in  $\Theta$  likely attributed to underground water. There is no data at 90 cm as the  $\Theta$  content readings were below 0, indicating the sensor was not making good contact with soil and was likely surrounded by an air pocket.



**Figure 5.12 Seasonal fluctuating hourly measurements of volumetric water content at various depths and indications of Field Capacity (FC) and Permanent Wilting Point (PWP) at 5 m from the tree within the working row.**

To observe if there were any fluctuations in  $T_c$  at three different  $\Theta$  levels, three dates were chosen (24 January 2019, 8 March 2019 and 4 April 2019) where the environmental variables ( $T_a$ ,  $R_s$ , VPD,  $ET_o$ ) varied (Figure 5.13). On 24 January temperature, VPD,  $R_s$  and  $ET_o$  were fairly high. On the 8 March 2019 there were variations in temperature,  $R_s$ , VPD and  $ET_o$ , which is typical for an overcast day receiving 0.56 mm rainfall. Conditions on 4 April 2019 were similar to those on 8 March 2019, however, no clouds were present on this day and no rain occurred. This day had the highest measured  $\Theta$ , taken as average down the soil profile. On 24 January 2019  $\Theta$  decline slightly from  $0.18 \text{ m}^3 \text{ m}^{-3}$  to  $0.17 \text{ m}^3 \text{ m}^{-3}$ , 8 March 2019 the  $\Theta$  started at  $0.12 \text{ m}^3 \text{ m}^{-3}$  and increased to  $0.15 \text{ m}^3 \text{ m}^{-3}$  at 12:00, on 4 April 2019,  $\Theta$  varied slightly from 0.2 to  $0.19 \text{ m}^3 \text{ m}^{-3}$  and represents the highest  $\Theta$  for this comparison with  $\Theta$  being close to field capacity (Figure 5.13A). When comparing Figure 5.13A with Figure 5.13B it can be seen that even when  $\Theta$  was high this did not always translate into higher  $T_c$  rates, suggesting that soil water content was not limiting  $T_c$ . Further the decreasing  $T_c$  in response to increasing  $\Theta$  on 8 March 2019 is evidence that  $T_c$  is not only limited by the  $\Theta$ , but more a function of the prevailing environmental conditions, such as the fluctuating VPD. This is further evident on 29 January 2019, whereby  $\Theta$  was sufficient, but the high VPD, temperature, solar radiation and reference evapotranspiration resulted in the lowest  $T_c$  between the three measurement dates.



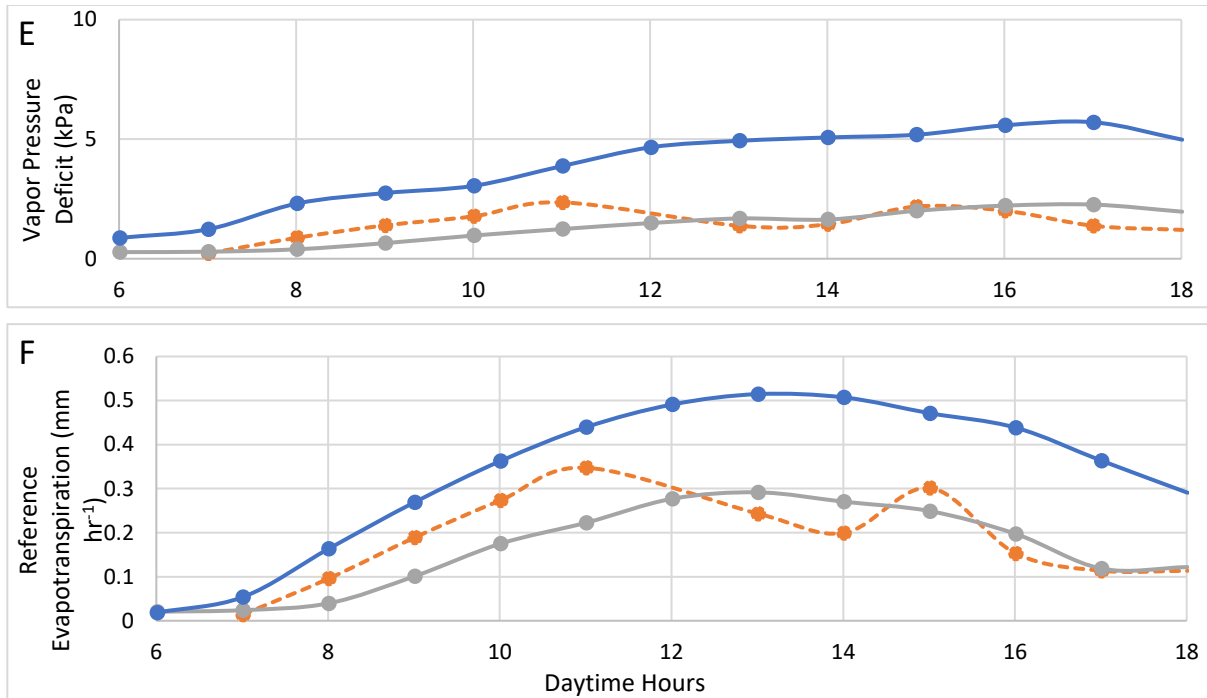


**Figure 5.13 Hourly comparison of various levels of A) volumetric water content in relation to B) canopy transpiration given varying environmental variables such as C) temperature (°C), D) solar radiation ( $\text{MJ m}^{-2} \text{h}^{-1}$ ), E) vapor pressure deficit (kPa) and F) reference evapotranspiration ( $\text{mm h}^{-1}$ ) on three selected date which are 24<sup>th</sup> January 2019, 8<sup>th</sup> March 2019 and 4<sup>th</sup> April 2019.**

#### 5.4. Discussion and Conclusion

Each atmospheric variable will differ in its impact on  $T_c$  as certain factors will have a more pronounced effect on  $T_c$  as a result of their potential to drive water loss from the leaf surface and the trees adaptive response to combat such water loss. It is also important to consider that different variables will become limiting at different times and will impact  $T_c$  rates throughout the day. The  $T_c$  rate had a good correlation with temperature, for both cultivars, and showed a linear relationship up until a plateau was reached at temperatures exceeding  $30^\circ\text{C}$ . A similar relationship was observed between  $T_c$  and VPD, as  $T_c$  increased rapidly between a VPD of 0-1.5 kPa, where after it started to plateau with increasing VPD. This agrees with the study by Ibraimo et al., (2016), where a VPD exceeding 1.4 kPa resulted in a restriction in  $T_c$  rates through stomatal closure. However, it was reported that maximum midday  $T_c$  rates could be attributed to hydraulic limitation rather than stomatal limitation alone, but the two processes are linked as hydraulic limitation requires the closing of stomata to prevent water potential to drop below the threshold for cavitation to occur (Rodríguez-Gamir et al., 2016). Therefore the  $T_c$  rate will be product of the balance existing between stomatal conductance, VPD and hydraulic conductance (Rodríguez-Gamir et al., 2016). There is an opportunity for additional research to investigate the validity of the aforementioned statement in pecan trees. This study could explore the feasibility of employing a



similar methodology to that conducted by Rodríguez-Gamir et al., (2016) on two distinct citrus rootstocks, *Poncirus trifoliata* (L.) Raf. and *Cleopatra mandarin* (*Citrus reshni* Hort ex Tan.). The proposed study would involve measuring whole tree transpiration alongside gas exchange parameters and evaluating root and shoot hydraulic conductance in pecan trees.

The  $T_c$  response to  $ET_o$  showed a similar pattern to VPD, whereby there was a linear correlation and tighter cluster of data at low  $ET_o$  values, whereafter a less pronounced increase was observed and more scattering of results, corresponding to threshold levels of 1.4 kPa VPD, 21 MJ m<sup>-2</sup> day<sup>-1</sup> and 4 mm day<sup>-1</sup> as reported by Ibraimo (2018). The results support the findings of Ibraimo (2018), who demonstrated that pecan  $T_c$  is tightly coupled to the atmosphere, (average decoupling coefficient ( $\Omega$ ) of 0.16), and as a result  $T_c$  is very responsive to changes in stomatal conductance.

To further understand how pecans respond to its immediate environment water potential measurements of sun, shade leaves and the stem were conducted, as the gradient between these components and soil water potential of the soil dictate water movement through the tree, to the atmosphere (Nobel, 2009). First was it important to assess possible water stress in the orchard, which would impact transpiration measurements causing an underestimation of unstressed seasonal water use estimates. During the study predawn water potential measurements were conducted to ensure that  $T_c$  was not limited and there was no evidence of stress in the orchard. All predawn measurements were above the threshold of -0.42 MPa identified by Taylor (2020). Further were chameleon sensors used in conjunction with soil water content measurements that indicated that there was sufficient PAW. The result from diurnal daily variation of leaf and stem water potential on three occasions determined that the diurnal pattern varies with leaf exposure to sun and shade conditions, where sun exposed leaves had a much lower water potential than the shade exposed leaves, with  $\Psi_{Stem}$  having the lowest values except for certain periods whereby  $\Psi_{Shade}$  values were lower. All  $\Psi$  measurements had variable results in response to different amounts of VPD, which is indicative of an isohydric response (Tardieu, 1998). This was observed between different measurement days, whereby on 11 April 2019 (Figure C), although VPD levels were the lowest of the three measurement dates,  $\Psi$  was also lowest and the second highest  $T_c$  rate was observed. This is in contrast to 4 December 2018 (Figure B) when the highest daily VPD was recorded and also the highest  $\Psi$  and the highest  $T_c$  rate between measurement periods. Pecan trees are quite resilient to increased atmospheric demand, especially if soil water content is not limiting, and can withstand  $\Psi_{stem}$  depressions of -2 MPa before a reduction in transpiration rate occurs through stomatal closure (Steinberg et al., 1990; Wells, 2015). From the current study whereby VPD was compared with  $\Psi$  it can be seen that the  $\Psi_{sun}$  does not decrease to a greater

extent during high VPD conditions compared to a cooler day with lower VPD. The phenomenon whereby the pecan tree is able to maintain a constant  $\Psi$  level during fluctuating atmospheric demand conditions is indicative of isohydric behaviour (Klein, 2014). Steinberg et al., (1990) and Deb et al., (2012) reported similar fluctuating hourly  $\Psi$  trends, where the sunlit and shaded leaf water potential declined at a similar same rate up until 12:00.

Pecan trees are reported to have a very efficient water transport system with a big taproot system that could contribute to the trees natural competitive advantage to obtain water at greater depths (Steinberg et al., 1990). Inherently pecan trees have a large water requirement therefore they are dependent on available soil water to sustain its water status. This dependency has been reported by Wells (2015) and Deb et al., (2012) whereby there exists a positive linear relationship between  $\Psi_{\text{Stem}}$  and  $\Theta$  from budbreak up until the end of nut sizing, but not during the kernel filling stage, as a moderate to heavy crop load could result in water stress regardless of soil water status. During the measurement period the  $T_c$  rates differed, not as a result of  $\Theta$  levels, but as a result of variable environmental conditions conducive for  $T_c$  to occur and differences canopy size. Further the decreasing  $T_c$  response to increasing  $\Theta$  on the 8 March 2019 is evidence that  $T_c$  rate is not only limited by the  $\Theta$  amount but more a function of the prevailing environmental conditions, such as fluctuating VPD, concluding that soil water was unlikely to be limiting  $T_c$ . Therefore, it can be seen that the leaves remain the final mediating component controlling water loss in response to prevailing environmental conditions and that fluctuating soil water content, at sufficient amounts at or above PAW, will not have a meaningful impact on  $T_c$ . The  $\Theta$  was maintained within PAW conditions for majority of the season, with fluctuating  $\Theta$  values observed between depths of 30 to 60 cm. At greater depths the  $\Theta$  fluctuated to a lesser extent as a result of limited roots found within that area. From the results it was seen that small diameter roots, typically associated with water and nutrient uptake (0 and 10 mm), were mostly concentrated in the top 60 cm, depending on the position of measurement relative to the tree. The number of small diameter roots where highest closest to the tree trunk, decreasing in number as distance from the tree increases. These small roots also decreased down the soil profile. From these results it can be seen that the zones with highest fluctuations in  $\Theta$  correlating with zones of highest fine root concentrations.

## CHAPTER 6      MODELLING PECAN EVAPOTRANSPIRATION

### 6.1.      Introduction

Judicious water application is vital for optimum fruit production, resulting in a large majority of fruit bearing orchards relying on irrigation, especially in arid and semi-arid climatic regions where rainfall is known to be scarce and inconsistent. Therefore, irrigation water management, through accurate quantification of total crop water use or evapotranspiration (ET), is an integral component to maximize orchard profitability, especially as more farmers are planting orchard crops.

The pecan nut industry in South Africa has experienced significant growth at an annual rate of approximately 2 to 3%, with an estimated planted area of 21,500 to 27,700 hectares. Of this area, at least 11,000 hectares are in Vaalharts and 2,100 hectares in the Upington region. South Africa has become the world's fourth-largest producer, with nut exports in 2018 reaching 16,196 tons and increasing to 21,000 tons in 2020. It is projected that production will further increase to over 37,300 tons by 2025 (A. Coetzee, personal communication, 12 August 2019; SAPPA, 2018). As the industry grows, the demand for irrigation increases, but there is limited knowledge of pecan water use under South African conditions. Currently, water management for pecan orchards relies on research from other countries or empirical models, potentially leading to inaccurate predictions of evapotranspiration (ET) and inadequate irrigation scheduling (Ibraimo, 2018). Different regions in South Africa have unique climates and management practices, causing crop coefficients (Kc) and ET to vary. To address this, modeling approaches have been developed to adjust pecan Kc based on specific climatic conditions and management practices, using weather variables, thermal time, fractional canopy cover, and crop height (Allen and Pereira, 2009; Allen et al., 1998b; Miyamoto, 1983; Samani et al., 2011; Sammis et al., 2004; Taylor et al., 2015; Wang et al., 2007c). However, it is essential to validate and calibrate these empirical modeling approaches in regions outside of their original development zone, as they may not be fully transferable to different conditions.

In the study by Ibraimo (2018), were the shortcomings highlighted of modelling pecan water use according to a four stage crop coefficient approach with values provided for stone fruit, as described by Allen et al. (1998b) in the FAO-56 approach. It was found that ET estimates were accurate on a seasonal basis, but results varied greatly on a monthly basis as it showed that pecans exhibit a six stage crop coefficient curve (Ibraimo, 2018). A second approach was tested

whereby a set of reference crop coefficients were adjusted according to canopy size, to derive orchard specific crop coefficients (Samani et al., 2011). It was further tested if the derived crop coefficients could be adjusted according to specific climatic conditions for that region by using a crop coefficient-growing degree day ( $K_c$ -GDD) relationship developed by Sammis et al., (2004). It proved to work at the Cullinan site as the crop coefficients were specific for that orchard, but was further hypothesized that it would not transferable to other hotter production regions (GDD exceeding 1500) as at these sites the production season is longer with different rates of canopy development at the onset of the season, and different rates of senescence at the conclusion of the season which would lead to different crop coefficients (Ibraimo, 2018). It was suggested to use an approach whereby the crop coefficient curve was adjusted according to phenological stages. Further to this suggestion, it was proposed that the approach would work well in orchards where  $E_s$  is a minor component of ET, however in orchards with canopy cover less than 80% the  $E_s$  can constitute a greater portion of ET. As a result the estimation of ET was suggested to be improved by separating measurements of  $E_s$  and  $T_c$  (Ibraimo, 2018).

The aim of this chapter is to validate if the crop specific modelling approach to determine  $K_c$ , as described by Ibraimo et al., (2016) and Ibraimo (2018). It was hypothesized that the GDD will exceed 1500 in this growing region leading to inaccurate estimation of  $K_{c-ref}$  when using an empirical approach to adjust the GDD- $K_{c-ref}$  curve, and therefore will have to be adjusted according to phenological stages, which will lead to more accurate estimates of ET. Further ET can be more accurately estimated by means of the dual crop coefficient approach than the single crop coefficient approach. This will make the use of the dual crop coefficient more transferrable to different regions of South Africa to obtain more accurate estimates of ET.

## 6.2. Materials and Methods

The process for model validation encompassed the validation of different methods, to assess if the conclusions made by Ibraimo et al., (2016) hold true. Firstly, the approach by Samani et al., (2011) to derive orchard specific  $K_c$  values, which can be adjusted for specific climatic conditions in a region using a  $K_c$ -GDD relationship (Sammis et al., 2004) was assessed. When GDD exceeded 1500 (which is typical of warm, dry growing areas), the  $K_{c-ref}$  values were adjusted according to phenological stages (derived from the  $K_t$  graphs) to obtain accurate ET estimates (Ibraimo, 2018). Secondly, the ability of the dual crop coefficient approach to obtain accurate estimations of ET in orchard with canopy cover less than 80% was assessed, as in this approach  $E_s$  is modelled separately.

In the first approach, the  $K_c$ , which encompasses  $E_s$  and  $T_c$ , was determined according to the guidelines set out by Samani et al., (2011) and modified by Ibraimo (2018) whereby a crop-specific modelling approach was followed that allows for the adjustment of  $K_c$  values according to canopy cover. This was achieved by empirically relating reference crop coefficients ( $K_{c-ref}$ ) for a mature orchard to canopy cover of the study orchard, as described by Samani et al., (2011);

$$K_c = (0.6035f_{c\text{ eff}} + 0.4808)K_{c-ref} \quad (28)$$

Where  $f_{c\text{ eff}}$  is effective fractional cover that was estimated monthly from ceptometer estimates, and  $K_{c-ref}$  is the crop coefficient of a mature reference orchard. Monthly  $K_{c-ref}$  values were obtained from the study conducted by Samani et al., (2011), that is representative of a well-managed orchard in New Mexico (Table 6). In order to account for seasons in the southern hemisphere the values were offset by 6 months.

**Table 6.1 Monthly pecan reference crop coefficients ( $K_{c-ref}$ ) for New Mexico, which were offset by 6 months to represent southern hemisphere seasons (Ibraimo et al., 2016; Samani et al., 2011).**

	Month								
	Sep	Oct	Nov	Dec	Jan	Feb	Mar	Apr	May
$K_{c-ref}$ New Mexico	0.39	0.59	0.87	1.02	1.04	1.24	1.26	0.84	0.39

The shape of the  $K_{c-ref}$  curve is impacted by thermal time, as demonstrated by Sammis et al., (2004) and as a result this crop coefficient curve needs to be adjusted for different regions in which average prevailing temperatures differ from those experienced in New Mexico where the approach was developed. In order to do this, Sammis et al., (2004) established a  $K_c$ -growing degree day (GDD) relationship as follows:

$$K_{c-ref} = -3.9 \times 10^{-12}GDD^4 + 1.1 \times 10^{-8}GDD^3 - 1.1 \times 10^{-5}GDD^2 + 4.3 \times 10^{-3}GDD + 3.3 \times 10^{-1} \quad (29)$$

Equation (29) was used to calculate daily  $K_{c-ref}$  values through the 2018-2019 production season in the Vaalharts region of South Africa, as seen in Table .

**Table 6.2 Average monthly pecan reference crop coefficients ( $K_{c-ref}$ ) for the Vaalharts study site during the 2018-2019 production season using the function described by Sammis et al., (2004).**

	Month								
	Sep	Oct	Nov	Dec	Jan	Feb	Mar	Apr	May
$K_{c-ref}$	0.41	0.74	0.92	0.94	1.01	1.04	0.08	0	0

Growing degree days were determined as:

$$\text{GDD} = \left( \frac{T_{\min} + T_{\max}}{2} \right) - 15.5 \quad (30)$$

and were calculated from weather data gathered from the automatic weather station (AWS), and a base temperature of 15.5 °C without a cut off temperature (Miyamoto, 1983). Due to limitations to this method to adjust  $K_{c\text{-ref}}$  values throughout the season using the relationship in equation 29 (Ibraimo (2018), a new method was proposed whereby the values of **Error! Reference source not found.** could be adjusted according to field observations. The six-stage crop growth curve was adjusted based on measured data from the pecan orchard at the trial site in Vaalharts during the 2018-2019 production season. The method of adjusting  $K_{c\text{-ref}}$  values to the specific climatic conditions experienced during the trial period were as follows (Ibraimo, 2018);

1. The dates of the entire growth season were numerically listed starting at bud-break up until complete leaf fall, with the day of bud break being day 1.
2. The growing season was divided into six growth stages, as seen in Table , based on the derived  $K_t$  values as accurate observations of phenological developmental stages were not completed (Herrera, 1990; Wells and Conner, 2007).
3. The  $K_{c\text{-ref}}$  value used is where it was constant throughout the growing stage, as seen in Table , for the following three stages; bud-break, pollination to early dough and shuck split.
4. The daily  $K_{c\text{-ref}}$  values for the growth stages where  $K_{c\text{-ref}}$  varies linearly was estimated with the day number within the growing season, with Equation (31) (Allen et al., 1998b).

$$K_{c\ i} = K_{c\ \text{prev}} + \left[ \frac{i - \sum L_{\text{prev}}}{L_{\text{stage}}} \right] (K_{c\ \text{next}} - K_{c\ \text{prev}}) \quad (31)$$

Whereby  $i$  is the day number of the growing season,  $K_{c\ i}$  is the  $K_c$  on day  $i$ ,  $L_{\text{stage}}$  is the length of stage under consideration and  $\sum(L_{\text{prev}})$  is the sum of lengths of all the previous stages,  $K_{c\ \text{prev}}$  is the  $K_c$  at the end of the previous stage and  $K_{c\ \text{next}}$  is the  $K_c$  at the onset of the next stage. The  $K_{c\text{-ref}}$  values based on climate adjustment, obtained from the Sammis et al., (2004) equation were not used for modelling purposes. The  $K_c$  for the orchard was estimated according to Equation 28 with the  $K_{c\text{-ref}}$  values of Table , and adjusted according to the growth stages.

**Table 6.3 Pecan growth stage classification through the course of the season (Herrera, 1990; Wells and Conner, 2007) and corresponding  $K_{c\text{-ref}}$  values as suggested by Ibraimo et al., (2016) and Samani et al., (2011).**

Growth Stage	Growth Stage Definition	$K_{c\text{-ref}}$
1. Bud-break	Emergence of leaf primordial	0.34

2. Pre-pollination	Occurrence of leaf expansion	0.34-0.92
3. Pollination to early dough	Stigmas of pistillate flowers turn from green to red until shell hardening is complete	0.94
4. Dough stage	Kernel is completely formed	0.94-1.18
5. Shuck split	Sutures of shuck begin to split apart	1.18
6. Leaf drop	Onset of leaf senescence	1.18-0.39

For the 2018/19 season was ET determined as the sum of  $T_c$  (average of the four 'Choctaw' and 'Wichita' trees respectively), determined using the heat ratio method (described in Chapter 3.6), and soil evaporation estimates ( $E_s$ ), determined using the FAO-56 evaporation model (Chapter 2.2.5). The estimation of the evaporation crop coefficient ( $K_e$ ) through the course of the season was done by means of the FAO-56 dual crop coefficient approach as described in Chapter 2.2.5 with the results of the process described in Chapter 4.4.3 (Allen et al., 1998b; Allen et al., 2005). Measurements of  $E_s$  conducted with the soil micro lysimeters were used for model parameterization, as this approach was successful in a pecan orchard in Cullinan, South Africa (Ibraimo, 2018). The method of micro-lysimeter measurements were described in Chapter 3.5. Measurements of  $E_s$  using the micro-lysimeters were used for model parameterization using eight days of  $E_s$  measurements, while model validation was done using eight days of  $E_s$  measurements, as described in Chapter 4.3.3. The values used to parameterize the model are provided in Table .

**Table 6.4 Values used to parameterize the FAO-56 dual crop coefficient model in order to estimate soil evaporation coefficient.**

Parameters	Trial Orchard
Soil surface layer depth ( $Z_e$ ) (m)	0.15
$\Theta_{FC}$ ( $m^3m^{-3}$ )	0.214
$\Theta_{PWP}$ ( $m^3m^{-3}$ )	0.09
Surface area wetted by irrigation ( $m^2$ )	98.52
Fraction of surface area wetted by irrigation	0.985
$K_{c\ max}$	1.4
Fraction of soil surface covered by the canopy	0.34-0.98



### 6.3. Results and Discussion

#### 6.3.1. Modelling ET of pecans

Transpiration crop coefficients ( $K_t$ ) followed a 6 stage crop coefficient curve as reported for pecan trees in Cullinan and in New Mexico (Ibraimo et al., 2016; Sammis et al., 2004). A peak in  $K_t$  values was found from March to May, which is associated with a flush of leaves and nut filling, as seen in LAI measurements (Figure 4.3). Throughout most of the season,  $K_t$  values were slightly higher for the 'Choctaw' trees than the 'Wichita' trees, reflecting the slightly higher transpiration rates and greater LAI of these trees (Chapter 4.2.2.). During the late spring and summer period the average  $K_t$  for the 'Wichita' trees was 0.60, whilst it was 0.72 for the same period for the 'Choctaw' trees. All the values presented in Figure 6.1 were smaller than 1.4 as it is not energetically possible for the  $K_t$  to exceed 1.4 for tall, rough tree crops (Allen et al., 2011c). The  $K_t$  values reached a peak LAI was a maximum and  $T_c$  rates were also at a maximum. This phase coincides with the oil accumulation phase which is an energy expensive process that requires higher photosynthetic rates, and therefore possibly higher stomatal conductance and  $T_c$ , leading to a maximum  $K_t$  values (Wood, 2003). After nut maturation the  $K_t$  value started to decline, as a result of the start of leaf senescence and decreased  $T_c$  rates. The black line in Figure 6.1 represents the average  $K_t$  between the two measurement cultivars, and the key dates when changes in the trend in  $K_t$  values were observed. This is important for determining the length of pecan growth stages, which influence the length of  $K_{c-ref}$  stages.

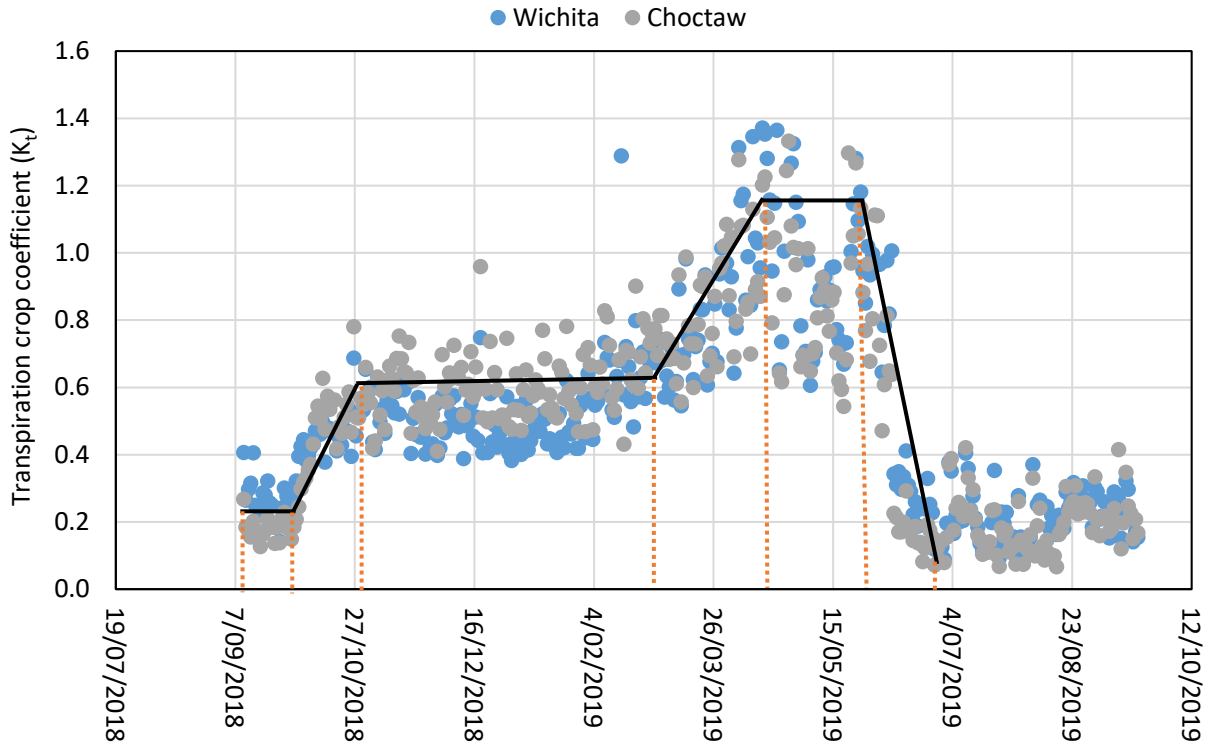


**Figure 6.1** Transpiration crop coefficients ( $K_t$ ) for the 2018-2019 production season for ‘Wichita’ (blue dots) and ‘Choctaw’ (grey dots) pecan trees, with the black line representing the average  $K_t$  between the two measured cultivars with red dotted lines indicating on what date changes occurred.

As suggested by Ibraimo et al., (2016), the key to applying this curve to other regions, is the adjustment for canopy cover and local climate conditions. The prevailing weather conditions impact canopy development and therefore also the length of the season, which is suggested to be controlled by the accumulation of thermal time (Sammis et al., 2004). When comparing the polynomial relationship between measured daily GDD and the resulting  $K_c$  derived by Sammis et al., (2004), and the  $K_t$  curves, for ‘Choctaw’ and ‘Wichita’, the shortcomings of this relationship are evident (Figure 6.2). In the Vaalharts region seasonal cumulative GDD exceeded 1500 and as hypothesized by Ibraimo (2018), if the relationship by Sammis et al., (2004) was used to derive  $K_c$  values for this region the values would be 0 before the end of the season. This is why it was deemed necessary to conduct measurements in the hotter pecan production regions of South Africa where the production season was longer, and the rate of canopy development and leaf senescence differ from the region in which previous measurements were conducted. Importantly, the  $K_t$  curve in relation to thermal time was very similar for the ‘Choctaw’ and ‘Wichita’ trees, with the most significant difference being a slight difference in magnitude of the  $K_t$  between 240 and 1200 GDD.

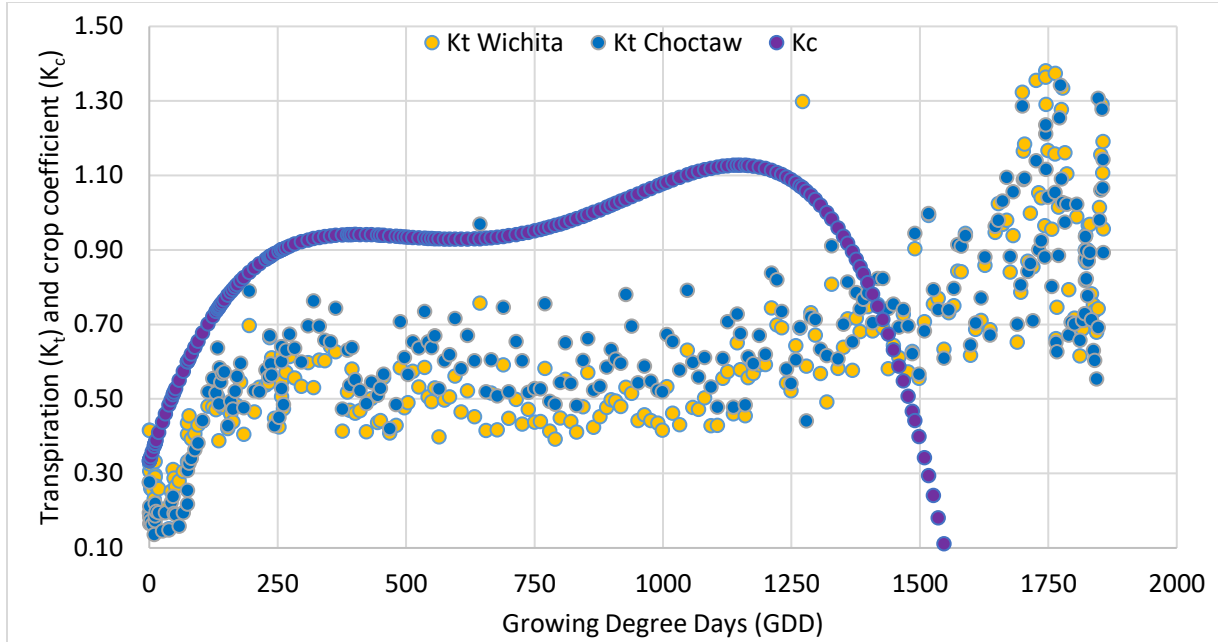


**Figure 6.2** The comparison between measured daily growing degree days (GDD) and the derived  $K_c$  values, as described by Sammis et al., (2004) (purple dots), in relation to  $K_t$  values for ‘Choctaw’ (blue dots) and ‘Wichita’ (yellow dots) pecan trees in the Vaalharts region.

As the empirical relationship of Sammis et al., (2004) was unable to account for the cumulative thermal time over a season in Vaalharts, it was necessary to adjust the  $K_{c-ref}$  of Samani et al., (2011) according to observed phenological stages. The  $K_{c-ref}$  curve adjusted according to the dates identified in Figure 6.1, which coincided with visual observations made within the orchard throughout the 2018-2019 season and can be seen in Figure 6.3. The stages are as follows (1) Bud-break, (2) Pre-pollination, (3) Pollination to early dough, (4) Dough stage, (5) Shuck split and (6) Leaf drop. These phenological stages help allow the adjustment of the  $K_{c-ref}$  curve to account for the longer season in Vaalharts, and can be done for any production region.

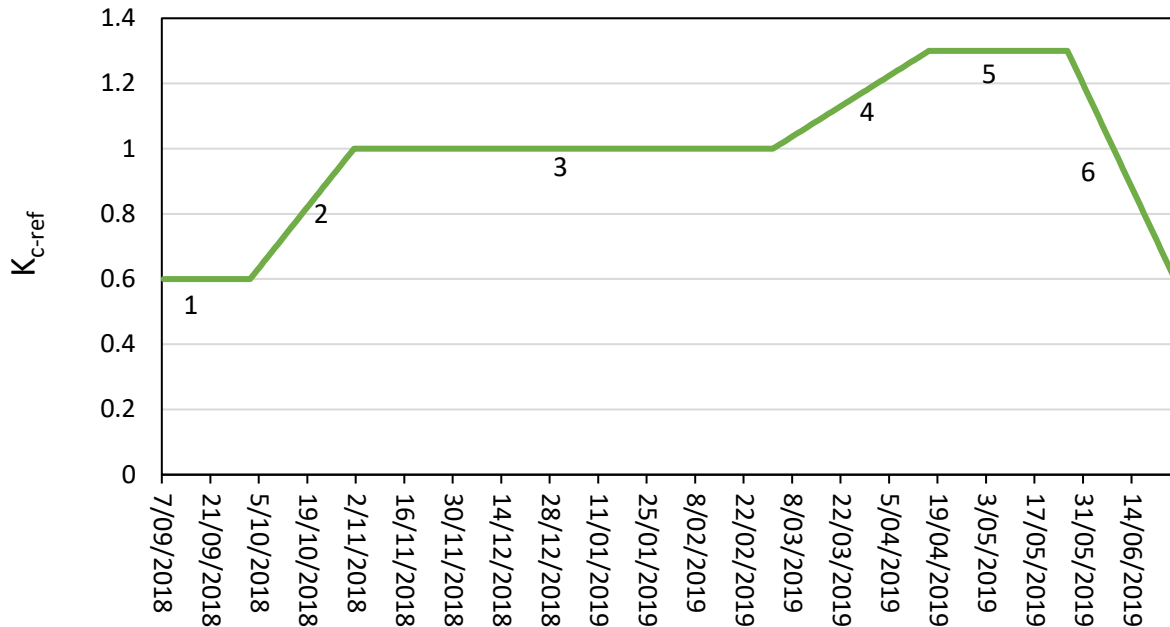


**Figure 6.3 Six stage reference crop coefficient ( $K_{c-ref}$ ) curve for a mature pecan orchard at Vaalharts for the 2018-2019 production season.**

The six stage  $K_{c-ref}$  (Figure 6.3) was then used with estimates of  $f_{c,eff}$  (Figure 6.4), to determine  $K_c$  values for the orchard that are needed to determine ET from weather data.

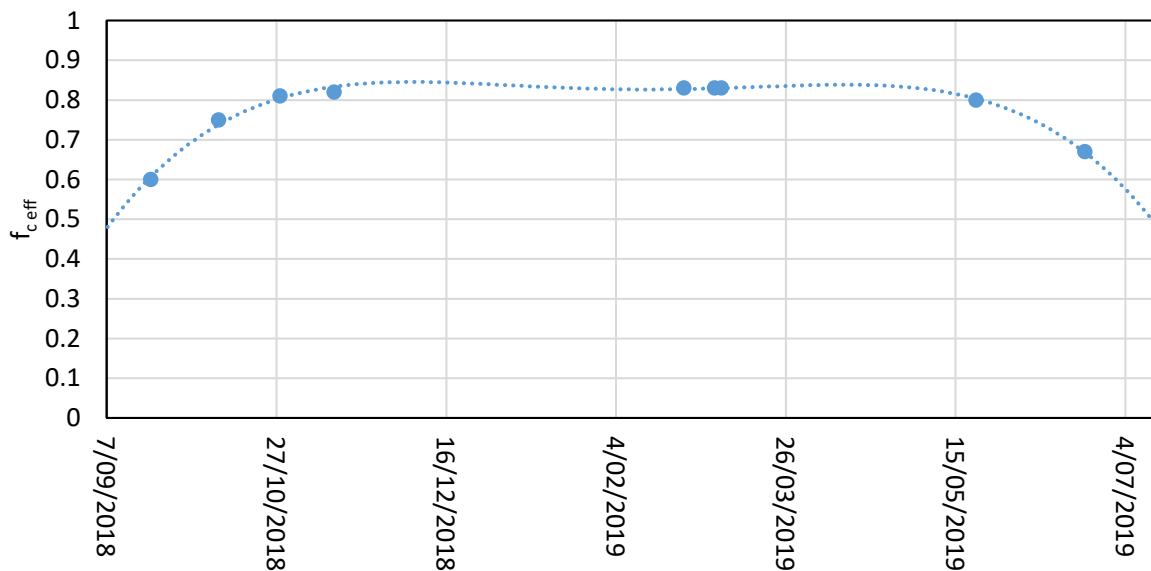


**Figure 6.4 Measured (marker) and extrapolated (line) effective fractional interception of photosynthetic active radiation in the Vaalharts pecan orchard for the 2018-2019 season.**

The ET was determined by multiplying the derived  $K_c$  value with measured  $ET_0$  values. The estimated ET values for pecans, during the 2018-2019 season, were then compared to

determined ET values (sum of modelled  $E_s$  and average  $T_c$  of eight pecan trees). The determined ET (sum of  $T_c$  and  $E_s$ ) differed from FAO-56 estimated ET over the season, whereby determined ET values were 1136 mm and estimated values 1204 mm for the 2018-2019 production season (Figure 6.5). There was a slight overestimation between the months of November 2018 and January 2019, when the canopy was still developing. After this point, there was good agreement between the two values. Over the course of the season there was a 6% overestimation of modelled values compared to actual measured values, which provided a more accurate estimation of ET than the methods employed by Ibraimo (2018) to estimate ET.

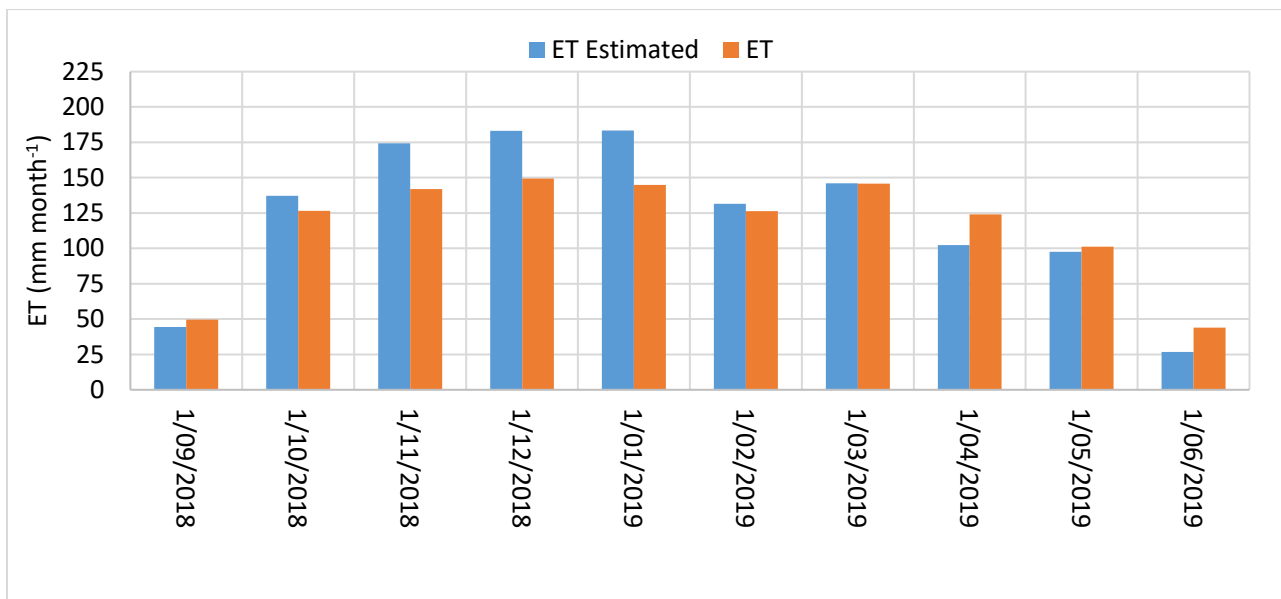


**Figure 6.5 Comparison between monthly estimated and actual evapotranspiration (ET) as described by Ibraimo (2018) with adjusted  $K_c$  values for a mature pecan orchard in Vaalharts during the 2018-2019 production season, according to phenological stages.**

The performance of the model was determined by comparing the accuracy of monthly ET modelling against determined monthly ET. From this comparison the  $R^2$  value was 0.86, which is at an acceptable standard. The D value was 0.91, RMSE 23.22, MAE of 13.60 and CRM of 1.01. The MAE is below the threshold of 20% which indicates that the slight deviation is still within acceptable limits. Based on the positive CRM value the deviation is attributed to a overestimation of the model.

#### 6.4. Conclusion

From the results can it be seen that the application of the empirical equation of Sammis et al., (2004) for adjusting  $K_c$  values according to thermal time does not hold true in Vaalharts that has higher GDD accumulation during its growing season. This method only applies to regions where

cumulative GDD for a season is less than 1500 and in Vaalharts for the 2018/19 season it was 1861. A different approach had to be used that could accommodate warmer growing conditions with a longer growing season, such as mentioned by Ibraimo (2018), whereby the crop coefficient curve was adjusted according to phenological stages. This allows for the accurate estimation of  $K_c$ , using the function described by Samani et al., (2011), which follows a six stage crop curve, which was determined from  $K_t$  values within this study. The method was shown to successfully estimate monthly ET of mature pecan trees in this study, when the adjusted  $K_{c-ref}$  values were further adjusted for canopy size as described by Samani et al., (2011). There was a slight overestimation by the model between November 2018 and January 2019, ultimately accounting for a 6% overestimation of estimated ET as compared to determined ET. This data suggests that by allowing for the adjustment of the  $K_{c-ref}$  curve according to local growing conditions and canopy cover, good estimates of monthly ET can be obtained.

## CHAPTER 7 GENERAL CONCLUSIONS

Measurement of seasonal evapotranspiration (ET), which can be partitioned into canopy transpiration ( $T_c$ ) and soil evaporation ( $E_s$ ), is becoming of increased importance for judicious irrigation scheduling in water scarce regions. This is of particular concern in South Africa where pecans are commonly produced in arid to semi-arid regions, characterized by low and erratic rainfall patterns. Furthermore as the area planted with pecan trees increases, (yearly increase of 2-3%, 27 700 ha under cultivation, (SAPPA, 2018)), the responsible use of irrigation water becomes more important. When comparing previous estimates of pecan ET with estimates from this study it is evident that ET varies significantly between production regions. From the current study in Vaalharts for a single season was the mixed cultivar orchard average ET 1184.5 mm, whilst in the study by Ibraimo (2018), conducted in Cullinan, lower ET values of approximately 1000 mm were reported, whereas the study by Miyamoto (1983) conducted in Las Cruces, New Mexico, reported higher ET values of 1300 mm and Sammis et al., (2004) reported 1215 mm for the same area. The difference in ET between Vaalharts and Las Cruces can be attributed to the irrigation technique, where flood irrigation is used in Las Cruces, which typically leads to higher  $E_s$  rates. In order to extrapolate measured ET data to other growing areas, accurate estimates of ET are necessary which can be achieved through crop modelling, given the time and cost constraints in conducting actual ET measurements. Determining the most appropriate model to use, in turn, requires an in-depth understanding of the process associated with pecan ET and its constituents ( $T_c$  and  $E_s$ ) and how these are influenced by a number of contributing factors.

Transpiration is an integral part of ET and will vary across a season as it is on the prevailing weather conditions and availability of water in the soil. There have been few concerted efforts to quantify pecan  $T_c$  as most of the research has focused primarily on ET determination. Pecan transpiration was reported to be tightly coupled to the atmosphere (decoupling coefficients ( $\Omega$ ) of 0.16) where numerous factors play an integral role in determining the water gradient out of the leaf that will ultimately impact  $T_c$  (Ibraimo, 2018). Ibraimo (2018) found that the primary weather variable driving  $T_c$  was vapor pressure deficit (VPD) and the second most contributing factor was solar radiation ( $R_s$ ) (Ibraimo, 2018). Andersen and Brodbeck (1988) suggested that pecans are very resilient to unfavorable atmospheric conditions that favor a greater water deficit between the leaf and the atmosphere and can endure high VPDs (3 kPa) without a reduction in  $T_c$ , given soil water is not limiting. The results within this study showed that  $T_c$  reached a plateau at a VPD greater than 1.5 kPa whereafter stomata was likely limiting  $T_c$ . Within hotter and drier pecan



production regions, such as Vaalharts, this could potentially limit total seasonal  $T_c$  if prolonged climatic conditions prevail with VPDs above 1.5 kPa. When measuring seasonal consumptive tree water use it is important that the tree does not experience water stress conditions as it will cause an underestimation of gathered data. According to predawn measurements, during certain window periods, there is confidence that the trees did not experience water stress, as all the values were higher than the minimum threshold of -0.42 MPa (Taylor, 2020). Further diurnal leaf ( $\Psi_{\text{leaf}}$ ) and stem ( $\Psi_{\text{stem}}$ ) water potential measurements were conducted through the course of the day. It was found that  $\Psi_{\text{leaf}}$  varied as a function of the sun or shade exposure, where sun exposed leaves experienced a declining  $\Psi_{\text{leaf}}$  up until 12:00 where after  $\Psi_{\text{leaf}}$  started increasing. From the current study whereby VPD was compared with  $\Psi$  it can be seen that  $\Psi_{\text{sun}}$  does not decrease to a greater extent during high VPD conditions compared to a cooler day with lower VPD. The phenomenon whereby the pecan tree is able to maintain a constant  $\Psi$  level during fluctuating atmospheric demand conditions is indicative of isohydric behaviour (Klein, 2014). Steinberg et al., (1990) and Deb et al., (2012) reported similar fluctuating hourly  $\Psi$  trends, where the sunlit and shaded leaf water potential declined at a similar same rate up until 12:00. Changes in canopy cover over a season also has a pronounced effect on the seasonal  $T_c$ , as the surface area from which transpiration occurs increases at the start of a season and decreases at the end of a season. The impact of canopy size on  $T_c$  was evident when comparing seasonal  $T_c$  between the two measurement cultivars, 925 mm for 'Choctaw' and 887 mm for 'Wichita'. 'Choctaw' trees had a higher leaf area index (LAI) towards the end of the season and this was reflected in higher seasonal  $T_c$  rates. In addition, 'Choctaw' trees also had the highest daily  $T_c$  rates ( $508 \text{ L tree}^{-1}$ ) as compared to 'Wichita' trees ( $425 \text{ L tree}^{-1}$ ).

When considering the components of ET separately, a more profound understanding can be achieved of how the variation of each component impacts ET. On a seasonal basis transpiration was the main contributor (78%) to ET, varying as canopy cover fluctuated, with  $E_s$  accounting for 22%. The  $E_s$  component was highest when canopy cover was sparse at the onset and end of the season, accounting for 36 and 52% in September 2018 and June 2019 respectively. The  $E_s$  component has the greatest potential when considering water saving techniques as it does not directly affect crop production. Within this study Stage 2 was more dominant as the macro-sprinklers provided large amounts of water during a single application, resulting in a low frequency of irrigation events. The longer soil water content can be maintained within Stage 2, the higher the water saving would be as the potential rate of evaporation is lower than within Stage 1 (Lehmann, 2008).

Soil evaporation varies on a daily and seasonal level as it is a function of the combination between supply (soil water) and demand (atmospheric variables driving evaporation) (Reinders, 2010; Or, 2013). As the water distribution from the macro-sprinkler was irregular around the tree base and the wetted areas exposed to solar radiation varied, an uneven  $E_s$  pattern was observed throughout the season. This was also the result of the deciduous nature of pecan orchards which causes variable canopy cover across the season. In addition the diurnal movement of the sun causing variation in shading of the surface during the course of the day. These results suggest that significant water saving can be made by considering methods that limit the application of water to only shaded areas underneath the canopy and to ensure that the irrigation wets a relatively small surface area, such as drip irrigation, and mulch application.

In order to ensure that soil moisture levels were not limiting  $T_c$ , a range of methods were deployed to continuously measure volumetric water content through the course of the season. These methods allowed a better understanding of the root density and distribution within the soil profile, as it could indicate if the irrigation is targeting root zones most effective for water uptake. It was found that the highest root density of small diameter roots (0-10 mm), closely associated with water and nutrient uptake, was found in the top 60 cm of the soil profile at various distances from the tree base. The amount of small diameter roots where highest closest to the tree base, decreasing in amount as distance from the tree increased. The frequency of small roots also decreased down the soil profile, with larger diameter roots becoming more prevalent as depth increased. The small root densities correlated with the zones where more soil water was available, with little evidence of drainage past 60 cm. Flux patterns of soil water content were observed, and it was found that in the zones where roots were sparsely distributed there was less variable soil water content pattern through the course of the season.

In this study measured  $T_c$  and modelled  $E_s$  were combined to provide estimates of ET on a daily, monthly and seasonal basis. The ET results from the current study varied when compared to a study conducted in cooler Cullinan (Ibraimo 2018), with the Vaalharts having a higher reference evapotranspiration ( $ET_0$ ), but also different irrigation techniques were used, where in Vaalharts macro-sprinklers (irrigation water use efficiency (IWUE) of 0.019-0.031 kg m<sup>-3</sup>) were used with a large wetting diameter compared to micro-sprinklers (IWUE of 0.086 kg m<sup>-3</sup>) used in Cullinan with a smaller wetting diameter. Water saving techniques should be focussed on increasing the IWUE of pecan trees in order to ensure the continued successful of cultivation of this crop in a semi-arid area. It was found that WUE efficiency varied according to bearing intensity, where WUE for 'Choctaw' trees was 0.24 kg m<sup>-3</sup> during an 'off-year', compared to 'Wichita' which was 0.40 kg m<sup>-3</sup>.

<sup>3</sup> during 'on-year'. The values were quite high compared to results found in Cullinan of  $0.14 \text{ kg m}^{-3}$  during an 'off-year' and  $0.23 \text{ kg m}^{-3}$  during an 'on-year' (Ibraimo, 2018), as well as Las Cruces with results varying between  $0.19 \text{ kg m}^{-3}$  (Miyamoto, 1983) and  $0.24 \text{ kg m}^{-3}$  (Sammis et al., 2004). The difference in results are attributed to higher evapotranspiration in pecan orchards in Las Cruces and the lower yield in Cullinan when compared to Vaalharts. When comparing WUE pecan to high yielding fruit tree crops such as table grapes (between  $1.69$  and  $7.71 \text{ kg m}^{-3}$  depending on irrigation method) (Du et al., 2008) or citrus ( $1.97 \text{ kg m}^{-3}$ ) (García-Sánchez et al., 2007), WUE is much lower in pecan trees as a result of its lower yields, it fails in comparison as pecans are low yielding crops. However, because they are high value crops water use productivity (WUP) was assessed to incorporate the economic value of the crop. The WUP differed between 'Choctaw' and 'Wichita' cultivars, where 'Wichita' trees had higher yields and better quality, and therefore a WUP of  $R26.05 \text{ m}^{-3}$  as compared to 'Choctaw', which had lower yields of lower quality and a WUP of  $R18.82 \text{ m}^{-3}$ . Using only one season's data in pecan orchards may not fully represent yield and ET variations due to the crop's alternate bearing nature. Analysing multiple seasons' data provides a more comprehensive understanding of climate, management effects, and influences on yield and ET. All the aforementioned (IWUE, WUE, WUP) could be increased by more judicious irrigation scheduling techniques which would involve accurately quantifying crop water use leading to more efficient water application, which will become increasingly important in areas with low and sporadic rainfall. From gathered data of IWUE, WUE and WUP variation was observed between cultivars, and will likely vary between years. The necessity therefore arise to quantify water use across a number of seasons and to test and validate robust crop modelling approaches that could give accurate ET estimations.

An important method for quantifying pecan water use under a wide range of conditions is through the application of crop modelling. In the study by Ibraimo (2018), were the shortcomings highlighted of modelling pecan water use according to a four stage crop coefficient approach with values provided for stone fruit, as described by Allen et al., (1998b) in the FAO-56 approach. It was found that ET estimates were accurate on a seasonal basis, but results varied greatly on a monthly basis as it showed that pecans exhibit a six stage crop coefficient curve (Ibraimo, 2018). A second approach was tested whereby a set of reference crop coefficients were adjusted according to canopy size, to derive orchard specific crop coefficients (Samani et al., 2011). It was further tested if the derived crop coefficients could be adjusted according to specific climatic conditions for that region by using a  $K_c$ -GDD relationship developed by Sammis et al., (2004). It proved to work at the Cullinan site as the crop coefficients were specific for that orchard, but as seen within this study that it would not transferable to other hotter production regions (GDD

exceeding 1500) as at these sites the production season is longer with different rates of canopy development at the onset of the season, and different rates of senescence at the conclusion of the season which would lead to different crop coefficients (Ibraimo, 2018). It was suggested to use an approach whereby the crop coefficient curve was adjusted according to phenological stages. The failure of the model is especially important under South African growing conditions as the  $K_{c-ref}$  curve, as developed by (Samani et al., 2011; Sammis et al., 2004) has limitations which includes the length of the season and upper limit of  $K_{c-ref}$ . Following the parameterisation of the model as suggested model, as suggested by Ibraimo et al., (2016), an  $R^2$  value of 0.86 and a 6% overestimation was found when compared to measured results. The accuracy of the model can be ascribed to the method whereby  $K_{c-ref}$  curve was adjusted for the study region using phenological stages (derived from the  $K_t$  curve within this study). This six stage crop reference coefficient curve was better suited to pecans as they exhibit a second flush late in the season during the nut filling stage. The  $K_{c-ref}$  values were then adjusted using canopy cover estimates as described by Samani et al., (2011). The resulting  $K_c$  values are then used in conjunction with  $ET_o$  to determine ET (Allen et al., 2005). The aforementioned measured ET values differed between cultivars in this study due to different growth flushes, it is also likely that values would differ between seasons, as growing conditions will differ between seasons. As this model validation only includes a single season further validation of the proposed model of Ibraimo (2018) is needed for consecutive years as well as testing its transferability in other pecan production regions of South Africa, and between different seasons to determine if the model holds true, as well as a revised polynomial function, as suggested by Sammis et al., (2004), but with a broader analysis range.

## References

- Abraha, M. G., and Savage, M. J. (2010). Validation of a three-dimensional solar radiation interception model for tree crops. *Agriculture Ecosystems & Environment* 139, 636-652.
- Achat, D., Bakker, M., and Trichet, P. (2008). Rooting patterns and fine root biomass of *Pinus pinaster* assessed by trench wall and core methods. *Journal of Forest Research* 13, 165-175.
- Allen, R. (2008). Quality assessment of weather data and micrometeorological flux-impacts on evapotranspiration calculation. In "Proceedings of annual meeting of the Society of Agricultural Meteorology of Japan Abstracts of International Symposium on Agricultural Meteorology 2008", pp. 25-41. The Society of Agricultural Meteorology of Japan.
- Allen, R., and Pereira, L. (2009). Estimating crop coefficients from fraction of ground cover and height. *Irrigation Science* 28, 17-34.
- Allen, R., Pereira, L., Howell, T., and Jensen, M. (2011a). Evapotranspiration information reporting: I. Factors governing measurement accuracy. *Agricultural Water Management* 98, 899-920.
- Allen, R., Pereira, L., Howell, T., and Jensen, M. (2011b). Evapotranspiration information reporting: II. Recommended documentation. *Agricultural Water Management* 98, 921-929.
- Allen, R., Pereira, L., Raes, D., and Smith, M. (1998a). Crop evapotranspiration-Guidelines for computing crop water requirements-FAO Irrigation and drainage paper 56. *Fao, Rome* 300, D05109.
- Allen, R. G., Pereira, L. S., Howell, T. A., and Jensen, M. E. (2011c). Evapotranspiration information reporting: I. Factors governing measurement accuracy. *Agricultural Water Management* 98, 899-920.
- Allen, R. G., Pereira, L. S., Raes, D., and Smith, M. (1998b). Crop evapotranspiration-Guidelines for computing crop water requirements-FAO Irrigation and drainage paper 56. *Fao, Rome* 300, D05109.
- Allen, R. G., Pereira, L. S., Smith, M., Raes, D., and Wright, J. L. (2005). FAO-56 dual crop coefficient method for estimating evaporation from soil and application extensions. *Journal of irrigation and drainage engineering* 131, 2-13.
- Andales, A., Wang, J., Sammis, T. W., Mexal, J. G., Simmons, L. J., Miller, D. R., and Gutschick, V. P. (2006). A model of pecan tree growth for the management of pruning and irrigation. *agricultural water management* 84, 77-88.
- Andersen, P., and Brodbeck, B. (1988). Net CO<sub>2</sub> assimilation and plant water relations characteristics of pecan growth flushes. *Journal of the American Society for Horticultural Science* 113, 444-450.
- Annandale, J., Benade, N., Jovanovic, N., Steyn, J., Du Sautoy, N., and Commission, W. R. (1999). Facilitating irrigation scheduling by means of the soil water balance model.
- Annandale, J., Steyn, J., Benadé, N., Jovanovic, N., and Soundy, P. (2005). Technology transfer of the Soil Water Balance (SWB) model as a user friendly irrigation scheduling tool. *WRC report No. TT251/05*.
- Arora, R., Wisniewski, M. E., and Scorza, R. (1992). Cold acclimation in genetically related (sibling) deciduous and evergreen peach (*Prunus persica* [L.] Batsch): I. Seasonal changes in cold hardiness and polypeptides of bark and xylem tissues. *Plant Physiology* 99, 1562-1568.
- Ayars, J., Trout, T., Mead, R., Phene, C., and Johnson, R. (1999). Crop coefficients for mature peach trees are well correlated with midday canopy light interception. In "III International Symposium on Irrigation of Horticultural Crops 537", pp. 455-460.
- Baker, J. V., and Van Bavel, C. (1987). Measurement of mass flow of water in the stems of herbaceous plants. Wiley Online Library.

- Barret, D. J., Hatton, T. J., Ash, J.E., and Ball, M.C. (1995). Evaluation of the heat pulse velocity technique for measurement of sap flow in rainforest and eucalypt forest species of South-Eastern Australia. *Plant, Cell & Environment* 18, 463-469.
- Bawazir, A., and King, J. (2004). Crop Evapotranspiration (ET) Study for Doña Ana County, New Mexico. *Las Cruces, NM: New Mexico Water Resources Research Institute. Technical Completion Report.*
- Becker, P., and Edwards, W. (1999). Corrected heat capacity of wood for sap flow calculations. *Tree Physiology* 19, 767-768.
- Begg, J. E., and Turner, N. C. (1976). Crop water deficits. In "Advances in agronomy", Vol. 28, pp. 161-217. Elsevier.
- Bellocchi, G., Rivington, M., Donatelli, M., and Matthews, K. (2011). Validation of biophysical models: issues and methodologies. In "Sustainable Agriculture Volume 2", pp. 577-603. Springer.
- Bonachela, S., Orgaz, F., Villalobos, F. J., and Fereres, E. (1999). Measurement and simulation of evaporation from soil in olive orchards. *Irrigation Science* 18, 205-211.
- Bonachela, S., Orgaz, F., Villalobos, F. J., and Fereres, E. (2001). Soil evaporation from drip-irrigated olive orchards. *Irrigation Science* 20, 65-71.
- Bowen, I. S. (1926). The ratio of heat losses by conduction and by evaporation from any water surface. *Physical review* 27, 779.
- Burgess, S. S., Adams, M. A., Turner, N. C., Beverly, C. R., Ong, C. K., Khan, A. A., and Bleby, T. M. (2001). An improved heat pulse method to measure low and reverse rates of sap flow in woody plants. *Tree physiology* 21, 589-598.
- Campbell, G., and Turner, N. (1990). Plant-soil-water relationships.
- Castel, J. (1996). Evapotranspiration of a drip-irrigated clementine citrus tree in a weighing lysimeter. In "II International Symposium on Irrigation of Horticultural Crops 449", pp. 91-98.
- Ceaglske, N. H., and Hougen, O. (1937). Drying granular solids. *Industrial & Engineering Chemistry* 29, 805-813.
- Cohen, S., Naor, A., Bennink, J., Grava, A., and Tyree, M. (2007). Hydraulic resistance components of mature apple trees on rootstocks of different vigours. *Journal of experimental botany* 58, 4213-4224.
- Cohen, Y., Fuchs, M., and Green, G. (1981). Improvement of the heat pulse method for determining sap flow in trees. *Plant, Cell & Environment* 4, 391-397.
- Consoli, S., and Papa, R. (2013). Corrected surface energy balance to measure and model the evapotranspiration of irrigated orange orchards in semi-arid Mediterranean conditions. *Irrigation science* 31, 1159-1171.
- Daamen, C. C., and Simmonds, L. P. (1996). Measurement of evaporation from bare soil and its estimation using surface resistance. *Water Resources Research* 32, 1393-1402.
- Daamen, C. C., Simmonds, L. P., Wallace, J. S., Laryea, K. B., and Sivakumar, M. V. K. (1993). Use of microlysimeters to measure evaporation from sandy soils. *Agricultural and Forest Meteorology* 65, 159-173.
- Deb, S. K., Shukla, M. K., and Mexal, J. G. (2012). Estimating midday leaf and stem water potentials of mature pecan trees from soil water content and climatic parameters. *HortScience* 47, 907-916.
- Domec, J. C., Noormets, A., King, J. S., Sun, G., McNulty, S. G., Gavazzi, M. J., Boggs, J. L., and Treasure, E. A. (2009). Decoupling the influence of leaf and root hydraulic conductances on stomatal conductance and its sensitivity to vapour pressure deficit as soil dries in a drained loblolly pine plantation. *Plant, Cell & Environment* 32, 980-991.
- Du, T., Kang, S., Zhang, J., Li, F., and Yan, B. (2008). Water use efficiency and fruit quality of table grape under alternate partial root-zone drip irrigation. *Agricultural water management* 95, 659-668.



- Eissenstat, D., Wells, C., Yanai, R., and Whitbeck, J. (2000). Building roots in a changing environment: implications for root longevity. *The New Phytologist* 147, 33-42.
- Evans, L. (1976a). Aspects of the comparative physiology of grain yield in cereals. In "Advances in Agronomy", Vol. 28, pp. 301-359. Elsevier.
- Evans, L. T. (1976b). Aspects of the comparative physiology of grain yield in cereals. In "Advances in Agronomy", Vol. 28, pp. 301-359. Elsevier.
- Fernandes-Silva, A. A., Ferreira, T. C., Correia, C. M., Malheiro, A. C., and Villalobos, F. J. (2010). Influence of different irrigation regimes on crop yield and water use efficiency of olive. *Plant and soil* 333, 35-47.
- Fernández, J., Alcon, F., Diaz-Espejo, A., Hernandez-Santana, V., and Cuevas, M. (2020). Water use indicators and economic analysis for on-farm irrigation decision: A case study of a super high density olive tree orchard. *Agricultural Water Management* 237, 106074.
- Ferreira, M. I., Valancogne, C., Daudet, F. A., Ameglio, T., Pacheco, C. A., and Michaelsen, J. (1996). Evapotranspiration and crop-water relations in a peach orchard. In "Evapotranspiration and irrigation scheduling. Proceedings of the International Conference, San Antonio, Texas", pp. 3-6.
- Flumignan, D. L., Faria, R. T. d., and Lena, B. P. (2012). Test of a microlysimeter for measurement of soil evaporation. *Engenharia Agrícola* 32, 80-90.
- Foken, T. (2008). The energy balance closure problem: an overview. *Ecological Applications* 18, 1351-1367.
- Foken, T., Aubinet, M., and Leuning, R. (2012). The eddy covariance method. In "Eddy covariance", pp. 1-19. Springer.
- García-Sánchez, F., Syvertsen, J. P., Gimeno, V., Botía, P., and Perez-Perez, J. G. (2007). Responses to flooding and drought stress by two citrus rootstock seedlings with different water-use efficiency. *Physiologia Plantarum* 130, 532-542.
- Garrot, D. J., Kilby, M. W., Fangmeier, D. D., Husman, S. H., and Ralowicz, A. E. (1993). Production, growth, and nut quality in pecans under water stress based on the crop water stress index. *Journal of the American Society for Horticultural Science* 118, 694-698.
- Goldsmith, R. (2013). Changing directions: the atmosphere-plant-soil continuum. *New Phytologist* 199, 4-6.
- Goodwin, I., Whitfield, D. M., and Connor, D. J. (2006). Effects of tree size on water use of peach (*Prunus persica* L. Batsch). *Irrigation Science* 24, 59-68.
- Granier, A. (1985). Une nouvelle méthode pour la mesure du flux de sève brute dans le tronc des arbres. In "Annales des Sciences forestières", Vol. 42, pp. 193-200. EDP Sciences.
- Granier, A. (1987). Evaluation of transpiration in a Douglas-fir stand by means of sap flow measurements. *Tree physiology* 3, 309-320.
- Granier, A., Loustau, D., and Bréda, N. (2000). A generic model of forest canopy conductance dependent on climate, soil water availability and leaf area index. *Annals of Forest Science* 57, 755-765.
- Green, S., and Clothier, B. (1988). Water use of kiwifruit vines and apple trees by the heat-pulse technique. *Journal of Experimental Botany* 39, 115-123.
- Green, S., and Clothier, B. (1999). The root zone dynamics of water uptake by a mature apple tree. *Plant and Soil* 206, 61-77.
- Green, S., Clothier, B., and Jardine, B. (2003). Theory and practical application of heat pulse to measure sap flow. *Agronomy Journal* 95, 1371-1379.
- Hatton, T. J., Catchpole, E. A., and Vertessy, R. A. (1990). Integration of sap flow velocity to estimate plant water use. *Tree Physiology* 6, 201-209.
- Heaton, E. K., Daniell, J. W., and Moon, L. C. (1982). Effect of Drip Irrigation of Pecan Quality and Relationship of Selected Quality Parameters. *Journal of Food Science* 47, 1272-1275.



- Herrera, E. A. (1990). Fruit Growth and Development of Ideal' and Western 'Pecans. *Journal of the American Society for Horticultural Science* 115, 915-923.
- Hetherington, A. M., and Woodward, F. I. (2003). The role of stomata in sensing and driving environmental change. *Nature* 424, 901.
- Holland, S., Heitman, J., Howard, A., Sauer, T., Giese, W., Ben-Gal, A., Agam, N., Kool, D., and Havlin, J. (2013). Micro-Bowen ratio system for measuring evapotranspiration in a vineyard interrow. *Agricultural and forest meteorology* 177, 93-100.
- Howell, T. (1994). Irrigation engineering, evapotranspiration. *Encyclopedia of agricultural science/edited by Charles J. Arntzen, Ellen M. Ritter*.
- Howell, T. (2003). Irrigation efficiency. p. 467–472. BA Stewart and TA Howell (ed.) *Encyclopedia of water science*. Marcel Dekker, New York. *Irrigation efficiency*. p. 467–472. In BA Stewart and TA Howell (ed.) *Encyclopedia of water science*. Marcel Dekker, New York.
- Ibraimo, N. A. (2018). Water use of deciduous and evergreen tree nut crops: a case study using pecans and macadamias.
- Ibraimo, N. A., Taylor, N. J., Steyn, J. M., Gush, M. B., and Annandale, J. G. (2016). Estimating water use of mature pecan orchards: A six stage crop growth curve approach. *Agricultural Water Management* 177, 359-368.
- Jarvis, A. J., Davies, W. J. (1998). The coupled response of stomatal conductance to photosynthesis and transpiration. *Journal of Experimental Botany*, 399-406.
- Jarvis, P. G., McNaughton, K. (1986). Stomatal control of transpiration: scaling up from leaf to region. In "Advances in ecological research", Vol. 15, pp. 1-49. Elsevier.
- Jensen, M., Harrison, D., Korven, H., and Robinson, F. (1980). The role of irrigation in food and fiber production. *The role of irrigation in food and fiber production.*, 15-41.
- Jones, H. G., Lakso, A. N., and Syvertsen, J. (1985). Physiological control of water status in temperate and subtropical fruit trees. *Horticultural reviews* 7, 301-344.
- Kallestad, J., Sammis, T., Mexala, J., and Gutschick, V. (2012). The impact of prolonged flood-irrigation on leaf gas exchange in mature pecans in an orchard setting. *International Journal of Plant Production* 1, 163-178.
- Kilby, M. (1980). Fall irrigation of pecans. *Pecan South*.
- Klein, T. (2014). The variability of stomatal sensitivity to leaf water potential across tree species indicates a continuum between isohydric and anisohydric behaviours. *Functional Ecology* 28, 1313-1320.
- Kool, D., Agam, N., Lazarovitch, N., Heitman, J., Sauer, T., and Ben-Gal, A. (2014). A review of approaches for evapotranspiration partitioning. *Agricultural and forest meteorology* 184, 56-70.
- Kozlowski, T. (1992). Carbohydrate sources and sinks in woody plants. *The Botanical Review* 58, 107-222.
- Lehmann, P., Assouline, S., and Or, D. (2008). Characteristic lengths affecting evaporative drying of porous media. *Physical Review E* 77, 056309.
- Ma, L., Hou, C. W., Zhang, X. Z., Li, H. L., Wang, Y., and Han, Z. H. (2013). Seasonal growth and spatial distribution of apple tree roots on different rootstocks or interstems. *Journal of the American Society for Horticultural Science* 138, 79-87.
- Mahrt, L. (1998). Flux sampling errors for aircraft and towers. *Journal of Atmospheric and Oceanic technology* 15, 416-429.
- Malm, N. R. (2003). "Climate Guide, Las Cruces, 1892-2000," New Mexico State University, Agricultural Experiment Station.
- Marshall, D. (1958). Measurement of sap flow in conifers by heat transport. *Plant physiology* 33, 385.

- Massonnet, C., Costes, E., Rambal, S., Dreyer, E., and Regnard, J. L. (2007). Stomatal regulation of photosynthesis in apple leaves: evidence for different water-use strategies between two cultivars. *Annals of botany* 100, 1347-1356.
- Mellouli, H., Van Wesemael, B., Poesen, J., and Hartmann, R. (2000). Evaporation losses from bare soils as influenced by cultivation techniques in semi-arid regions. *Agricultural Water Management* 42, 355-369.
- Mielke, E. (1981). Effect of stress on pecan photosynthesis. In "Proc. Western Pecan Conf", pp. 47-65.
- Miyamoto, S. (1983). Consumptive water use of irrigated pecans. *Journal of the American Society for Horticultural Science* 108, 676-681.
- Miyamoto, S. (1989). Scheduling irrigation for pecans. In "International Symposium on the Culture of Subtropical and Tropical Fruits and Crops 275", pp. 513-522.
- Miyamoto, S. (1990). Scheduling irrigation for pecans. *Acta Horticulturae* 275, 513-522.
- Miyamoto, S., Henggeler, J., and Storey, J. B. (1995). Water management in irrigated pecan orchards in the southwestern United States. *HortTechnology* 5, 214-218.
- Monteith, J. L. (1965). Evaporation and environment. In "Symposia of the society for experimental biology", Vol. 19, pp. 205-234. Cambridge University Press (CUP) Cambridge.
- Nardini, A., and Salleo, S. (2000). Limitation of stomatal conductance by hydraulic traits: sensing or preventing xylem cavitation? *Trees* 15, 14-24.
- Nobel, P. (2009). *Physicochemical and Environmental Plant Physiology*—Academic Press. Oxford.
- Or, D., Lehmann, P., Shahraeeni, E., and Shokri, N. (2013). Advances in soil evaporation physics—A review. *Vadose Zone Journal* 12.
- Othman, Y., Van Leeuwen, D., Heerema, R., and Hilaire, R. S. (2014). Midday stem water potential values needed to maintain photosynthesis and leaf gas exchange established for pecan. *Journal of the American Society for Horticultural Science* 139, 537-546.
- Payero, J. O., and Irmak, S. (2008). Construction, installation, and performance of two repacked weighing lysimeters. *Irrigation Science* 26, 191-202.
- Penman, H. L. (1948). Natural evaporation from open water, bare soil and grass. *Proceedings of the Royal Society of London. Series A. Mathematical and Physical Sciences* 193, 120-145.
- Pereira, L. S., Allen, R. G., Smith, M., and Raes, D. (2015). Crop evapotranspiration estimation with FAO56: Past and future. *Agricultural Water Management* 147, 4-20.
- Pou, A., Medrano, H., Tomàs, M., Martorell, S., Ribas-Carbó, M., and Flexas, J. (2012). Anisohydric behaviour in grapevines results in better performance under moderate water stress and recovery than isohydric behaviour. *Plant and soil* 359, 335-349.
- Rana, G., and Katerji, N. (2000). Measurement and estimation of actual evapotranspiration in the field under Mediterranean climate: a review. *European Journal of agronomy* 13, 125-153.
- Reinders, F.B. (2010). Standards and guidelines for improved efficiency of irrigation water use from dam wall release to root zone application. WRC Report 466/10.
- Rico, C., Pittermann, J., Polley, H. W., Aspinwall, M. J., and Fay, P. A. (2013). The effect of subambient to elevated atmospheric CO<sub>2</sub> concentration on vascular function in *Helianthus annuus*: implications for plant response to climate change. *New Phytologist* 199, 956-965.
- Rieger, M., and Daniell, J. (1988). Leaf water relations, soil-to-leaf resistance, and drought stress in pecan seedlings. *Journal of the American Society for Horticultural Science (USA)*.

- Rodríguez-Gamir, J., Primo-Millo, E., and Forner-Giner, M. Á. (2016). An integrated view of whole-tree hydraulic architecture. Does stomatal or hydraulic conductance determine whole tree transpiration? *PloS one* 11, e0155246.
- Rodríguez-Gamir, J., Intrigliolo, D. S., Primo-Millo, E., and Forner-Giner, M. A. (2010). Relationships between xylem anatomy, root hydraulic conductivity, leaf/root ratio and transpiration in citrus trees on different rootstocks. *Physiologia plantarum* 139, 159-169.
- Roman, D., Novick, K., Brzostek, E., Dragoni, D., Rahman, F., and Phillips, R. (2015). The role of isohydric and anisohydric species in determining ecosystem-scale response to severe drought. *Oecologia* 179, 641-654.
- Rosa, R. D., Paredes, P., Rodrigues, G. C., Alves, I., Fernando, R. M., Pereira, L. S., and Allen, R. G. (2012). Implementing the dual crop coefficient approach in interactive software. 1. Background and computational strategy. *Agricultural Water Management* 103, 8-24.
- Ryan, M. G., and Yoder, B. J. (1997). Hydraulic limits to tree height and tree growth. *Bioscience* 47, 235-242.
- Sack, L., Cowan, P., Jaikumar, N., and Holbrook, N. (2003). The 'hydrology' of leaves: co-ordination of structure and function in temperate woody species. *Plant, Cell & Environment* 26, 1343-1356.
- Sade, N., Gebremedhin, A., and Moshelion, M. (2012). Risk-taking plants: anisohydric behavior as a stress-resistance trait. *Plant signaling & behavior* 7, 767-770.
- Samani, Z., Bawazir, A. S., Bleiweiss, M., Skaggs, R., Longworth, J., Tran, V. D., and Pinon, A. (2009a). Using remote sensing to evaluate the spatial variability of evapotranspiration and crop coefficient in the lower Rio Grande Valley, New Mexico. *Irrigation Science* 28, 93-100.
- Samani, Z., Bawazir, A. S., Bleiweiss, M., Skaggs, R., Longworth, J., Tran, V. D., and Pinon, A. (2009b). Using remote sensing to evaluate the spatial variability of evapotranspiration and crop coefficient in the lower Rio Grande Valley, New Mexico. Springer.
- Samani, Z., Bawazir, S., Skaggs, R., Longworth, J., Piñon, A., and Tran, V. (2011). A simple irrigation scheduling approach for pecans. *Agricultural water management* 98, 661-664.
- Sammis, T., Mexal, J., and Miller, D. (2004). Evapotranspiration of flood-irrigated pecans. *Agricultural water management* 69, 179-190.
- Sammis, T. W. (1980). Comparison of Sprinkler, Trickle, Subsurface, and Furrow Irrigation Methods for Row Crops 1. *Agronomy Journal* 72, 701-704.
- Sande, D. N., Mullen, J. D., and Nzaku, K. (2009). "Amenity benefits and public policy: An application to the Georgia Pecan Industry."
- SAPPA (2018). Industry Statistics. SAPPA.
- Saravanapavan, T., and Salvucci, G. D. (2000). Analysis of rate-limiting processes in soil evaporation with implications for soil resistance models. *Advances in water resources* 23, 493-502.
- Sargent, R. G. (2013). Verification and validation of simulation models. *Journal of simulation* 7, 12-24.
- Saxton, K., Rawls, W. J., Romberger, J., and Papendick, R. (1986). Estimating generalized soil-water characteristics from texture 1. *Soil science society of America Journal* 50, 1031-1036.
- Schlünder, E. U. (1988). On the mechanism of the constant drying rate period and its relevance to diffusion controlled catalytic gas phase reactions. *Chemical Engineering Science* 43, 2685-2688.
- Schultz, H. R. (2003). Differences in hydraulic architecture account for near-isohydric and anisohydric behaviour of two field-grown *Vitis vinifera* L. cultivars during drought. *Plant, Cell & Environment* 26, 1393-1405.

- Shahraeeni, E., Lehmann, P., and Or, D. (2012). Coupling of evaporative fluxes from drying porous surfaces with air boundary layer: Characteristics of evaporation from discrete pores. *Water Resources Research* 48.
- Shokri, N., Lehmann, P., and Or, D. (2010). Evaporation from layered porous media. *Journal of Geophysical Research: Solid Earth* 115.
- Shokri, N., Lehmann, P., Vontobel, P., and Or, D. (2008). Drying front and water content dynamics during evaporation from sand delineated by neutron radiography. *Water resources research* 44.
- Shokri, N., and Or, D. (2011). What determines drying rates at the onset of diffusion controlled stage-2 evaporation from porous media? *Water Resources Research* 47.
- Shuttleworth, W. J., and Wallace, J. (1985). Evaporation from sparse crops-an energy combination theory. *Quarterly Journal of the Royal Meteorological Society* 111, 839-855.
- Sinclair, T. R., Tanner, C., and Bennett, J. (1984). Water-use efficiency in crop production. *Bioscience* 34, 36-40.
- Smith, D., and Allen, S. (1996). Measurement of sap flow in plant stems. *Journal of Experimental Botany* 47, 1833-1844.
- Smith, M., and Ager, P. (1988). Effects of soil flooding on leaf gas exchange of seedling pecan trees. *HortScience* 23, 370-372.
- Sorensen, R., Jones, T., Campbell, G., and Montes-Helu, M. (1999). Heat pulse needles to measure pecan tree transpiration. *Applied Engineering in Agriculture* 15, 651.
- Sparks, D. (2002). Rainfall governs pecan stand homogeneity in native, wild habitats. *Journal of the American Society for Horticultural Science* 127, 860-868.
- Sparks, D. (2005). Adaptability of pecan as a species. *HortScience* 40, 1175-1189.
- Sperry, J. S. (2000). Hydraulic constraints on plant gas exchange. *Agricultural and forest meteorology* 104, 13-23.
- Sperry, J. S., Meinzer, F. C., and McCulloh, K. A. (2008). Safety and efficiency conflicts in hydraulic architecture: scaling from tissues to trees. *Plant, Cell & Environment* 31, 632-645.
- Steinberg, S. L., McFarland, M. J., and Worthington, J. W. (1990). Comparison of trunk and branch sap flow with canopy transpiration in pecan. *Journal of experimental botany* 41, 653-659.
- Stirzaker, R., Mbakwe, I., and Mziray, N. R. (2017). A soil water and solute learning system for small-scale irrigators in Africa. *International Journal of Water Resources Development* 33, 788-803.
- Sun, H., Liu, C., Zhang, Y., and Zhang, X. (2004). Study on soil evaporation by using micro-lysimeter [J]. *Journal of hydraulic engineering* 8, 114-118.
- Swanson, R., and Whitfield, D. (1981). A numerical analysis of heat pulse velocity theory and practice. *Journal of experimental botany* 32, 221-239.
- Tardieu, F., and Simonneau, T. (1998). Variability among species of stomatal control under fluctuating soil water status and evaporative demand: modelling isohydric and anisohydric behaviours. *Journal of Experimental Botany* 49, 419-432.
- Taylor, N., Kunene, S., Pandor, M. (2020). Stick-tights and vivipary in pecans. *Department of Plant and Soil Sciences, University of Pretoria*.
- Taylor, N., Mahohoma, W., Vahrmeijer, J., Gush, M. B., Allen, R. G., and Annandale, J. G. (2015). Crop coefficient approaches based on fixed estimates of leaf resistance are not appropriate for estimating water use of citrus. *Irrigation science* 33, 153-166.
- Taylor, N. J., and Gush, M. B. (2014). The water use of selected fruit tree orchards (Volume 1): Review of available knowledge. *Water Research Commission Report*, 14.
- Trenberth, K. E., Fasullo, J. T., and Kiehl, J. (2009). Earth's global energy budget. *Bulletin of the American Meteorological Society* 90, 311-324.



- Tsuda, M., and Tyree, M. T. (2000). Plant hydraulic conductance measured by the high pressure flow meter in crop plants. *Journal of Experimental Botany* 51, 823-828.
- Twine, T. E., Kustas, W., Norman, J., Cook, D., Houser, P., Meyers, T., Prueger, J., Starks, P., and Wesely, M. (2000). Correcting eddy-covariance flux underestimates over a grassland. *Agricultural and Forest Meteorology* 103, 279-300.
- Vandegheuchte, M. W., and Steppe, K. (2013). Sap-flux density measurement methods: working principles and applicability. *Functional Plant Biology* 40, 213-223.
- Villalobos, F. J., Testi, L., Orgaz, F., García-Tejera, O., Lopez-Bernal, A., González-Dugo, M. V., Ballester-Lurbe, C., Castel, J. R., Alarcón-Cabañero, J. J., and Nicolás-Nicolás, E. (2013). Modelling canopy conductance and transpiration of fruit trees in Mediterranean areas: a simplified approach. *Agricultural and forest meteorology* 171, 93-103.
- Wang, H., and Liu, C. (2007). Soil evaporation and its affecting factors under crop canopy. *Communications in soil science and plant analysis* 38, 259-271.
- Wang, J., Miller, D. R., Sammis, T. W., Gutschick, V. P., Simmons, L. J., and Andales, A. A. (2007a). Energy balance measurements and a simple model for estimating pecan water use efficiency. *Agricultural water management* 91, 92-101.
- Wang, J., Sammis, T. W., Andales, A. A., Simmons, L. J., Gutschick, V. P., and Miller, D. R. (2007b). Crop coefficients of open-canopy pecan orchards. *Agricultural Water Management* 88, 253-262.
- Wang, J., Sammis, T. W., Andales, A. A., Simmons, L. J., Gutschick, V. P., and Miller, D. R. (2007c). Crop coefficients of open-canopy pecan orchards. *agricultural water management* 88, 253-262.
- Ward, F. A., and Pulido-Velazquez, M. (2008). Water conservation in irrigation can increase water use. *Proceedings of the National Academy of Sciences* 105, 18215-18220.
- Wells, L. (2015). Irrigation water management for pecans in humid climates. *HortScience* 50, 1070-1074.
- Wells, L. (2017). "Pecan: America's Native Nut Tree," University of Alabama Press.
- Wells, L., and Conner, P. (2007). Southeastern pecan growers' handbook.
- White Jr, A., and Edwards, J. (1978). Soil profile distribution and seasonal growth of pecans roots. In "Proceedings of the Annual Convention Southeast Pecan Growers Association".
- Willis, W. (1960). Evaporation from Layered Soils in the Presence of a Water Table 2.1. *Soil Science Society of America Journal* 24, 239-242.
- Willmott, C. J. (1981). On the validation of models. *Physical geography* 2, 184-194.
- Wilson, K., Goldstein, A., Falge, E., Aubinet, M., Baldocchi, D., Berbigier, P., Bernhofer, C., Ceulemans, R., Dolman, H., and Field, C. (2002). Energy balance closure at FLUXNET sites. *Agricultural and Forest Meteorology* 113, 223-243.
- Wolstenholme, B. (1979). The ecology of pecan trees, Part 1. *Characteristics of the native habitat. Pecan Quart* 13, 32-35.
- Wood, B. W. (1988). Fruiting affects photosynthesis and senescence of pecan leaves. *Journal of the American Society for Horticultural Science*.
- Wood, B. W., Conner, P. J., and Worley, R. E. (2002). Insight into alternate bearing of pecan. In "XXVI International Horticultural Congress: Key Processes in the Growth and Cropping of Deciduous Fruit and Nut Trees 636", pp. 617-629.
- Wood, B. W., Conner, P. J., and Worley, R. E. (2003). Relationship of alternate bearing intensity in pecan to fruit and canopy characteristics. *HortScience* 38, 361-366.
- Wood, B. W., Payne, J. A., and Grauke, L. J. (1994). An overview of the evolution of the US pecan industry. In "Pecan Technology", pp. 1-11. Springer.
- Wood, B. W., Smith, M. W., Worley, R. E., Anderson, P. C., Thompson, T. T., and Grauke, L. (1997). Reproductive and vegetative characteristics of pecan cultivars. *HortScience* 32, 1028-1033.

- Yamanaka, T., Takeda, A., and Shimada, J. (1998). Evaporation beneath the soil surface: Some observational evidence and numerical experiments. *Hydrological Processes* 12, 2193-2203.
- Yamanaka, T., Takeda, A., and Sugita, F. (1997). A modified surface-resistance approach for representing bare-soil evaporation: Wind tunnel experiments under various atmospheric conditions. *Water Resources Research* 33, 2117-2128.
- Yang, S., and Tyree, M. T. (1993). Hydraulic resistance in *Acer saccharum* shoots and its influence on leaf water potential and transpiration. *Tree Physiology* 12, 231-242.
- Zeggaf, A. T., Takeuchi, S., Dehghanisani, H., Anyoji, H., and Yano, T. (2008). A Bowen ratio technique for partitioning energy fluxes between maize transpiration and soil surface evaporation. *Agronomy Journal* 100, 988-996.